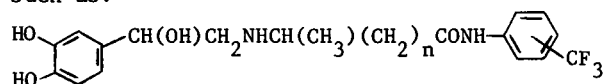


M-PM-SymI-1 BIOPHYSICS OF CARRIER-DRUG CONJUGATES. M. Goodman, M. Hassan and E. Scoffone, Dept. of Chemistry, University of California, San Diego, La Jolla, CA 92093 and V. Madison, Dept. of Physical Chemistry, Hoffmann-La Roche, Inc., Nutley, NJ 07110

In search for new drug analogs with higher potency and specificity, we have synthesized many catecholamine derivatives such as:



The biological activity is based on cAMP accumulation in a mouse sarcoma (S49) cell line. The results are *p*-CH₃ 10 x isoproterenol; *m*-CF₃ 1 x isoproterenol; *o*-CF₃ 10⁻³ x isoproterenol. The biological activity also depends on the number of methylenes in the spacer group. We carried out extensive computer simulations to characterize the conformational properties of these molecules including molecular dynamics and energy minimizations, using empirical energy expressions in the form of a Valence Force Field. The molecular dynamics provide information on the flexibility of the compounds and the interactions among different groups, while the energy minimizations allow the determination of the most stable conformations. Particularly interesting is the study of the folding properties of these molecules which examine the interactions between the two aromatic groups. These effects may be central to biological activity. We believe this theoretical study in conjunction with the synthesis and biological testing of new analogs can help in the understanding of the relationship between structure and activity of these compounds and the design of new drugs.

M-PM-SymI-2 DE NOVO DESIGN AND SYNTHESIS OF A PROTEIN by Jane S. Richardson and David C. Richardson, Duke University, and Bruce W. Erickson, Rockefeller University.

We are engaged in an effort to design, synthesize, and study entirely novel small proteins as model systems of protein folding and catalysis. The first step in such design is choice of a suitable overall architecture: it must be large enough to form a stable tertiary structure (including built-in tolerance for future sequence changes), small enough for practical synthesis, and well enough understood to allow rational design of the detailed sequence. We have chosen to make a small beta barrel protein with two identical halves joined at their C-termini by a covalent cross-linker whose tail attaches them to the resin during synthesis. Each half is designed to form a 4-strand antiparallel beta sheet with up&down topology. The sequence was chosen by optimizing and compromising many simultaneous criteria: strong prediction of the beta strands, precise location of the tight turns (to control the topology), good side chain fit of the hydrophobic sheet faces that pack together and solubility for the outer faces, favorable pair combinations for the side chains on neighboring strands, ease of synthesis, allowance for later changes to make a binding pocket at one end and specific cleavage sites to allow sequencing those changes, etc. The sequence is: Ac-STVTARQPNVTYISIPNTATVRLPNYTLISIG. Synthesis of the protein (called betabellin) was recently completed, and we are now trying to purify, characterize, and crystallize it.

M-PM-SymI-3 INTERFACIAL FACTORS IN THE DESIGN OF BIOMEDICAL MATERIALS, R.E. Baier, Advanced Technology Center, Calspan Corporation, PO Box 400, Buffalo, NY 14225 and Department of Biophysics, State University of New York at Buffalo, New York 14214.

There are many biotechnological needs to either encourage or inhibit attachment, adhesion, growth, or activity of biological entities at their junctions with synthetic materials. An emerging specialty of interfacial biophysics serves these needs by developing structure/function correlations of surface-localized substances. Structural aspects are deduced from surface compositional analyses via multiple attenuated internal reflection infrared spectroscopy, energy-dispersive x-ray and electron spectroscopy, and contact angle techniques to determine outermost atomic clusters, together with surface morphology by ellipsometry, scanning electron microscopy, and profilometry. Functional data are acquired by critical surface tension determination, contact and zeta potential measurement, evaluation of protein adsorption and conformation changes, immunologic tests, and morphometric studies of adherent cells. The most significant current successes of this approach are seen in artificial hearts and substitute blood vessels, while progress is being made with truly nontoxic, fouling-resistant coatings for ships, heat exchangers, and food processing equipment. These rely mainly on surface-energy-controlled materials that mimic natural boundaries with saline media, such as those of healthy vascular endothelium, oral mucosa, or the modified skin of porpoises and killer whales. Percutaneous leads, dental and orthopedic implants benefit, conversely, from surface modifications that produce scrupulous cleanliness and strong bioadhesion. Future prosthetic devices are designed as biosynthetic composites, such as tanned umbilical cord vessels and custom-grown, mesh-reinforced tissues.

M-PM-SymI-4

CONTROLLED DRUG RELEASE SYSTEMS

by Robert Langer, MIT

Despite major advances in polymeric systems little attention has been given to developing systems for the controlled release of large molecules (M.W. > 1000) such as polypeptide hormones. However, advances in genetic engineering may allow the commercial production of a variety of useful macromolecular drugs, such as growth hormones. Since these are potent compounds, all with very short *in vivo* half-lives, it will be critical to develop delivery systems for them. In early studies, we demonstrated that small ethylene-vinyl acetate copolymer pellets could release many different macromolecules in bioactive form for over 100 days *in vitro* and *in vivo*. By combining simple fabrication parameters such as drug particle size, loading, and coating - release rates for any drug could be changed several thousand fold. Microstructural studies show that the incorporation of powdered macromolecules during polymer matrix casting creates a series of interconnecting channels through which dissolved drug can diffuse. In order to achieve constant rates, a hemispheric device laminated with an impermeable coating, except of a small cavity in the center face, was developed. Constant release was achieved for over 60 days. Monte-Carlo computer methods are currently being explored to model these systems. Bioerodible polymer systems based on polyanhydrides are also being explored. In order to provide increased release rates on demand, a polymer-drug delivery system containing small magnetic beads was designed. Release rates were controlled by an oscillating external bar magnet. When exposed to the magnetic field, polymer matrices released up to 30 times more drug. Applications for both magnetic and non-magnetic systems include the delivery of insulin, vaccines, interferon, and enzymes.

M-PM-A1 DIFFUSION-ENHANCED LANTHANIDE ENERGY TRANSFER AS A PROBE OF MACROMOLECULAR ELECTROSTATICS: PH DEPENDENCE OF ENERGY TRANSFER TO MYOGLOBIN. T.G. Wensel and C.F. Meares, Chemistry Department, University of California, Davis, California 95616.

The use of diffusion-enhanced lanthanide energy transfer to study macromolecular electrostatics was investigated using the heme in sperm whale met-(aquo)myoglobin as energy acceptor. Energy transfer from a series of Tb(III) chelates of similar size and shape, but having net electric charges of +1, -1, or 0, was measured as the charge on myoglobin was varied from +6 to 0 by pH titration. The rate constant for energy transfer from the neutral chelate indicates that the 8 Å diameter probe can closely approach an edge of the heme, in accord with the heme accessibility apparent from crystallographic models. The rate constants for the positively and negatively charged chelates differ from each other by a factor of about 4 and from the rate constant for the neutral probe by factors of about $\frac{1}{2}$ and 2 respectively at a protein charge of +6 (pH 6). Near the isoionic point (8.2) the rate constants for all three chelates converge. By using the three probes and varying experimental conditions, it has been demonstrated that these effects are due to electrostatic rather than chemical interactions. The sizes of the effects are consistent with the known charge of myoglobin at each pH, and in fair agreement with theoretical predictions from a simple model.

M-PM-A2 PORPHYRIN CORE EXPANSION AND ELECTRONIC STRUCTURE IN THE NEUTRAL pH FORM OF COPPER CYTOCHROME c*, J. A. Shelnutt, Sandia National Laboratories, Albuquerque, NM; K. D. Straub, VA Medical Center, Little Rock, AR; P. M. Rentzepis, Bell Laboratories, Murray Hill, NJ; M. Gouterman and E. R. Davidson, University of Washington, Seattle, WA

The pH-dependent resonance Raman and absorption spectra of copper cytochrome c are examined. Large shifts in the Raman core-size marker lines are observed in the neutral pH form of copper cytochrome c relative to the protein at pH extremes (pH 2 and pH 13). Five-coordinate copper-porphyrin complexes exhibit similar, but somewhat smaller, shifts in the core-size marker lines. The Raman shifts represent a significant expansion (0.03 Å) of the porphinato core in the neutral form. Further, analysis of the $\pi \rightarrow \pi^*$ absorption spectral changes using the 4-orbital model indicates a substantial destabilization of the top-filled $a_{2u}(\pi)$ orbital in the neutral pH form of the protein. The result is a red shift of all $\pi \rightarrow \pi^*$ bands, a decrease in the separation of the α and Soret bands, and a reversal in the α and β band intensity ratio. Iterative extended Huckel molecular orbital calculations for model copper porphyrins show destabilization of the a_{2u} orbital caused by addition of a σ -donating axial ligand. Thus, the calculations support previous interpretations of spectral changes based on addition of an axial fifth ligand. They further predict an observed strong uv band near 350 nm in the neutral form to be a $d_{z^2} \rightarrow e_g(\pi^*)$ charge-transfer band. Finally, spectral changes are consistent with dimerization of the porphyrins in the copper cytochrome c dimers at the pH extremes.

* This work was performed at Sandia National Laboratories, supported by the U. S. Department of Energy (DOE) under Contract # DE-AC04-76-DP00789.

M-PM-A3 COMPARISON OF THE MAGNETIC PROPERTIES OF DEOXY AND PHOTODISSOCIATED MYOGLOBIN. Heinrich Roder, Todd B. Sauke and Hans Frauenfelder, Dept. of Physics, University of Illinois, Urbana, IL 61801.

A superconducting magnetometer was used to measure the magnetic susceptibility of photodissociated carbon monoxy myoglobin over the temperature range from 1.7 to 25 K at 10 and 50 kG. The spin and the crystal field parameters of the iron ion were extracted by a spin Hamiltonian approach. Under equivalent conditions the magnetic susceptibility of deoxy myoglobin was measured. In both experiments the CO-bound protein was used as a diamagnetic reference. Above about 5 K the metastable photolysed state and the equilibrium deoxy form of myoglobin are magnetically indistinguishable and can be fitted with $S = 2$ and $g = 2$. The transition from spin 0 to spin 2 and the conformational changes known to accompany these electronic changes thus also occur after photolysis at low temperature. At the lowest temperatures distinct differences become apparent, indicating a somewhat smaller zero-field splitting in the photo product as compared to the ligand-free state at equilibrium. In qualitative agreement with observations made by other techniques, our results imply that in the heme region of myoglobin substantial structural relaxation occurs after photodissociation, even at 1.7 K. These results are important for the interpretation of the ligand binding kinetics after flash photolysis at low temperature and contribute to the understanding of the relationship between electronic structure and function in heme proteins.

M-PM-A4 FERRICYTOCHROME C: REFOLDING AND METHIONINE-80-SULFUR IRON LINKAGE. Yash P. Myer, Department of Chemistry, State University of New York at Albany, Albany NY 12222.

The role of methionine-80-sulfur ligation to heme iron in ferricytochrome c during refolding has been examined. Urea-denatured horse heart ferricytochrome c in the presence of imidazole, 0.5 M, pH 7.0, was studied using stopped-flow and equilibrium measurements at 407.5 nm. Thermodynamically, Imd-cytochrome c folds and unfolds via a single transition with (Urea) of 5.9 M. Kinetically the refolding is a tri-phasic process: (i) a slow, urea-independent phase, time constant of 22 ± 6 s and an amplitude of 10-13%; (ii) an intermediate reaction, with a slightly positive urea-dependent rate constant, average time constant of 150 ms; and (iii) a fast phase with negative urea dependence of the rate constant from 4-6 M urea and positive dependence above the 6 M concentration, with the largest time constant, 25 ± 6 ms, at 5.8 M urea, the mid-point of the transition. The amplitudes of the intermediate and the fast phases exhibit reciprocity with increasing urea concentrations, favoring the intermediate form at higher concentrations, while maintaining an almost constant sum of the two amplitudes throughout the range. The temperature dependence of the three apparent rate constants yielded activation energies of 14, 19 and 23 ± 3 Kcal/mole, respectively. These findings show that the slow reaction, time constant in decaseconds, does not require, directly or indirectly, the formation of the Met-80-S linkage to iron but the formation of this linkage does determine the over all course of the refolding dynamics. A model involving direct refolding of two unfolded forms, U_f and U_i , in a urea-dependent equilibrium, and concurrently, in a urea-independent equilibrium with the form refolding with a slow reaction, has been proposed for the folding of Imd-cytochrome c.

M-PM-A5 RESONANCE RAMAN STUDIES ON IRON-CARBON BOND LENGTHS IN CARBONMONOXY AND CYANO-MET COMPLEXES OF THE MONOMERIC INSECT HEMOGLOBIN CTT III. Ellen A. Kerr, Bojan Benko, Nai-Teng Yu and Klaus Gersonde*, School of Chemistry, Georgia Institute of Technology, Atlanta, GA 30332 and *Abteilung Physiologische Chemie, Rheinisch-Westfälische Technische Hochschule, D-5100 Aachen, Germany.

Soret-excited resonance Raman spectroscopy yields direct information regarding the iron-carbon bonding interactions in the cyano-met and carbonmonoxy complexes of hemoglobin III from Chironomus thummi thummi (CTT III) in solution. Multiple-isotope exchanges allow us to identify the Fe(III)-CN^- stretching at 453 cm^{-1} , the Fe(III)-C-N^- bending at 412 cm^{-1} , the Fe(II)-CO stretching at 500 cm^{-1} , the Fe(II)-C-O bending at 574 cm^{-1} and the C-O stretching at 1960 cm^{-1} .

The resonance Raman data, in conjunction with those obtained from heme model complexes with well-known Fe-C bond distances, strongly suggest that the Fe(III)-CN^- bond ($\sim 1.91 \text{ \AA}$) is longer than the Fe(II)-CO bond ($\sim 1.80 \text{ \AA}$), in disagreement with those of x-ray crystallographic studies (W. Steigemann and E. Weber (1979) *J. Mol. Biol.* **127**, 309) in which the Fe-C bond lengths were reported as 2.2 \AA in cyano-met and 2.4 \AA in carbonmonoxy CTT III. Based on Badger's rule and normal mode calculations, the x-ray structural data would lead to the prediction of 266 cm^{-1} for the Fe(II)-CO stretching frequency in CTT III·CO, which was not observed. On the other hand, we estimate the Fe-CO bond length as $1.78\text{-}1.80 \text{ \AA}$, which is very similar to the 1.80 \AA value in human Hb·CO crystals (J. M. Baldwin (1980) *J. Mol. Biol.* **136**, 103). We have also estimated the Fe-C-O angle as $169^\circ \pm 5^\circ$, somewhat larger than the 161° value by Steigemann and Weber.

M-PM-A6 THE ENVIRONMENT OF HEME COORDINATED CO IN HEMOPROTEINS AS SEEN BY MAGNETIC RELAXATION AND INFRARED SPECTROSCOPY. A COMPARISON OF MAMMALIAN HEMOGLOBINS, GLYCERA DIBRANCHIATA HEMOGLOBIN AND CYTOCHROME c PEROXIDASE. By James D. Satterlee, Department of Chemistry, The University of New Mexico, Albuquerque, New Mexico 87131.

Analysis of ^{13}CO relaxation data for human hemoglobin A, rabbit hemoglobin sperm whale myoglobin, and Glycera dibranchiata monomer hemoglobin may be interpreted in view of a specific interaction for the distal histidine (E-7). Further, a comparison of infrared stretching frequencies for heme coordinated CO in these proteins and yeast cytochrome c peroxidase (CcP) confirms the uniqueness of CcP and the Glycera monomer. Of particular interest is that cytochrome c peroxidase, alone, exhibits a 2 cm^{-1} deuterium isotope effect for the CO stretching vibration.

M-PM-A7 THE SPECTROSCOPIC DIFFERENCES BETWEEN α AND β SUBUNITS IN HEMOGLOBIN. Peter P.

Chuknyiski, Periakaruppan T. Manoharan, and Joseph M. Rifkind. Laboratory of Cellular & Molecular Biology, NIH, NIA, Gerontology Research Center, Baltimore, MD 21224.

X-ray studies indicate a different heme environment for α and β subunits in hemoglobin. These differences influence ligand affinities under certain conditions. While the spectra of isolated subunits are somewhat different, there is little spectroscopic data to indicate this difference within the intact tetramers. We have been able to clearly distinguish the α and β -chains in two types of spectroscopic studies. A temperature dependent red shift of the solet and 555 nm absorption bands in deoxy HbA has been observed. In the temperature range from 0°-28°C these changes produce a linear dependence of the extinction coefficient on the temperature. A dramatic distinction in this linear temperature dependence is observed between deoxy α -SH and β -SH subunits. The slope of the temperature dependence for α -SH subunits is much higher than for deoxy HbA, while for the β -SH subunits the slope of the temperature dependence is much lower than for deoxy HbA. The calculated average temperature dependence for deoxy α -SH and β -SH subunits has a slope with a value 0.87 relative to that of deoxy HbA, while it is almost the same as that found for oxy HbA. We have, furthermore, found that in the temperature range of 210-250 K methemoglobin forms reversible low spin complexes with the distal histidine. The ESR spectra of these complexes show two components. By Cu oxidation of the β -chains, it was possible to show that the α -chain complex has $g_1 = 2.92$, $g_2 = 2.26$ and $g_3 = 1.46$, while the β -chain complex has $g_1 = 3.066$, $g_2 = 2.34$ and $g_3 = 1.46$. This difference between the α -chains and β -chains are indicative of distinctions in the ligand pockets of both chains. A somewhat altered relative position of the distal histidine could produce these changes in the g -values.

M-PM-A8 HYDROGEN EXCHANGE KINETICS AND SOLUBILITY PROPERTIES OF METHEMOGLOBIN AND

METHEMOGLOBIN COMPLEXES by Gabriel B. Ogunmola, Andrew Demehin, Ben Hallaway, Paul Sanford Roger Gregory, Andreas Rosenberg, University of Minnesota, Minneapolis, MN 55455. We have applied hydrogen exchange kinetics and solubility studies in PEG to study the distribution of the conformational states of methemoglobin at different pH and temperatures. Polyethylene glycol (PEG) enabled us to study the solubilities of methemoglobin without the necessity of high salt which screens important electrostatic properties. Variation in solubility of methemoglobin in PEG is determined principally by excluded volume of polymer and the hemoglobin molecules. Across the pH, methemoglobin undergoes a characteristic structural transition close to its isoelectric point (IEP) in a way that suggests a redistribution of configuration of charged groups on the protein IEP and gives rise to different deviation from ideal behaviour on either side of the IEP. Hydrogen exchange studies, on the other hand, suggest similar results, there being across the pH, a redistribution of fluctuations of different energy barriers with a characteristic transition close to the IEP of the molecule and an exchange rate of the internal protons which reflects the internal motions associated with large amplitude fluctuations of the molecule. Hence, changes in the electrostatic stabilization energy of the folded structure would make significant contribution to the redistribution of fluctuations in the molecule. Differences in the solubility of methemoglobin and its azide complexes across the pH suggest a more favourable binding of azide ion to the crystalline phase than in solution. This would indicate that lattice forces in the crystal allow as much conformational fluctuation in the molecule as in solution. Our data suggests that the thermodynamic parameters of the ligand binding in the crystalline phase could be discussed with the same set of parameters of fluctuation in the solution phase.

M-PM-A9

WITHDRAWN

M-PM-A10 THE RATE OF CONFORMATIONAL CHANGE IN HEMOGLOBIN A AND HEMOGLOBIN KANSAS MEASURED BY MODULATED EXCITATION. F.A. Ferrone*, M. Coletta**, S. Basak*, A.J. Martino*, and M. Brunori.**
*Department of Physics, Drexel University, Philadelphia, PA, 19104
**University of Rome, Rome, Italy.

We have constructed an apparatus which uses modulated excitation for studying the rate of conformational change between the R and T quaternary structures of hemoglobin. The principles of the method have been previously described [F.A. Ferrone and J.J. Hopfield, *Proc. Nat. Acad. Sci. USA*, **73**, 4497, (1976)]; however, the instrument has several novel features. The probe beam employs a microspectrophotometer; the excitation beam is provided by an argon ion laser modulated by an acousto-optic modulator. This apparatus allows us to measure signals from DC to 100 kHz, while the photolysis level can be continuously varied from 0 to 100%. Absorption, in-phase and out-of-phase spectra are simultaneously collected by an on-line computer. We have used this apparatus to follow the transition between R and T structures at three-fold ligation in the carboxy derivative of hemoglobin A and hemoglobin Kansas ($\beta 102 \text{ Asn} \rightarrow \text{Thr}$).

(Work at Drexel supported by NIH grant AM30239.)

M-PM-A11 POLYMERIZATION OF SICKLE CELL HEMOGLOBIN IN THE PRESENCE OF OXYGEN. F.A. Ferrone, Department of Physics, Drexel University, Philadelphia, PA, 19104.

It has recently been proposed that sickle cell hemoglobin polymerizes by a double nucleation mechanism. In such a mechanism, sickle cell hemoglobin polymers are formed by two pathways. One pathway consists of homogeneous nucleation of polymers from bulk solution; the other pathway is the heterogeneous nucleation of polymers onto the surface of polymers already formed by either pathway. This model has been quantitatively successful in describing all known kinetic data. Combined with recent work on oxygen binding to sickle hemoglobin polymers, it is now possible to calculate the time course of polymerization in the presence of oxygen. We have assumed the distribution of intracellular concentrations as obtained by Coletta et al. [*Nature*, **300**, 194 (1982)], and that, to a good approximation, only molecules in the T quaternary structure polymerize, while molecules in the R structure contribute equally to the excluded-volume non-ideality. We also assume that the oxygen saturation remains fixed. With these assumptions we have computed distributions of tenth-times for various levels of oxygen saturation. We find that even for oxygen saturations of 50%, almost half the population of cells polymerizes in less than one second.

Work supported by NIH grant HL21802.

M-PM-A12 Cloning of Human Erythropoietin Gene. Sylvia Lee-Huang, Dept. of Biochemistry, NYU School of Medicine, N.Y., N.Y. 10016.

Human erythropoietin (Ep) is a glycoprotein hormone (34K daltons). As the prime regulator of red blood cell production, its major functions are to promote erythroid differentiation and to initiate hemoglobin synthesis. An understanding of the mode of Ep action is of obvious importance; however, research in this area has been limited by an insufficient supply of the pure hormone. We have been engaged in the development of techniques for improved Ep purification and this has enabled the preparation of sufficient quantities of pure material for the production of monoclonal antibodies. These antibodies were used for the identification of Ep mRNA and the screening of recombinant plasmid containing Ep gene sequences. Poly(A)⁺RNA was prepared from the kidney of a patient suffering from renal carcinoma with elevated Ep titer. cDNA was synthesized and inserted into the Pst I site of pBR322 by homopolymeric dC:dG tailing. The recombinant plasmids were transformed into *E. coli*. Recombinant colonies (Tet^R, Amp^S) were initially screened by colony hybridization with [³²P]-cDNA probes from methylmercury size fractionated mRNA enriched in Ep message. Positive colonies were further screened immunologically by *in situ* RIA with monoclonal anti-Ep. Three clones were identified that expressed the Ep gene as a β -lactamase fusion protein. They contain inserts of approximately 0.2, 0.6, and 1.4 Kb. DNA from these clones hybrid select human Ep mRNA and whose translation product immunoreacts with monoclonal anti-Ep. Protein extracts from these clones also react specifically with monoclonal antibodies to human Ep on Western blots. Pure Ep competes with these fusion proteins for antibody binding. Supported by NIH grants HL 21683 and HL 30862.

M-PM-B1 TRANSPORT THEORY FOR MAGNETIC RESONANCE. J. Schotland, J.S. Leigh, Jr., & B. Chance, Department of Biochem/Biophys., Univ. of Penna., Phila., PA 19104

A general theory of transport processes was developed for magnetic resonance. The density matrix equations for magnetic relaxation were modified to include the effects of stochastic transport of a nucleus between magnetically distinct states. The transition probability for a jump between x and x' is $W(x',x)$. Let $\rho(x,t)$ denote the density matrix, L the Liouvillian operator, R the relaxation operator and L_d the transport operator. Then $i \partial_t \rho = L\rho + R\rho + L_d\rho$ (1) with the ansatz $L_d\rho(x,t) = \int [W(x',x)\rho(x',t) - W(x,x')\rho(x,t)] dx'$ (2). In the small jump limit (1) & (2) may be rewritten as

$$i \partial_t \rho = L\rho + R\rho + \sum_{i,j} A_{ij} \frac{\partial(x_i \rho)}{\partial x_j} + \frac{1}{2} \sum_{i,j} B_{ij} \frac{\partial^2 \rho}{\partial x_i \partial x_j} \quad (3)$$

where A_{ij} and B_{ij} are the first and second moments of the process $W(x,x')$. Choosing the Bloch form of the relaxation operator and calculating expectations values of I_z yields

$$\partial_t M_z = (M_0 - M_z)/T_1 + \sum_{i,j} A_{ij} \frac{\partial(x_i M_z)}{\partial x_j} + \frac{1}{2} \sum_{i,j} B_{ij} \frac{\partial^2 M_z}{\partial x_i \partial x_j} \quad (4)$$

where M_z is the z component of the magnetization and T_1 is the spin-lattice relaxation time. The above formation is applicable to a description of general convection and diffusion effects. For $W(x,x')$ an isotropic diffusion process, (4) reduces to the usual modified Bloch diffusion equation $\partial_t M_z = (M_0 - M_z)/T_1 + D \nabla^2 M_z$ with diffusion coefficient D .

M-PM-B2 ^{13}C -NMR STUDY OF MOTIONS AND PROTONATION STATE OF SEMISYNTHETICALLY INCORPORATED ^{13}C -ENRICHED AMINO ACIDS AT THE N-TERMINAL OF SPERM WHALE MYOGLOBIN. David G. Maskalick, Mark R. Busch, George W. Neireiter, David E. Harris, Frank R. N. Gurd, Department of Chemistry, Indiana University, Bloomington, Indiana 47405.

The internal motions of amino acid side chains and protein backbone segments should influence and in turn be affected by charge-charge interactions, steric constraints, hydrophobic forces, and hydrogen bonding. ^{13}C -enriched glycine, alanine, and isoleucine have been substituted for the NH_2 terminal valine of sperm whale myoglobin using semisynthetic techniques. The addition of a single methyl group to the side chain can alter the $\text{pK}_a^{\text{NH}_2}$ by as much as 0.3 pH units indicating a delicately balanced set of charge-charge interactions between the αNH_2 group and the rest of the protein. From the T_1 and NOE values the generalized order parameter and the effective correlation time for internal motions were calculated using the Lipari-Szabo model-free approach (JACS 104, 4546-4570, (1982)). Meaningful differences in the amplitude of motion were obtained only when the uncertainties in the T_1 and NOE values were less than $\pm 10\%$. The internal motions of $[\text{Ala}^1]\text{Mb}$ and $[\text{Gly}^1]\text{Mb}$ were of greater amplitude when $\text{pH} > \text{pK}_a^{\text{NH}_2}$. Within the framework of the wobbling-in-a-cone model $31^\circ < \theta^\alpha < 57^\circ$ and the restricted diffusion model $47^\circ < \gamma^\alpha < 129^\circ$. Internal correlation times for these motion models were on the picosecond time scale but were associated with orders of magnitude uncertainties. The two methyl group rotations in isoleucine are free and the $\text{C}^\beta\text{-C}^\gamma$ and $\text{C}^\alpha\text{-C}^\beta$ bonds exhibit restricted rotations while the $\text{C}^\alpha\text{-C}^\beta$ bond is nearly devoid of rotational mobility. Uniform ^{13}C -enrichment was crucial for the extraction of unique motion parameters for successive bond rotations. (Supported by U.S. Public Health Service Research Grants HL-05556 and HL-14680.)

M-PM-B3 STRUCTURE-FUNCTION RELATIONSHIPS IN SHORT-CHAIN ACYL-ACYL-CARRIER-PROTEINS FROM *E. COLI*. K. H. Mayo and J. H. Prestegard, Department of Chemistry, Yale University, 225 Prospect Street, New Haven, CT 06511.

Acyl-Carrier-Proteins (ACPs) are known to play a key metabolic role in the synthesis of fatty acids and phospholipids in both prokaryotic and eukaryotic organisms. All known ACPs share the capacity to carry a growing fatty acid chain bound through a thioester linkage to a 4'-phosphopantetheine prosthetic group, phosphodiester linked to a serine of ACP. The suggestion that structural properties of acyl-ACPs may be responsible for variations in activities of enzymes of the fatty acid synthetase system toward different acylated species has stimulated much interest in the study of structure/function relationships of acyl-ACPs. The study of acyl-ACPs also renders potential insight into protein-fatty acid interactions in general. In this present study, ^{19}F -NMR, ^1H -NMR and nuclear Overhauser techniques at 500 MHz have been used to investigate structural perturbations of *E. coli* ACP upon acylation by acetyl, butyryl, hexanoyl and octanoyl fatty acid chains. Results are discussed in terms of the proposed tertiary structural model for ACP (Mayo, Tyrell, and Prestegard (1983) Biochemistry 22, 4485-4493). They indicate a possible structural interaction of the acyl-chain with Phe-50 of ACP and demonstrate significant variations in interaction as acyl chains are elongated.

This work was supported by NIH grant (GM-32243).

M-PM-B4 COMBINATION OF SATURATION TRANSFER (ST) AND TWO DIMENSIONAL (2D) NMR TECHNIQUES TO DETECT THE PARTICIPATION OF NMR-INVISIBLE POOLS IN EXCHANGE REACTIONS

A.P. Koretsky, V.J. Basus, T.L. James, M.P. Klein, and M.W. Weiner. VA Med Center, Depts. of Med. and Pharm. Chem. Univ. of Cal. San Francisco, and Lawrence Berkeley Lab., Univ. of Cal., Berkeley, CA.

^{31}P NMR ST studies of creatine kinase (CK) *in vivo* have been complicated by competing reactions and the possible involvement of small metabolite pools not detected by NMR. (e.g. ADP). Under some circumstances ST and 2D techniques may differ in their sensitivity to detect the presence of NMR-invisible pools. To investigate this possibility, ^{31}P NMR ST and 2D experiments were performed at 97.2 MHz on an equilibrium solution of CK and its reactants; ADP was not detected. Saturation of the phosphocreatine (PCr) resonance led to a 37% reduction of the γ -ATP peak, and saturation of the γ -ATP resonance led to a 34% reduction in PCr magnetization. Forward and reverse rates for the reaction were equal (7.3 $\mu\text{moles/sec}$). Saturation of the γ -ATP resonance also led to a reduction of β -ATP magnetization. This could be explained by either a negative nuclear Overhauser effect (NOE) or direct saturation of the small β -ADP pool, exchanging with β -ATP. The presence of CK was necessary for this effect. Saturation of the β -ATP did not affect γ -ATP. Examination of the 2D spectrum indicated cross-peaks of equal intensity between PCr and γ -ATP. The absence of cross peaks between γ and β -ATP was consistent with the hypothesis that the ST result was not due to a NOE, but rather to an exchange between the small β -ADP pool and β -ATP. Therefore, ST detected exchange between an NMR invisible and an NMR-visible pool, whereas 2D NMR did not. These results suggest that a comparison of ST and 2D NMR may have application to the study of other exchange systems which involve NMR-invisible pools.

M-PM-B5 CONFORMATIONAL PROPERTIES OF MOUSE EPIDERMAL GROWTH FACTOR.

K. H. Mayo (Introduced by: P. B. Moore), Department of Chemistry, Yale University, 225 Prospect Street, New Haven, CT 06511.

Mouse epidermal growth factor (mEGF), a protein hormone effector molecule that regulates cellular development and division, has been investigated using proton nuclear magnetic resonance (NMR) and nuclear Overhauser (NOE) techniques at 500 MHz. Proximity relationships derived from NOE data place stringent limitations on possible models for the molecule. The data are analyzed in terms of model building based on the predictive Chou-Fasman secondary structural algorithm applied to mEGF (Holladay, Savage, Cohen, and Puett (1976) *Biochemistry* 15, 2624-2633). Experimental results indicate mEGF to be a globular protein and assign regions of β -turns as predicted by the Chou-Fasman algorithm and of tiered- β -sheets as proposed by model building studies of the protein. pH titration data demonstrate a His-22 pKa of 7.1 indicating a salt bridge formation between His-22 and another residue. The His-22 pKa is also reflected in the chemical shift changes of several other resonances as a function of pH. Nuclear Overhauser methods yield evidence for a pH-induced conformational transition in mEGF associated with the breaking of the His-22 salt bridge.

This work was supported by NIH grant (GM-32243).

M-PM-B6 ^1H NMR of INTACT MUSCLE AT 11 TESLA. Carlos Arús*, Michael Bárány, William, M.

Westler*, and John. L. Markley (Intro. Louis H. Schliselfeld). College of Medicine, University of Illinois at Chicago IL 60612 and Department of Chemistry, Purdue University, West Lafayette, IN 47907

^1H NMR spectra of intact frog, chicken and human skeletal muscles, and porcine heart were recorded at 470 MHz with the Plateau and Gueron pulse sequence for the suppression of water, $90^\circ_y, \tau, 90^\circ_y$, with $\tau = 180 \mu\text{sec}$, and with radiofrequency on resonance with the water peak (J. Am. Chem. Soc. 104, 7310, 1982). Under these conditions a minimum of 250 times molar decrease in the water signal was achieved. The resolution of the spectra was enhanced by trapezoidal multiplication of the FID prior to Fourier transformation. A few transients (1-12) were required to resolve the resonances from the protons of muscle metabolites. Only cytosolic metabolites, lactic acid, creatine, phosphocreatine, carnosine, anserine, free amino acids, α -glycerophosphorylcholine, choline, carnitine and ATP, contributed to the spectra. The previously unobserved exchangeable protons of these metabolites were also recorded and thereby phosphocreatine at 7.3 ppm could be separated from creatine at 6.7 ppm. During aging of frog muscle, changes in levels of phosphocreatine, creatine and lactic acid were followed by ^1H NMR. Furthermore, the acidification of the intracellular pH was monitored during aging from the chemical shifts of the C4-H, C2-H and NH protons of the histidine ring of carnosine. High resolution proton spectra were also obtained with human muscle biopsies showing changes in lactic acid and creatine content between normal and diseased muscles. The simultaneous measurement of levels of lactic acid, phosphocreatine, creatine and intracellular pH illustrate the potential of ^1H NMR for studying muscle metabolism. (Supported by MDA, Shriners Hospitals and NIH RR 01077).

M-PM-B7 ^{13}C NMR OF INTACT TISSUE AT 11 TESLA. Michael Bárány, Carlos Arús, Alice M. Wyrwicz, William M. Westler, and John L. Markley. University of Illinois at Chicago, IL 60612 and Purdue University, West Lafayette, IN 47907

The natural abundance ^{13}C NMR spectra of various tissues were recorded at 118.2 MHz. At this high field as many as 25 resonances can be resolved in liver, arising from carbons of glycogen, glucose, fatty acids, glycerol, choline and ethanolamine. Similarly a large number of resonances are seen in a secretory tissue, seminal vesicles. Characteristic for the spectra of skeletal muscle are the resonances of creatine and lactic acid. ^{13}C NMR may be used for a spectroscopic mapping of tissues, e.g. a great similarity between human quadriceps and rat soleus muscles is shown. Changes in the concentration of soluble tissue metabolites, e.g. lactic acid, may be followed by comparing the integer of a metabolite peak with that of the external standard dioxane peak. In normal muscle the carbons of membrane-bound phospholipids have limited mobility. However, in diseased muscle about 20% of these phospholipids are highly mobile. The membrane-phospholipids may also be mobilized by drugs. In muscle, trifluoperazine, a phenothiazine, is the most potent mobilizer. Chlorpromazine, a drug from the same family, is much less effective, whereas metofane, a halogenated anesthetic, and verapamil, a calcium channel blocker, have no effect at all. Drugs which perturb muscle membranes also inhibit glycolysis in muscle, as shown by the absence of accumulated lactic acid in the ^{13}C spectra, and drugs which are ineffective on these membranes have no influence on glycogen breakdown either. We have also mobilized the phospholipids in liver membranes with trifluoperazine and to a greater extent with metofane. (Supported by MDA, Shriners Hospitals, NIH RR 01077, NIH GM 29520 and K04GM 00503).

M-PM-B8 ^{23}Na AND ^{39}K NMR STUDIES OF PERFUSED, BEATING, RAT HEARTS: PERFUSION WITH SHIFT REAGENTS. M.M. Pike, J.C. Frazer, D. Dedrick, J.S. Ingwall, P.D. Allen, T.W. Smith, and C.S. Springer; NMR Laboratory; Harvard Medical School; Boston, MA 02115

The title studies have been conducted on Langendorff preparations. The heart rate and pressure are monitored continuously via an elastic balloon inserted in the left ventricle. There are a number of compartments where cations may reside. We eliminate most of the bath signal by maintaining a flowing mannitol bathing solution and some of the ventricular signal by filling the balloon with H_2O . The vascular (and presumably the residual ventricular and atrial) signal can be shifted downfield instantly upon introduction of $\text{Dy}(\text{TTHA})^{3-}$ (10 mM shifts ^{23}Na signal ca. 2 ppm) into the perfusing buffer solution. (There is negligible permanent effect on the heart rate.) Within one minute of the shift of the ^{23}Na vascular peak, most of the remaining unshifted intensity shifts downfield with an interesting time course. This shifted intensity probably represents NMR-visible interstitial Na^+ and the time lag is due to the kinetics of the shift reagent (SR) crossing the coronary capillary walls. Finally, a small peak (ca. 1/75 of the total intensity) remains near the unshifted position for long perfusion times. This is assigned to the NMR-visible intracellular Na^+ . This can be confirmed by lowering the K^+ (and Ca^{2+}) level of or by introducing ouabain into the perfusate. Each of these inhibits the action of the sarcolemmal Na^+/K^+ pumps (and causes the heart to stop beating). The intensity of the unshifted peak is increased to a significantly higher value. In the low K^+ experiment, restoration of the K^+ (Ca^{2+}) in the perfusate causes the heart to resume beating and the intracellular Na^+ level to fall back to normal. Both the ouabain and the SR can be washed out to restore the normal single sharp peak (^{23}Na , ca. 30 Hz).

M-PM-B9 MOLECULAR DYNAMICS AND OPTICAL SPECTROSCOPY OF PROTEINS. Ronald M. Levy and Olivia Rojas Department of Chemistry, Rutgers University, New Brunswick, New Jersey 08903. Richard Freisner, Department of Chemistry, University of Texas, Austin, Texas 78712

Computer simulations based on detailed atomic potential functions provide an extremely powerful method for studying the spectroscopic properties of large molecular systems. Because of the very high sensitivity of high resolution optical probes such as Fourier transform infrared (FTIR), resonance Raman, and coherent anti-Stokes Raman Spectroscopy (CARS), these techniques contain a large amount of structural and dynamical information. If computer simulations on realistic potential surfaces are to be useful for interpreting these optical experiments, it is essential that methods be developed which incorporate anharmonic effects on the calculated spectra since these effects often dominate the spectral changes. A quasi-harmonic approximation is described by which classical computer simulations on multi-dimensional potential surfaces can be used to estimate the effects of anharmonicity on vibrational spectra. A temperature dependent effective quadratic hamiltonian is parameterized using the results of a computer simulation on the exact potential surface. The quasi-harmonic hamiltonian defines a set of normal modes and frequencies which are (Duschinsky) rotated and shifted with respect to the harmonic values. The results of the quasi-harmonic calculations for the infra-red absorption of a model α -helix are compared with reference calculations in the harmonic approximation at a series of temperatures between 5°K and 300°K. Extension of the method to the calculation of vibrational spectra from quantum Monte-Carlo simulations is discussed.

M-PM-B10 RESOLUTION OF 3 AND 4 COMPONENT QUENCHED TYROSINE DECAYS: USE OF A FLUORESCENCE TO DECONVOLUTE A FLUORESCENCE. Enoch W. Small and Louis J. Libertini, Dept. of Biochemistry and Biophysics, Oregon State University, Corvallis, Oregon 97331.

In tyrosine fluorescence decay studies on chromatin and chromosomal proteins we often encounter complex decay kinetics, even for relatively simple systems. For example, we have detected five different fluorescence emissions for histone H1, a class A protein with only a single tyrosine residue. Two long wavelength components which peak at 340 and 400 nm are present when H1 is denatured, but disappear on salt-induced refolding. Also, the more typical H1 tyrosine fluorescence at 300 nm can be resolved into three components. Two components with lifetimes of 1.0 and 2.1 ns correspond to the denatured H1 and one with a lifetime of 4.1 ns derives from the single tyrosine in the refolded protein. We have developed a new approach which we call F/F deconvolution for handling such complex decays. In a normal fluorescence decay experiment a scatter sample is used to obtain a measured excitation and this excitation is then used to deconvolute the fluorescence. For F/F deconvolution the fluorescence is, instead, deconvoluted by using a measured single exponential fluorescence in the place of an excitation. The approach eliminates errors due to the wavelength dependence of the instrument response and can be used to cancel specific decays from the analysis. We have tested F/F deconvolution using measured decays of tyrosine quenched by varying amounts of KI and have shown that this approach can improve the accuracy of determining sub-nanosecond lifetimes. We have summed the measured tyrosine decays and shown that F/F deconvolution can dramatically improve decay resolution capabilities. For example, a decay with lifetimes of 1.3, 2.2 and 3.3 ns can be correctly resolved. Also, a synthetic fourth component can be added to three tyrosine decays and all four components correctly resolved. (Supported by NIH Grant GM 25663)

M-PM-B11 ANALYSIS OF FLUORESCENCE DECAY KINETICS FROM VARIABLE-FREQUENCY PHASE SHIFT AND MODULATION DATA by Joseph R. Lakowicz, Enrico Gratton, Gabor Laczko, Henryk Cherek and Mark Linkeman, University of Maryland School of Medicine, Department of Biological Chemistry, Baltimore, Maryland 21201 and University of Illinois, Department of Physics, Urbana, Illinois 61801.

It has recently become possible to measure fluorescence phase shift and modulation data over a wide range of modulation frequencies. Fluorescence phase shift and modulation data were obtained for one, two and three-component mixtures of fluorophores at modulation frequencies ranging from 1 to 140 MHz. These data were analyzed using a least-squares procedure to determine the values of the lifetimes and fractional intensities for a mixture of exponentially decaying fluorophores. Using the data obtained at a single emission bandpass, the lifetimes and pre-exponential factors of two-component mixtures were easily and reliably resolved if the lifetimes differed by a factor of two. With currently available instrumental stability, and single emission-bandpass data, three-component mixtures could just be resolved if the overall range of decay times was ten-fold, (1.3, 4.4 and 12 nsec). Measurement of phase and modulation data at several emission wavelengths where the ratio of the pre-exponential factors varied considerably enhanced our ability to resolve closely spaced two and three-component decays. Two-component mixtures could be resolved if the lifetimes differed by 30% (4.4 and 6.2 nsec). Also, the multiple-wavelength data allowed resolution of the lifetimes and fractional intensities of a three-component mixture. These results demonstrate that use of an appropriate range of modulation frequencies allows resolution of multi-exponential decay laws using a variable-frequency phase fluorometer with speed and precision.

M-PM-C1 PHOTOREMOVAL OF NIFEDIPINE REVEALS THE LIKELY MECHANISM OF ACTION OF THIS Ca⁺⁺ ANTAGONIST. A.M. Gurney, J.M. Nerbonne & H.A. Lester. Biology Div., Caltech, Pasadena, CA 91125

"Calcium antagonists" are thought to act via channel blockade, although several questions remain about the mechanisms by which they inhibit Ca⁺⁺ influx in cardiac and smooth muscle. Nifedipine, a potent and widely used calcium antagonist, contains an o-nitrobenzyl moiety and is photolabile; the reactions leading to photoconversion are complete in $< 100 \mu s$ and irradiation destroys the molecule's activity. In whole-cell recordings from cultured, ventricular myocytes from neonatal rat heart, nifedipine reduces the amplitude of the Ca⁺⁺ current, $ID_{50} \approx 0.5 \mu M$, and this effect can be reversed by light flashes of 1 ms duration produced by a xenon flashlamp. Blockade is independent of membrane potential and nifedipine does not display "use-dependence". In the presence of $0.5 \mu M$ nifedipine, with 140 mM Cs⁺ in the recording pipette to block outward currents, and either Ca⁺⁺ (5-10 mM) or Ba⁺⁺ (10 mM) as the current carrier, flashes increased the amplitude of the current (1.5 - 2 fold) within a few msec. The time to peak equals (to within 10%) the normal time of activation of the current (6-7 ms in Ba⁺⁺ and 2-3 ms in Ca⁺⁺, 23°C) and shows similar voltage-dependence. Membrane repolarization is not necessary for removal of the nifedipine induced suppression of the Ca⁺⁺ current. These results imply that nifedipine binds mainly to the closed, resting state of the channel. If 140 mM Cs⁺ is replaced with K⁺ in the pipette and Ca⁺⁺ is present in the bath, flashes in the presence of nifedipine not only increase the amplitude of the current, but also accelerate its rate of decay. As this effect is not observed when Ba⁺⁺ carries the current it is likely due to an increased Ca⁺⁺-dependent K⁺ current. Support: GM-29836, Del E. Webb Foundation, Fulbright-Hays travel grant.

M-PM-C2 PHOTO-INACTIVATION OF Ca²⁺ ANTAGONISTS IN FROG AND MAMMALIAN HEART: VOLTAGE-DEPENDENCE OF Ca²⁺ CHANNEL UNBLOCKING. M.Morad, T.Allen & Y.E.Goldman, Dept. of Physiol., Univ. of Penna., Phila., PA and M.D.I.B.L., Salsbury Cove, ME.

We have shown that in frog heart rapid photo-inactivation of dihydropyridine Ca²⁺-antagonists causes recovery of the slow inward current (I_{Si}) and developed tension if the light pulse is applied during diastole (Nature 304:635-638, 1983). Comparative experiments in cat ventricular muscle showed that I_{Si} recovered fully on the first depolarizing pulse following the flash, but in contrast to frog heart, 5-8 beats were required for complete recovery of suppressed tension. These results suggest that in mammalian heart replenishment of internal Ca²⁺ pools is required before tension is fully recovered. In order to analyze the voltage dependence of Ca²⁺ channel unblocking, frog ventricular strips were voltage clamped using a single sucrose gap voltage clamp technique. In strips treated with nifedipine, if a 100 μsec pulse of 300-400 nm light was applied during the action potential or a depolarizing clamp, little recovery occurred during that depolarization. However, recovery of tension and I_{Si} was complete on the subsequent depolarization. Voltage-dependence of unblocking was measured by applying two depolarizing pulses to zero mV separated by a 300 msec holding interval at various potentials (V_h). The light pulse was applied 50 msec into the first depolarizing pulse. Recovery of tension and Ca²⁺-current during the second depolarizing pulse depended on V_h . At V_h positive to -20 mV no recovery occurred, but as V_h became more negative than -20 mV, tension and I_{Si} partially recovered. At potentials negative to -40 mV recovery was complete. These findings suggest that membrane repolarization is required for the photo-inactivated drug to release its block of the Ca²⁺-channel.

M-PM-C3 PARALLEL CHANGES OF Ca CURRENT AND IMMUNOGLOBULIN SECRETION DURING THE TISSUE CULTURE CYCLE IN HYBRIDOMAS SECRETING IMMUNOGLOBULIN. Y. Fukushima and S. Hagiwara, Department of Physiology, Jerry Lewis Neuromuscular Research Center, UCLA School of Medicine, Los Angeles, CA 90024.

Multiple myeloma is a neoplastic disease of B lymphocytes. Most myeloma cell lines secrete monoclonal antibodies in the same manner as clonally expanded normal B lymphocytes. A particular myeloma cell line, S194, synthesizes IgA but does not secrete immunoglobulin. By using the whole cell variation of the patch electrode voltage clamp technique, we have shown a Ca current in the membrane of this cell line. During this previous study we were impressed by a large variation of the maximum observable Ca current between individual cells. From the majority of cells only a vestige of Ca current could be recorded.

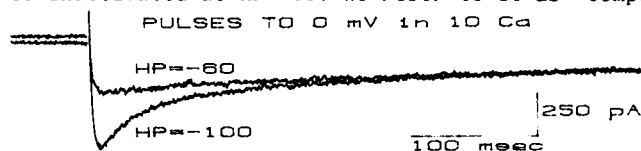
We have now studied two cell lines made by hybridization of S194 myeloma and splenic B lymphocytes. The resulting hybridoma cell lines secrete IgG and IgM. In these cells we found significantly larger Ca current than in S194 myeloma cells. We measured the Ca current and the immunoglobulin secretion as the cells grew in culture after renewing the culture medium. We observed that the Ca channel density and the immunoglobulin secretion per cell per unit time showed parallel changes during the tissue culture cycle. The Ca channel blocker D600 suppressed the immunoglobulin secretion at the concentration which blocked the Ca channel. We tentatively suggest that Ca influx through the Ca channel is required during immunoglobulin forming and/or secreting processes.

M-PM-C4 DECAY OF TWO Ca-DEPENDENT PROCESSES IN VOLTAGE-CLAMPED *APLYSIA* NEURONS. J.W. Deitmer and R. Eckert. Department of Biology, UCLA, Los Angeles, CA 90024.

Following Ca²⁺ influx during membrane depolarization, transiently elevated free Ca²⁺ at the inner face of the membrane undergoes a decline toward its resting value. To examine this process, the time course of the Ca-dependent K tail current ($I_{K(Ca)}$ tail) and the time course of removal of Ca-dependent inactivation of calcium current were determined at 13°C in neurones L-3 and L-6 of *A. californica* following depolarizing voltage-clamp pulses from $V_h = -40$ mV. Measurements of the $I_{K(Ca)}$ tail began 300 ms after repolarization to avoid the rapidly decaying voltage-dependent tail currents. The $I_{K(Ca)}$ tail approximated a bi-exponential time course; following a 100ms pulse to 0 mV, τ_1 and τ_2 typically were 0.7 s and 17 s, respectively. Removal of inactivation of the Ca current, determined under similar conditions by the paired pulse method, also roughly approximated a bi-exponential in which τ_1 and τ_2 typically were 1 s and 10 s. However, the τ_2 component of removal of inactivation had a much larger relative amplitude than did the τ_2 of the $I_{K(Ca)}$ tail. Thus, removal of Ca-dependent inactivation proceeds significantly more slowly than the decay of $I_{K(Ca)}$. The $I_{K(Ca)}$ tail and the removal of Ca inactivation both became somewhat slower if the amplitude and/or duration of the prepulse (and hence Ca²⁺ influx) were increased. Injection of EGTA virtually eliminated all trace of the $I_{K(Ca)}$ tail. The EGTA clearly was less effective, however, in fully blocking Ca inactivation, but it significantly increased the rate of removal of inactivation. Possible reasons for the differences in relaxation kinetics and sensitivity to injected EGTA exhibited by these two Ca-dependent processes will be discussed. Supported by USPHS NS 8364, NSF BNS 80-12346, BNS 82-03843, and a Max Kade Foundation Fellowship to J.W.D.

M-PM-C5 TWO COMPONENTS OF CALCIUM CHANNEL CURRENT IN CHICK DORSAL ROOT GANGLION CELLS. Martha C. Nowicky, Aaron P. Fox and Richard W. Tsien, Departments of Neuroanatomy and Physiology, Yale University School of Medicine, New Haven, CT 06510.

Membrane currents were recorded from chick dorsal root ganglion cells in culture with gigaseal pipettes in the whole cell voltage clamp mode. To suppress Na and K channel currents, the pipette contained 120 mM CsCl, 10 mM EGTA, 2 mM MgCl₂, and 5 mM HEPES, and the external solution included TEA in place of Na as well as 200 nM TTX. Under these conditions, depolarizations from a holding potential (HP) of -60 mV elicited clear inward calcium currents. With 10 mM Ca outside, the inward current reached a maximum of 1-5 nA at +10 to +20 mV, corresponding to a current density of ~200 pA/pF. Little or no decay of the inward current was seen during long depolarizations (>500 msec) from a holding potential (HP) of -60 mV. However, at HP=-100 mV or more negative, the inward current was larger and showed a more obvious phase of decay (see fig.) The decay ($t_{1/2} \sim 45$ msec) was unaffected by replacing external Ca with Ba. Substantial inward current remained after the early phase of decay was complete: currents evoked by depolarizations from the different HPs never crossed. We attribute the extra current evoked from -100 mV to a component of calcium current which is inactivated at HP=-60. We refer to it as "component I" because it activates at more negative



potentials and inactivates faster than the component which remains with HP=-60 mV ("component II"). Both components were totally abolished by 100 μ M Cd. Supported by grants from NINCDS, NHLBI, and the Canadian Heart Foundation.

M-PM-C6 EVIDENCE FOR TWO TYPES OF Ca CHANNELS IN GH3 CELLS. Donald R. Matteson and Clay M. Armstrong. Department of Physiology, University of Pennsylvania, Philadelphia, Pa. 19104.

In the literature there are indications for more than one type of Ca channel. We present evidence here that GH3 cells may have two distinct types of Ca channels. Cells were voltage clamped using the whole cell variation of patch clamp technique. Na currents were blocked with TTX and K currents were eliminated by filling electrodes with Cs. Ca channel current could be carried by Ca, Ba or Sr. With Ba as charge carrier, the channels have both fast (~150 μ s) and slow (~1.5 ms) components of deactivation following a 5 ms pulse to +20 mV. As pulse duration increases from 5 to 100 ms the slow component disappears, the fast component remains unchanged or increases in size, and the channels inactivate little if at all. The activation threshold for the slow component is more negative than for the fast. In the presence of Ca, most cells exhibit only the slow tail following a 5 ms pulse to +20 mV. The tail disappears as the length of the pulse is increased, indicating that the channels inactivate. Some cells in Ca also show the fast deactivation phase following depolarization to +20 mV or more. Switching the external solution from 25 mM Ba to 20 mM Ba + 5 mM Ca decreased current during the pulse by about 50%, reduced the fast tail and left the slow tail unchanged. Thus the current eliminated by addition of Ca had fast deactivation kinetics and did not inactivate.

These results are consistent with the existence of two types of Ca channels in GH3 cells. The first type has a low activation threshold, slow deactivation kinetics, and they inactivate. The second type has a higher threshold, fast deactivation kinetics, and they do not appear to inactivate.

M-PM-C7 INACTIVATION AS A MECHANISM FOR Ca CURRENT DECAY IN INTACT SKELETAL MUSCLE FIBERS OF THE FROG. E. Stefani and G. Cota. Department of Physiology and Biophysics, Centro de Investigación del IPN, Apartado Postal 14-740, México, D.F. 07000, MEXICO.

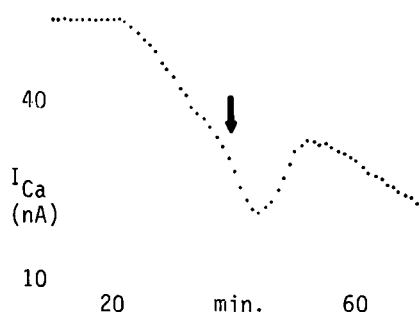
The three microelectrode voltage clamp technique near the fiber end was used on cutaneous pectoris muscle fibers of *Rana moctezuma*. Ca currents (I_{Ca}) were recorded after blocking K currents in I_{Ca} recording solution at 23°C (mM/l): TEA-CH₃SO₃ 120, Ca(CH₃SO₃)₂ 10 and sucrose 350. Two pulse inactivation experiments were performed with prepulse durations of 2 sec, an interval of 0.5 sec and a test pulse of 1 sec to 0 mV. The holding potential was -100 mV. I_{Ca} during the test pulse was reduced to 0.57 of the control I_{Ca} with a prepulse to 0 mV. This prepulse elicited near maximal I_{Ca} . Larger prepulses approaching the Ca equilibrium potential and eliciting smaller I_{Ca} did not remove inactivation. For example, a prepulse to +50 mV which produced less than 10% of the maximal time integral of I_{Ca} , inactivated to 0.62 the I_{Ca} during the test pulse. This confirms that Ca entry is not a requirement to produce inactivation. In other experiments we recorded I_{Ca} in a Ca buffer system (mM/l): Ca-maleate 123; (TEA)₂-maleate 15 and 3,4-diaminopyridine 1. The time constant of decay (τ_d) of I_{Ca} practically remained unchanged in this solution. For example, at -5 mV, $\tau_d=0.99\pm.14$ sec (4). In I_{Ca} recording solution, $\tau_d=1.33\pm0.12$ sec (5) at -20 mV and $\tau_d=0.90\pm0.08$ sec (1) at 0 mV. This observation confirms that the decay of I_{Ca} cannot be explained by Ca depletion in the tubular system in intact fibers in hypertonic solution.

This work was supported by CONACyT (México), grant PCCBNAL-790022.

M-PM-C8 TEMPORARY REVERSAL OF CALCIUM CURRENT WASHOUT IN INTERNALLY PERFUSED SNAIL NEURONS.

Bruce Yazejian and Lou Byerly, Dept. of Biol. Sci., USC, Los Angeles, CA.

It has been shown previously that in internally perfused neurons of the snail *Lymnaea stagnalis*, the Ca current is unstable and washes out with time. The time course of the washout is sigmoidal with the current falling to half of its initial value after 30-40 min. of perfusion. We report here a temporary reversal of the washout with internal perfusion of an enriched solution containing 2 mM ATP and 3 mM Mg²⁺. Our results differ from those of Doroshenko et al. (Neuroscience 7:2125, 1982) in that we find the inclusion of cAMP in the enriched solution is not necessary for the reversal.



Our procedure diverges from theirs by the buffering of both internal calcium (with 5 mM EGTA) and pH (with 100 mM HEPES). Perfusion with the enriched solution never causes the Ca current to rise to a value greater than the initial value measured in unenriched solution. The rate of washout after the temporary reversal is slower than that before the addition of the enriched solution. This suggests that ATP is involved in the stabilization of the Ca current. Currently we are investigating the mechanism through which ATP is acting. Perfusion with an internal solution enriched only with theophylline (up to 10 mM) has no effect on the washout. Supported by NS 15341.

M-PM-C9 CAN SARCOLEMMAL BOUND Ca BE IMPORTANT IN THE REGULATION OF Ca INFLUX VIA Ca CHANNELS? Donald M. Bers and Arthur Peskoff. Division of Biomedical Sciences, University of California, Riverside, CA 92521 and Departments of Biomathematics and Physiology, UCLA, Los Angeles, CA 90024.

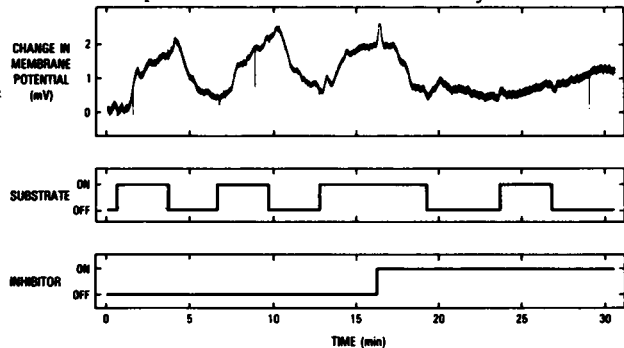
Striking correlations have been previously reported (Bers et al., Am. J. Physiol., 240:H576-H583, 1981) between the amount of Ca bound to the external surface of cardiac sarcolemma (SL) and the contractility of various cardiac muscle preparations under a variety of experimental conditions. It was suggested that SL bound Ca might be directly related to Ca influx and thence to tension development (either directly or via control of SR Ca release). If SL bound Ca plays a role in regulating Ca influx, what might the physical basis for this regulation be? Let us first consider a hemisphere of given radius from the external opening of the Ca channel. From Ca binding experiments we can estimate the amounts of Ca bound to the SL and in solution in this hemisphere. The ratio of SL bound Ca to Ca in solution is inversely proportional to the radius of the hemisphere. For example, at 2 mM Ca, 90% of the Ca within 40 nm of the channel (~ 200 x channel radius) would be SL bound (or 50% at 350 nm). This is exclusive of other Ca binding sites which may exist in the glycocalyx in this region and also does not include the surface cation concentrating effect of fixed negative charges on the SL surface in the diffuse double layer. If one assumes a single channel current of 1 pA, the diffusion equation predicts that the [Ca] near the channel opening would decrease significantly. The [Ca] in these regions should also be the most highly buffered by SL bound Ca. This bound Ca may thus "feed" the channel and provide a mechanism explaining correlations which exist between SL Ca binding, Ca influx and tension development. While the qualitative conclusion is intuitively clear, evaluation of the quantitative contribution of SL bound Ca to Ca current must simultaneously incorporate: 1) diffusion effects, 2) surface charge effects, 3) Ca binding characteristics, and 4) changes in local electrical fields.

M-PM-D1 FUNCTIONAL CHANNELS EXTRACTED FROM THE SQUID GIANT AXON PREPARATION. R. M. Torres, R. Coronado, and F. Bezanilla, Dept. of Physiology, UCLA, Los Angeles, CA 90024 and Dept. of Pharmacology, Univ. of North Carolina, Chapel Hill, NC 27513.

We have used the technique of bilayer formation on the tip of a patch pipette (Coronado and Latorre, *Biophys. J.* 43:231,1983) to assay the presence of functional channels extracted from the squid giant axon preparation. Two methods for extraction were used. In the first method, the two giant axons from a single squid were carefully dissected and cleaned of all adjacent fibers and connective tissue. The axoplasm was removed and discarded by rolling it out or by cutting the axon open. Following homogenization, sonication and centrifugation, the supernatant was added to the bath so that vesicle fusion could occur with the bilayer formed at the tip of the pipette. In the second method, the axon was dissected as before, cut open and the axoplasm removed. This cut-open axon was dipped repeatedly in a bath with a monolayer on its surface. Finally, a bilayer was formed on the tip of the pipette from this monolayer. Fire polished pipettes had aperture diameters of less than 2 μm . The experiments were performed at 16°C using 50% PE and 50% PS as lipids. We observed unitary events of different magnitudes which were cation selective. Among them, two types of events are clearly identified. The first type of channel shows a $P_K/P_{Na} \approx 4$, has very little or no voltage dependence and a conductance of about 50 pS in 270 mM K. This channel may be responsible for the resting conductance of the squid axon (leakage). The second type of channel shows a $P_K/P_{Na} \approx 40$, is voltage dependent and has a conductance of about 18 pS in 270 mM K. This channel shows bursting activity and has the properties of the K channel of the squid axon. (Supported by USPHS grant GM30376.)

M-PM-D2 TRANSDUCTION OF REDOX ENERGY INTO TRANSMEMBRANE VOLTAGE BY CYTOCHROME C OXIDASE FROM THE THERMOPHILIC BACTERIUM PS3 RECONSTITUTED INTO PLANAR LIPID BILAYERS. T. Hamamoto and M. Montal, Depts. of Biology and Physics, University of California at San Diego, La Jolla, CA 92093

Cytochrome c oxidase (cytox) generates a proton electrochemical potential gradient across membranes. The nature and number of charges translocated per mole of substrate oxidized is controversial and could be solved by direct measurements of membrane potential (ΔV) [1]. Here, the purified 3-subunit cytox from the thermophilic bacterium PS3 (from N. Sone [2]) was reconstituted into planar lipid bilayers formed at the tip of patch pipets [3] and the open circuit ΔV was directly measured. Bilayers were continuously perfused with buffer (0.2M KCl, 10mM CaCl₂, 10mM Tricine, pH 7.2), substrate (50 μM phenazine methosulfate + 2.5mM ascorbate) and inhibitor (1mM KCN) according to the pulse sequence shown in the figure. Perfusion with substrate generated a ΔV ($\sim 2\text{mV}$, positive in the substrate side) that was inhibited by cyanide. These results demonstrate the direct transduction of redox energy into ΔV and validate this approach to characterize the ΔV generated by cytox. [1] Montal, in *Perspec. in Membr. Biol.* (1974) 591, Acad. Press. [2] Sone & Hinkle, *JBC*, 257(1982) 12600. [3] Suarez-Isla, et al. *Biochem.* 22(1983) 2319. Supported by NIH, DAMR and JSPS.



M-PM-D3 INCORPORATION OF Ca^{2+} -ACTIVATED K^+ CHANNELS FROM RABBIT INTESTINAL SMOOTH MUSCLE SARCOLEMMMA, INTO PLANAR BILAYERS. X. Cecchi, D. Wolff, O. Alvarez and R. Latorre. Departamento de Biología, Facultad de Ciencias Básicas y Farmacéuticas, Universidad de Chile, Santiago.

Interaction of vesicles from rabbit intestinal smooth muscle sarcolemma with planar lipid bilayers (Phosphatidylethanolamine: Phosphatidylserine - 7:3) promotes the incorporation of K^+ selective channels. The conductance of these channels fluctuate between two states: closed \longleftrightarrow open, and the fraction of time that the channels remain in the open state, ($f(V)$), is dependent on the electrical potential difference across the bilayer and the Ca^{2+} concentration in the solution. When the Ca^{2+} concentration is 1mM, $f(V)$ is 0.5 at -60mV (Voltage was applied to the cis aqueous solution; the opposite trans side was defined as ground.) At a Ca^{2+} concentration of 2 μM , the $f(V)$ value of 0.5 is obtained at +60mV. In symmetrical solutions of 100mM KCl 5mM MOPS-K (pH 7.0) the unitary conductance is 292 pS. The addition of TEA to the trans side produces a voltage-independent decrease of the conductance. On the other hand trans Cs^+ , produces a voltage-dependent inhibition of the conductance. Recently, a channel of similar characteristics has been described in isolated smooth muscle cells from frog stomach. This findings suggest that this kind of channels are common to smooths muscle cells. Supported by University of Chile Grant B-1224-8333 and NIH Grant GM-28992

M-PM-D4 INTERACTION OF DIFFERENT CHEMICAL FORMS OF ALAMETHICIN IN LIPID BILAYERS. James E. Hall, Igor Vodyanoy, T.M. Balasubramanian⁺ and Garland R. Marshall⁺ (Univ. of Calif., Irvine, CA 92717 and ⁺ Washington University, St. Louis, MO 63110)

Three different alamethicin analogues have been prepared which alone produce current voltage (I-V) curves having very different symmetries about the origin. If peptide is added to one side of the membrane (the *cis* side), F4 conductance turns on when the voltage on the *cis* side is positive, Boc 2-20 produces a perfectly symmetrical I-V curve, and BG 1 turns on when the voltage is negative. These analogues also influence each other. If Boc 2-20 is initially added to one side of the membrane, it produces a symmetric I-V curve which can be used as a reference for the effects of the other analogues. F4 added to the *cis* side shifts the positive branch of the Boc 2-20 I-V curve to lower voltage. F4 added to the *trans* side shifts the negative branch of the I-V curve to lower voltage. The opposite is true. Further BG 1 and F4 interact only when added to opposite sides of the membrane. When added to the same side, they give a conductance which is just the sum of what each would give in the absence of the other.

These results imply that the c-termini of the monomers forming the hybrid open channels must be on the same side of the membrane for successful interaction.

M-PM-D5 FLUCTUATIONS OF ENERGY PROFILES IN ONE-PARTICLE CHANNELS INDUCE COUPLING BETWEEN FLUXES OF DIFFERENT PERMEANT SPECIES. S. Ciani. Dept. of Physiology, UCLA, Los Angeles, Calif. 90024.

Models for permeation through channels, extended to allow for transitions of the pore between states with different energy profiles, have been shown to predict features generally considered indicative of multi-ion occupancy: e.g. maxima for the conductance dependence on ion concentration (Läuger, Stephan and Frehland, BBA, 602 (1980) 167-180). For a simple one-site, two-barrier pore, fluctuating between two states, "normal" and "polarized", characterized by different energy peaks, we have shown that in the mixture of two species, A and B (either both charged, or both neutral, or one charged and one neutral), the flux of each is coupled to the driving force of the other via cross coefficients, L_{AB} and L_{BA} , which can be given as functions of the concentrations, C_A and C_B , of the membrane potential and of the various rate constants, and which become equal when the driving forces are sufficiently small that the flux equations can be linearized. A requirement for coupling is that the peaks of the two barriers, as sensed by both species, shift unequally in the transition between the two states, so that the difference between their values in the "normal" state be different from that in the "polarized" one. Coupling can be positive or negative, depending on whether the relative shifts of the two peaks for the two species are in the opposite or in the same direction, and the value of the cross coefficients, as functions of both C_A and C_B , increases, reaches a maximum and vanishes at high concentrations.

This model for transport in a single-particle channel provides a very simple mechanism whereby the flux of a neutral permeant species can be driven by the electro-chemical potential gradient of an ion. (Supported by a grant from MDA).

M-PM-D6 HYDROSTATIC PRESSURE EFFECTS ON TRANSPORT OF CARRIER-CATION COMPLEXES AND OF HYDROPHOBIC ANIONS. B. E. Aldridge and L. J. Bruner, Department of Physics, University of California, Riverside, CA 92521.

Bilayer membranes formed from diphytanoyl phosphatidylcholine/decane solutions were studied at hydrostatic pressures to 100 MPa ($\sim 1,000$ atm). Carrier-mediated conductance of K^+ ions by both valinomycin and nonactin decreased by about a factor of three as pressure was increased from ambient to 100 MPa. Since the viscosity of bulk alkane liquids increases by a comparable factor over this pressure range, application of the Stokes-Einstein relation suggests that the barrier to transport in these cases is equivalent to that provided by a fluid film having the hydrodynamic properties of a bulk liquid hydrocarbon.

The kinetic parameters characterizing transient conductance observed at low concentrations ($\sim 10^{-7}M$) of the hydrophobic anions, dipicrylamine and tetraphenylborate, on the other hand, are essentially independent of pressure over the same range. These observations suggest that either, a) the microenvironment of the translocating anion is more water-like than hydrocarbon-like, or b) transport is non-diffusive, being accomplished by a single thermally activated transition over a barrier having its origin in electrostatic or chemical bonding forces. Additional observations on pressure dependent conductance at higher concentration ($10^{-5} - 10^{-4}M$) of hydrophobic anions will be discussed.

Supported by NSF grant PCM-7926672.

M-PM-D7 THE POLARITY OF CARBOXYLIC IONOPHORES AND THEIR COMPLEXES.

B. C. PRESSMAN, DEPT. OF PHARMACOLOGY, U. OF MIAMI MEDICAL SCHOOL, MIAMI, FL 33101.

HPLC chromatography on a C18 reversed phase column has been exploited for evaluating the polarity of cation complexes of carboxylic ionophores. The eluant was 80% acetonitrile containing: (1) 0.02% HAC; (2) tetramethylammonium diethylmalonate buffer, pH 7.2; (3) diethylmalonate + CF_3SO_3^- salts of the test cations (Li^+ , Na^+ , K^+ , Rb^+ , Cs^+). Ionophores tested (100 g each) include lasalocid, monensin, nigericin, salinomycin, etc. Virtually all ionophore samples examined contained several components, only some of which were active as ionophores as ascertained by two phase binding tests with ^{22}Na or ^{86}Rb . Most ionophores, when ion paired with tetramethylammonium, showed extremely short retention times (R_t) < 5 min [flow 2 ml/min], often < 1 min) reflecting high polarity indicative of an open ionophore conformation preferring polar solvents and membrane interfaces. Protonated and inclusion-complexed ionophore species have longer R_t 's (5-30 min) indicative of conformations with polar groups focused inward, which can traverse the low polarity membrane interior. In general, R_t 's are proportional to the tightness of complexation, i. e. how well the polar groups are enclosed. For monensin (Na^+ selective) K^+ complex $R_t = 5.5$ min; Na^+ complex, $R_t = 6.3$. For nigericin (K^+ selective) K^+ complex $R_t = 12.0$ vs 2.7 for the Na^+ complex. C5-ring-substituted lasalocids provide a simple lyotropic series. For the protonated lasalocids, the following R_t 's were observed for the various C5 substituents: H, 6.2; Cl, 7.2; Br, 7.7; I, 8.2. Thus each species of each ionophore has a unique polarity, a function of cation species complexed and the intrinsic atomic constituents. Each ionophore sample has multiple components which must be resolved for determination of definitive physical and biological properties of each structure depicted in the literature. Supported by NIH Grant HL-23932.

M-PM-D8 EFFECT OF Ca^{+2} -ANTAGONISTS ON THE Ca^{+2} UPTAKE ASSOCIATED WITH THE ACROSOME REACTION OF SEA URCHIN SPERM. J. García-Soto and A. Darszon. Dept. of Biochem., CINVESTAV-IPN, México City.

In most animal species the sperm must first undergo the acrosome reaction—an exocytotic event—in order to fertilize the egg. The acrosome reaction in sea urchin sperm is induced by a jelly coat surrounding the egg and requires Ca^{+2} and Na^+ in the sea water, at pH 8. This induction is accompanied by Ca^{+2} and Na^+ influx as well as K^+ and H^+ efflux. The mechanism involved in these ionic movements is unknown. The Ca^{+2} -channel blocker D600 inhibits both acrosome reaction and Ca^{+2} uptake. At pH 9 in sea water the acrosome reaction is triggered without jelly. By substituting Na^+ for choline in the medium, we found that the triggering by high pH does not require extracellular Na^+ . That the acrosome reaction occurs at pH 9, with or without Na^+ , correlates with an increase in Ca^{+2} uptake which is comparable to that induced by jelly. The acrosome reaction and Ca^{+2} uptake triggered at high pH are also inhibited by D600. These results suggest that the Ca^{+2} uptake associated with the jelly-induced acrosome reaction does not depend directly on the Na^+ influx. Since Ca^{+2} uptake induced either with jelly or high pH shows sensitivity to D600, it is suggested that the same transport system operates at both triggering conditions. According to the effect of D600, it is proposed that ionic channels are involved in the Ca^{+2} transport associated with the acrosome reaction. This proposal is supported by our finding that the acrosome reaction and Ca^{+2} uptake are inhibited by nisoldipine, a highly specific blocker of Ca^{+2} channels in excitable cells.

M-PM-D9 DEDUCTIONS ABOUT THE ELASTIC ENERGY STORAGE MECHANISM OF ERYTHROCYTE MEMBRANE SKELETON FROM THE DEPENDENCE OF THE MEMBRANE ELASTIC MODULUS ON TEMPERATURE HISTORY. Richard E. Waugh, University of Rochester Medical Center, Rochester, NY 14642.

The effect of temperature history on the elastic shear modulus of red blood cell membrane has been examined. The experiments were undertaken to determine if the observed increase in surface elastic shear modulus with decreasing temperature could be due to an increase in the number of spectrin tetramers in the membrane skeleton. Ungewickell and Gratzer (Eur. J. Biochem. 88:379, 1978) have shown that the ratio of spectrin tetramers to dimers is highly temperature-dependent, and that the interconversion occurs very slowly at low temperatures. Therefore, by quenching cells incubated at high temperature the tetramer-dimer ratio at the incubation temperature can be "captured" and preserved at the low temperature. Cells were preincubated at temperatures ranging from 30°C to 42°C, then quenched to 0°C and the surface elastic shear modulus was measured by micropipette aspiration at 5.0°C. If the change in the number of tetramers on the membrane makes a significant contribution to the change in the membrane shear modulus, there should be a difference in the moduli measured at 5°C depending on the temperature at which the cells were incubated prior to quenching. No such differences were found, indicating that the decrease in shear modulus with increasing temperature is not due to a decrease in the number of spectrin tetramers on the membrane. These results support the assumptions of a previous thermodynamic analysis (Waugh and Evans, Biophys. J. 26:115, 1979), which indicates that the elastic energy storage mechanism of the red cell membrane skeleton is predominantly enthalpic in nature and that the entropy of the membrane skeleton increases with deformation. (Supported by NIH grants No. HL 26485 and HL 18208.)

M-PM-D10 SPONTANEOUS FORMATION OF STABLE UNILAMELLAR VESICLES.

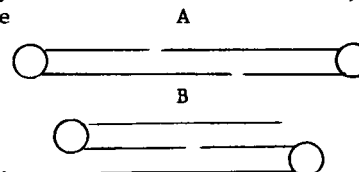
N.E. Gabriel and M.F. Roberts, Massachusetts Institute of Technology, Cambridge, MA 02139.

Stable unilamellar vesicles spontaneously form by mixing long-chain lecithins with small amounts of micellar short-chain lecithins. Dipalmitoyl-PC (20 mM) and diheptanoyl-PC (5 mM) form vesicles of about 800 Å in aqueous solution. Examination of the 500 MHz ^1H NMR spectrum of these aggregates shows two $\text{N}(\text{CH}_3)_3$ peaks visible without added lanthanide ions. Rather than reflecting inside/outside lecithin molecules, these peaks are attributed to diheptanoyl-PC and the separate dipalmitoyl-PC molecules. With the addition of Pr^{+3} to the exterior buffer, three $\text{N}(\text{CH}_3)_3$ resonances are observed: two relatively invariant peaks (a narrow one from diheptanoyl-PC, a broad one from dipalmitoyl-PC on the interior layer) and a downfield shifted component (due to the exterior monolayer of dipalmitoyl-PC and any diheptanoyl-PC). If Pr^{+3} is encapsulated in the vesicles and EDTA added to the exterior, then virtually all of the sharp diheptanoyl-PC signal shifts downfield. Thus, most of the short-chain species is on the inner monolayer.

Stability studies have been conducted by encapsulating the fluorescent dye 6-carboxyfluorescein inside the vesicles. These vesicles are relatively stable (i.e., little change in fluorescence intensity) over the temperature range 25 to 55°C and for several days; addition of Triton X-100 dramatically increases the fluorescence by disrupting the vesicles. These easily formed unilamellar vesicles may be useful for liposome-based drug delivery.

M-PM-D11 A NEW STRUCTURAL MODEL FOR MIXED CHAIN LECITHINS. T. J. McIntosh, S. A. Simon, J. C. Ellington, and N. A. Porter, Departments of Anatomy, Physiology and Chemistry, Duke University, Durham, NC 27710.

Multilamellar suspensions of mixed chain phosphatidylcholines have been studied extensively by calorimetry and Raman spectroscopy by Huang and colleagues (Biochem. 20: 6086 and Biochem. 22: 2775). They have found that the order in the gel state hydrocarbon chains is greatest when the difference in length of the two acyl chains is large, such as in $\text{C}_{18:10}$ PC. They have proposed the packing model shown in A, which is consistent with the X-ray data of Tardieu et al. (J. Mol. Biol. 75: 711) obtained at 1% water content. However, we have found that the X-ray parameters are quite different at higher water contents (10% and above). For fully hydrated gel state $\text{C}_{18:10}$ PC we observe a single sharp wide-angle reflection at 4.11 Å, indicating that the hydrocarbon chains are more tightly packed than in normal gel state PC bilayers and that there is no chain tilt. The calculated lipid thickness is only 36 Å, compared to the predicted value of about 45 Å for model A, and the area/molecule is 3 times the area/hydrocarbon chain. Moreover, the lipid thickness increases upon melting to the liquid crystalline state (where the thickness and area/molecule are similar to other liquid-crystalline PC's). These data are inconsistent with the packing arrangement shown in A, and we propose that in hydrated gel state $\text{C}_{18:10}$ PC the chains are packed as in model B. This model is consistent with all spectroscopic and X-ray data, and is novel in that there are 3 chains per head group at the lipid-water interface.

**M-PM-D12 CONCENTRATION OF CHOLESTEROL IN LIPOSOMAL MEMBRANES: MAINTENANCE AND RELATIONSHIP TO ENCAPSULATION OF MARKER.** Stanley R. Bouma, David M. Finley, and P. Ashok Aiyappa. Diagnostics Division, Abbott Laboratories, North Chicago, IL 60064.

Large multilamellar vesicles containing the water-soluble dye calcein (bis[N,N-bis-(carboxymethyl)aminomethyl] fluorescein) were prepared by hydrating thin films of sphingomyelin and cholesterol. The molar proportions of cholesterol to sphingomyelin prior to hydration ranged from 1:4 to 4:1.

In most cases, these proportions were maintained in the liposomal membranes after hydration, whether liposomes were prepared at room temperature or at or above 45°C. An exception was liposomes prepared at room temperature from films of cholesterol:sphingomyelin in the ratio of 4:1 -- these liposomes contained a reduced proportion of cholesterol.

The proportions of cholesterol:sphingomyelin present in the hydrated liposomal membrane were maintained after one week, during which time the liposomes experienced six excursions of slow temperature change (4° to 50° to 4°, at about 4 min/°C).

Encapsulation of calcein was maximal in liposomes containing at least 50% cholesterol. Although encapsulation decreased after each excursion of temperature change, the rate of decrease was minimal for proportions of cholesterol:sphingomyelin approaching 50:50.

M-PM-E1 LOCALIZATION OF MONOCLONAL ANTIBODIES TO DICTYOSTELIUM MYOSIN AND EFFECTS OF THESE ANTIBODIES ON MYOSIN MOTILITY IN VITRO. P.F. Flicker, G. Peltz, P. Parham, M.P. Sheetz, J.A. Spudich, Dept. of Structural Biology, Stanford University School of Medicine, Stanford, CA 94305.

The locations of the binding sites of monoclonal antibodies specific for Dictyostelium myosin have been correlated with the effects of these antibodies on the rate of myosin movement in vitro. Antibodies bound to myosin molecules were visualized in the electron microscope using rotary shadowing. For each antibody, 30-50 examples were measured to determine the site of binding. Myosin movement was assayed by the method of Sheetz and Spudich (1983. *Nature* 303:31). As expected, antibodies that bind to the myosin head region inhibit myosin movement. One antibody binds to the heavy chain portion of the head region and inhibits the rate of movement by 50%, whereas an antibody specific for the 18,000 dalton light chain inhibits movement completely. In contrast, three antibodies which bind to various positions along the tail have no effect on the rate of myosin movement. The binding sites of these antibodies have been mapped to regions about 480, 700 and 1370Å from the head-tail junction (1850Å total length of tail). An additional feature of the antibody which binds 1370Å from the heads is that it inhibits myosin filament formation. Interestingly, three other independent monoclonal antibodies which also bind to the tail all inhibit myosin movement completely. Blocking experiments suggest that these antibodies bind to spatially related sites. Images of myosin molecules with bound antibody reveal that these sites are approximately 1200Å from the head-tail junction. These studies provide a preliminary map of regions of the myosin molecule important for motility. (NIH GM 25240 to JAS.)

M-PM-E2 ROLE OF THE C-TERMINAL REGION OF THE HEAVY CHAIN IN THE ACTIN-ACTIVATED ATPase ACTIVITY AND FILAMENT FORMATION OF ACANTHAMOEBA MYOSIN II. Jacek Kuznicki, Graham P. Cote and Edward D. Korn, NHLBI, NIH, Bethesda, MD 20205.

The actin-activated Mg^{2+} -ATPase activity of myosin II from Acanthamoeba is regulated by phosphorylation of 3 serine residues located at the end of the tail of the heavy chain. Only the dephosphorylated form of myosin II has high actin-activated ATPase activity. A 9,000 Da fragment containing all 3 phosphorylation sites is cleaved from the heavy chain by chymotrypsin. The light chains are undigested since they have unchanged mobility, in both SDS and urea PAGE. This chymotryptic-cleaved myosin was used to determine the role of the 9,000 Da segment of the tail of the heavy chains. The cleaved myosin retains complete Ca^{2+} -ATPase activity, however, its Mg^{2+} -ATPase activity is no longer activated by actin at pH 7.0 regardless of the Mg^{2+} concentration. Chymotryptic-cleaved myosin remains in the supernatant after centrifugation in the airfuge in the presence of 10 mM $MgCl_2$, although dephosphorylated and phosphorylated myosin II sediment under these conditions. The sedimentation coefficient of chymotryptic-cleaved myosin is about 6.5 S, slightly bigger than the monomer (4.8 S) but very much smaller than the values for the filaments formed by dephosphorylated (152 S) and phosphorylated (30 S) myosin under the same conditions. As measured in the analytical ultracentrifuge, chymotryptic-cleaved myosin does not copolymerize with dephosphorylated myosin. On the other hand, preparations of chymotryptic-cleaved myosin appear to aggregate as judged by light scattering. From the data, we conclude that the C-terminal 9,000 Da peptide of the myosin II heavy chain is required for actin-activated ATPase activity and possibly for formation of normal filaments.

M-PM-E3 ROLES OF CALCIUM AND NUCLEOTIDES IN REACTIVATED CONTRACTION OF LYSED CELL MODELS OF TELEOST RETINAL CONES. K. Porrello and B. Burnside. U. of California, Berkeley. (Intr. by Alan Bearden).

We have previously reported that dark-adapted retinas can be lysed with the detergent Brij-58 to obtain cone motile models which undergo Ca^{++} - and ATP-dependent reactivated contraction. Here we further dissect the roles of ATP and Ca^{++} 1) by characterizing the Ca^{++} and ATP requirements in more detail, 2) by analyzing the effects of ITP and the ATP analog ATPγS, and 3) by testing the effects of cAMP on reactivated cone contraction. Cone models contracted at rates proportional to the free Ca^{++} concentration between 3×10^{-8} and $10^{-6}M$. Reactivated contraction was inhibited by the calmodulin inhibitors trifluoperazine (10μM) and R24571 (10μM). Nucleotide requirements were similar to those of smooth muscle; i.e. when one nucleotide was supplied alone, contraction was highly specific for ATP. Not only ITP and ATPγS, but also GTP, CTP and AMPPNP failed to support reactivated contraction. However, if lysed cones were initially incubated with ATPγS and then subsequently incubated with ITP, cones contracted to an extent comparable to that observed with ATP. Since ATPγS can be used by kinases but not by myosin ATPase and ITP can be used by myosin ATPase but not by kinases, our results strongly suggest a role for myosin phosphorylation in Ca^{++} regulation of cone contraction. Also, as observed with skinned smooth muscle, adding cAMP to contraction medium strongly inhibits reactivated cone contraction. (Supported by NSF grant PCM 80-11972 and GM 32566).

M-PM-E4 CROSS-LINKING OF SMOOTH MUSCLE MYOSIN. S. Boström,¹ M. Ikebe² and D. J. Hartshorne,² ¹Hässel Research Labs., Mölndal, Sweden; ²Muscle Biology Grp., Univ. of Arizona, Tucson, AZ 85721

Two conformers of smooth muscle myosin have been identified and correspond to the folded (10S) and the extended (6S) forms. Each are distinguished by different enzymatic properties and the alteration of ATPase activities follows closely the conformational transition (Ikebe et al., *Biochemistry* 22:4580 (1983)). To investigate further the relationship between myosin conformation and enzymatic activity we have cross-linked dephosphorylated myosin in the 10S form. The conditions of cross-linking with dimethylsuberimide were as described by Trybus et al. (*Proc. Natl. Acad. Sci. USA* 79:6151 (1982)). The sedimentation pattern of the cross-linked myosin showed predominately a single component identical to the 10S species both at high (0.35M) and low (0.15M) KCl concentrations. The cross-linked myosin retained ATPase activity. Both the Ca^{2+} - and Mg^{2+} -ATPases showed only a slight effect of KCl, in contrast to very marked effects observed with native myosin. The increase in K^+ EDTA-ATPase with increasing KCl concentrations was linear and again was distinct from the pattern observed with native myosin. Actin-activated ATPase of dephosphorylated 10S cross-linked myosin was low (~ 1 nmole/min/mg myosin) and was increased only slightly on phosphorylation. However, the level of phosphorylation for the cross-linked species was less than that for native myosin and could explain the lack of actin-activation. Alternatively the low degree of actin activation, and also the other enzymatic activities that were altered, could be due to the "freezing" of myosin in the 10S conformation. The influence of coincident chemical modification remains to be established.

Work supported by grants HL 23615 & 20984, National Institutes of Health.

M-PM-E5 TRINITROPHENYLATION OF SMOOTH MUSCLE MYOSIN by S. Srivastava & D.J. Hartshorne, Muscle Biology Group, University of Arizona, Tucson, AZ 85721.

The reaction of 2,4,6-trinitrobenzene sulfonate (TNBS) with skeletal and cardiac muscle myosins has been well documented. In this report we present some observations on the reaction of TNBS with turkey gizzard myosin. The amount of "rapidly reactive lysine" was found to be between 1.4 and 1.6 moles per mole myosin. The second order rate constant for the reaction was $470 \text{ M}^{-1} \text{ S}^{-1}$. (The program for the curve fitting technique used to calculate this value was kindly supplied by Dr. J. Gergely.) This rate is in good agreement with the rate constant of inactivation of K^+ EDTA-ATPase activity of myosin upon trinitrophenylation. Unlike skeletal and cardiac myosins the level of Mg^{2+} - and Mg^{2+} -actin ATPase activities of myosin were unaffected by trinitrophenylation. However, the actin-activated ATPase activity of reacted myosin did not require light chain phosphorylation and the levels of actin-activated ATPase activity for trinitrophenylated myosin in the dephosphorylated and phosphorylated forms were equivalent. The phosphorylation reaction itself remained Ca^{2+} -dependent and the level of phosphate incorporated into the light chains was not altered by trinitrophenylation. The trinitrophenyl group was restricted to the heavy chains of myosin and was quantitatively recovered in subfragment 1. Limited tryptic hydrolysis (enzyme substrate weight ratio 1:100) of subfragment 1 yielded 3 major peptides of $M_r \sim 50,000$, $\sim 28,000$ and $\sim 25,000$. The trinitrophenyl group was localized in the 28,000 peptide.

Work supported by grant HL-23615 from the National Institutes of Health.

M-PM-E6 PREPARATION OF SUBFRAGMENT-2 AND LIGHT MEROMYOSIN (LMM) FROM GIZZARD MYOSIN ROD; LOCATION OF THE CLEAVAGE SITE. H. Suzuki, A. Wong, R.C. Lu, and J.C. Seidel, Dept. of Muscle Res., Boston Biomed. Res. Inst., and Dept. of Neurology, Harvard Med. School, Boston, MA.

Gizzard subfragment-2 [S-2(G)] and light meromyosin [LMM(G)] can be prepared by chymotryptic digestion of myosin rod prepared with papain. Insoluble LMM(G) is separated from S-2(G) by sedimentation in the presence of 35 mM NaCl, 20 mM Na-phosphate, pH 6.0, 10 mM MgCl_2 and 0.1 mM DTT. The resulting S-2(G) has an apparent subunit molecular weight 45,000 by gel electrophoresis in sodium dodecyl sulfate (SDS-PAGE), significantly greater than that of short S-2 from rabbit skeletal muscle ($M_r=40,000$) but less than that of skeletal long S-2 ($M_r=60,000$). S-2(G) having the same molecular weight can be obtained by digesting chymotryptic HMM with papain. LMM(G), prepared from myosin rod has an apparent chain weight of 85,000 (Okamoto et al., *J. Biochem.* 88:361,1980). Comparison of the NH_2 -terminal sequence of LMM(G) with the primary structure of skeletal muscle and nematode myosins suggest that the NH_2 -terminus of LMM(G) is at residue 327 of the rod. Assuming that no portion of the rod is lost on chymotryptic cleavage, S-2(G) and LMM(G) would have 326 and 772 residues, respectively, in agreement with their relative mobilities on SDS-PAGE. Assuming a coiled-coil structure like that of tropomyosin, the length of S-2(G) and LMM(G) can be estimated as 46 and 108 nm, respectively. It appears that the chymotryptic cleavage site is close to one of the bends in the 10S form of myosin (Onishi & Wakabayashi, *J. Biochem.* 92:871,1982; Trybus et al., *PNAS* 79:6151,1982). Supported by grants from NIH (AM-28401, HL-15391 & HL-23249), AHA (81 767) and MDA.

M-PM-E7 THE EFFECT OF PHOSPHORYLATION AND THE PROTEIN CONFORMATION ON THE BINDING OF GIZZARD MYOSIN TO F-ACTIN. H. Suzuki, W.F. Stafford, III and J.C. Seidel, Dept. of Muscle Research, Boston Biomedical Research Institute, and Dept. of Neurology, Harvard Medical School, Boston, MA

Between 0.15 and 0.25 M NaCl in the presence of MgATP, gizzard and arterial myosin can exist in either of two monomeric conformational states having sedimentation coefficients of 6 and 10S, respectively; phosphorylation of the 20 Kdal light chain or increasing ionic strength favors the 6S form (Suzuki et al., 1978; Suzuki et al., 1982; Trybus et al., 1982). We have found the same results in the presence of MgAMPPNP. In addition, both the binding of unphosphorylated myosin (UM) to skeletal muscle F-actin and the fraction of UM in the 6S conformation increase sharply with increasing ionic strength, suggesting that the 6S form binds more strongly than the 10S form. Under these conditions phosphorylated myosin (PM), which contains a greater fraction in the 6S conformational form than does UM, binds more strongly than UM. Above 0.25 M NaCl, where both myosins are in the 6S form, there is no difference between the binding of PM and UM. In the presence of Mg-pyrophosphate both PM and UM exist exclusively in the 6S form and bind equally well to actin at all NaCl concentrations tested. The simplest interpretation of these data is that phosphorylation promotes the binding of myosin to actin by shifting an equilibrium between 6 and 10S forms toward the 6S form, although we cannot rule out some direct effect of phosphorylation on the affinity of myosin for actin. Supported by grants from NHLBI (HL-15391, HL-23249 and HL-26229) and MDA.

M-PM-E8 REQUIREMENT OF Ca^{2+} AND TROPOMYOSIN (TM) FOR ACTIN-ACTIVATED ATPase ACTIVITY OF PHOSPHORYLATED FORMS OF PULMONARY AND GIZZARD MYOSIN WITH GIZZARD OR SKELETAL MUSCLE ACTIN. Sumitra Nag, Narindar Nath, Aida Carlos and John C. Seidel, Dept. of Muscle Research, Boston Biomedical Research Institute and Dept. of Neurology, Harvard Medical School, Boston, MA

At low concentrations of Mg^{2+} , activation of ATPase activity of phosphorylated gizzard myosin (PGM) by gizzard actin requires Ca^{2+} and TM (Nag & Seidel, 1983), but activation of phosphorylated pulmonary myosin (PPM) by skeletal actin does not (Chacko & Rosenfeld, 1982). Our present results show that the activation of phosphorylated pulmonary myosin by gizzard actin, is like that of gizzard myosin, requiring both Ca^{2+} and TM. Either Ca^{2+} or TM alone, increase activity not more than twofold, while both together produce a tenfold increase. A comparison of skeletal and gizzard actin reveals that activity with skeletal actin, which at 25° does not require Ca^{2+} , acquires Ca^{2+} dependence at lower temperatures. This is true for both types of phosphorylated myosin. At 15° the activity of PGM is not activated by skeletal actin unless both Ca^{2+} and TM are present. These results are consistent with a myosin linked regulation, modulated by the type of actin. The magnitude of the Ca^{2+} dependence also varies with changes in Mg^{2+} concentration, ionic strength and temperature, for both myosins. In general, Ca^{2+} sensitivity increases with decreasing Mg^{2+} concentration or temperature and with increasing ionic strength. PPM and PGM differ in the concentrations of Mg^{2+} or NaCl at which maximal Ca^{2+} dependence is observed. The relatively small effects of Ca^{2+} and TM on ATPase activity of phosphorylated arterial myosin seen in previous studies, may be attributable to the use of skeletal muscle actin and non-optimal assay conditions. Supported by grants from NHLBI (HL-15391 & HL-23249) and MDA.

M-PM-E9 STRETCH-INDUCED PHOSPHORYLATION OF THE 20,000-DALTON LIGHT CHAIN OF MYOSIN IN ARTERIAL SMOOTH MUSCLE. Kate Bárány, Ronald F. Ledvora*, David L. VanderMeulen, John Barron* and Michael Bárány. Department of Physiology and Biophysics and Department of Biological Chemistry, University of Illinois at Chicago, College of Medicine, Chicago, IL 60612

Helical strips from porcine carotid arteries were mounted in muscle chambers for tension measurements. Active tension was produced by K^+ or norepinephrine stimulation. Stretching to 1.7 times the resting length of the strips reversibly prevented active tension development. The phosphorylation of the 20,000-dalton light chain of myosin in the functionally different strips was assessed by two-dimensional gel electrophoresis and scanning. Maximal phosphorylation was found upon K^+ or norepinephrine challenge of strips at resting length, which developed active tension, and also in stretched strips, which did not produce active tension. These results show that the contractile event is not a prerequisite for phosphorylation. Furthermore, stretching alone also induced maximal light chain phosphorylation even in the absence of K^+ or norepinephrine. The stretch-induced light chain phosphorylation was not affected by exhaustive washing of the muscle with Ca^{2+} -free physiological salt solution, treatment of the muscle with verapamil, or by a short exposure to EGTA. Prolonged EGTA-treatment abolished the stretch-induced light chain phosphorylation. All evidence suggest that upon stretch, Ca^{2+} is released from intracellular sources and this Ca^{2+} activates the myosin light chain kinase producing phosphorylation of the light chain. (Supported by NIH NS-12172 and Chicago Heart Association).

M-PM-E10 COMPARISON OF THE ATPase ACTIVITIES OF PHOSPHORYLATED AND THIOPHOSPHORYLATED CHICKEN GIZZARD MYOSIN. Richard J. Heaslip* and Samuel Chacko, Department of Pathobiology, University of Pennsylvania, Philadelphia, Pa.

Actomyosin containing endogenous light chain kinase was prepared from gizzard by ammonium sulphate fractionation (35 - 70%) of the muscle extract. After incubation in 0.1mM CaCl_2 , 10mM MgCl_2 and either 2.5mM ATP or 0.5mM ATP γ S, the phosphorylated myosin was purified free of other proteins by gel filtration on a sepharose 4B-CL column. Purified thiophosphorylated (TPM) and phosphorylated (PM) myosin were compared with respect to their ATPase activities in high (0.5M KCl) and in low (0.02M KCl) ionic strength solutions. The PM and TPM had K^+ -EDTA stimulated ATPase activities of 1.26 ± 0.07 and 1.33 ± 0.09 $\mu\text{mol Pi/mg/min}$, respectively. Ca^{2+} -activated ATPase activity in 0.5M KCl was 0.73 ± 0.03 for both myosins. The ATPase activity of both PM and TPM in high ionic strength was inhibited by 5mM Mg^{2+} (0.07 ± 0.01 and 0.04 ± 0.01 $\mu\text{mol Pi/mg/min}$, respectively). In low ionic strength, the Mg-ATPase activities of PM and TPM were very low (0.022 ± 0.003 and 0.033 ± 0.010 respectively). When the 20K light chain was fully phosphorylated, gizzard actin (molar ratio M:A=1:16) containing gizzard tropomyosin (molar ratio A:Tm=6:1) activated the Mg-ATPase activity of PM and TPM to 0.134 ± 0.017 and 0.143 ± 0.028 respectively. In addition, for both PM and TPM the actin-activated ATPase activity was Ca^{2+} -dependent at free Mg^{2+} concentrations of < 3 mM. Removal of Ca^{2+} (pCa8) at these free Mg^{2+} concentrations caused up to 80% decrease in the actin-activated ATPase activity of these myosins. Hence, the thiophosphorylated and phosphorylated gizzard myosin are similar with respect to their enzymatic characteristics. (Supported by grants from NIH. RJH is an American Heart Association Fellow).

M-PM-E11 EFFECT OF Ca^{2+} and Mg^{2+} on the ACTIN-ACTIVATED ATP HYDROLYSIS BY PHOSPHORYLATED HMM PREPARED FROM ARTERIAL SMOOTH MUSCLE. Edward A. Kaminski* and Samuel Chacko, Department of Pathobiology, University of Pennsylvania, Philadelphia, Pa. (Introduced by R.E. Davies)

Actin-activated ATP hydrolysis by phosphorylated arterial myosin is Ca^{2+} dependent at Mg^{2+} concentrations which cause the myosin to bind 2 moles Ca^{2+} per mole (Chacko and Rosenfeld Proc. Natl. Acad. Sci. 79:292, 1982). Soluble heavy meromyosin (HMM) was prepared from phosphorylated arterial myosin by chymotryptic digestion and purified by gel filtration on Sepharose 6B. Actin-activated ATPase activity of the phosphorylated HMM was measured either at constant Mg^{2+} and variable Ca^{2+} or at constant pCa $^{2+}$ and variable Mg^{2+} concentrations. At constant (0.05 M) ionic strength and pCa5, the actin-activated ATPase activity increased as a function of Mg^{2+} concentration until the free Mg^{2+} reached between 1-2 mM; this was followed by a decrease in activity to a very low level at 8 mM free Mg^{2+} . Removal of Ca^{2+} at 1 mM Mg^{2+} lowered the actin-activated ATPase activity (40-60% inhibition). These experiments demonstrated that Mg^{2+} and Ca^{2+} had a direct effect on actin-activated ATP hydrolysis. This effect was not due to aggregation of the myosin and was independent of the rod portion of the myosin molecule. (Supported by grants from NIH; E.A. Kaminski is an MDA Fellow)

M-PM-E12 EFFECT OF MgCl_2 ON THE PROPERTIES OF SMOOTH MUSCLE MYOSIN. M. Ikebe, R.J. Barsotti and D.J. Hartshorne, Muscle Biology Group, University of Arizona, Tucson, AZ 85721

Ikebe et al. (Biochemistry 22:4580 (1983)) showed that under specific conditions phosphorylation of myosin induces the transition from 10S to 6S. This change is paralleled by an increase in viscosity and an alteration in enzymatic activities. The effect of Mg^{2+} and its relationship to myosin conformation was studied because several groups have demonstrated a requirement for high Mg^{2+} concentrations in vitro and also that Mg^{2+} can induce tension in skinned smooth muscle fibers. The actin-activated ATPase of turkey gizzard myosin in the presence of EGTA increased with increasing concentrations of MgCl_2 and reached a maximum (~ 15 nmoles/min/mg) at 30 mM. (For comparison the actin-activated ATPase of phosphorylated myosin was ~ 20 nmoles/min/mg). The Mg^{2+} -dependent increase in ATPase occurred without detectable phosphorylation of myosin. In parallel experiments carried out with monomeric myosin the increase in MgCl_2 concentrations effected the transition of 10S to 6S as detected by sedimentation velocity and viscosity measurements. For skinned chicken gizzard fibers in the absence of Ca^{2+} an increase in MgCl_2 induced tension. The level of MgCl_2 necessary to produce maximum tension was variable (10-20 mM total). The Mg^{2+} -tension was not accompanied by myosin phosphorylation as determined by urea-gel electrophoresis. Relaxed fibers contained $8 \pm 3\%$ phosphorylation compared to $11 \pm 5\%$ phosphorylation for fibers analyzed at the peak of Mg^{2+} -tension. (Normal contractions resulted in $50 \pm 9\%$ phosphorylation.) The Mg^{2+} -induced tension occurred with ITP in the presence and absence of Ca^{2+} . These findings suggest that high Mg concentrations may alter myosin conformation, independent of phosphorylation, and effect the biological activities of smooth muscle myosin. Work supported by grants HL 23615 & 20984, NIH.

M-PM-F1 PEELED MAMMALIAN SKELETAL MUSCLE FIBERS: REVERSIBLE BLOCK OF Cl^- -INDUCED TENSION TRANSIENTS BY D600 AND D890. SUE K. DONALDSON, ROBERT DUNN, JR., AND DANIEL HUETTEMAN, DEPARTMENT OF PHYSIOLOGY AND DEPARTMENT OF MEDICAL NURSING, RUSH UNIVERSITY, CHICAGO, ILLINOIS 60612

Single skeletal fibers from rabbit adductor magnus muscles were peeled in an aqueous relaxing solution ($\text{pCa} \approx 7.0$) and mounted in photo-diode force transducer for continuous monitoring of isometric tension generation. Bathing solutions, used for the peeled fibers were all at $\text{pH} = 7.0$ and $22 \pm 1^\circ\text{C}$ and contained 66mM (choline + K^+), 4mM Na^+ , 2mM MgATP^{2-} , 15mM CP^{2-} (added as tris,CP), 15 U/ml CPK, $0.02\text{--}4\text{mM}$ EGTA, variable $[\text{Ca}^{2+}]$, 1mM Mg^{2+} , and imidazole buffer (concentration variable to make ionic strength = 0.15M). Ca^{2+} release from the peeled fibers was stimulated by bathing solution substitution of choline Cl for K propionate at constant $[\text{K}^+][\text{Cl}^-]$ (Cl^- -induced release) and was monitored as isometric tension generation. The mechanism for Cl^- -induced Ca^{2+} release in mammalian peeled fibers appears to involve ionic depolarization of T-tubules. Ca^{2+} channel blockers D600 and D890 block the Cl^- -induced but not the caffeine-induced tension transient in the mammalian peeled fibers at concentrations of 10^{-6}M . Following addition of either D600 or D890 to the bathing solutions the first Cl^- -induced tension transient is not blocked but subsequent ones are. The inhibitory effect of either drug was eliminated by washing it off or by exposing the fiber to $10^{-5.6}\text{M}$ Ca (4mM EGTA) in the presence of the drug. Since D890 is permanently charged, the site of action of both drugs is probably on the cytoplasmic side of the membranes in the peeled mammalian skeletal fibers. Supported by grants from Muscular Dystrophy Association of America and NIH (HL23128, AM31511).

M-PM-F2 CONTRACTILE ACTIVATION IN STRIATED MUSCLE FIBERS WITH A SIMPLE TRANSVERSE TUBULAR SYSTEM.

Todd Scheuer and Wm. F. Gilly, Hopkins Marine Station of Stanford University, Pacific Grove, CA.

Scorpion striated muscle possesses a transverse tubular (T-) system in which the short, radially oriented tubules have prominent mouths. Diadic couplings between the well-developed sarcoplasmic reticulum and transverse tubules are structurally similar to those in vertebrates. Contractile activation in scorpion (*Uroctonus mordax*) fibers was characterized at 20°C with a 2-microelectrode voltage clamp method. Threshold amplitude for just-detectable sarcomere shortening was determined for voltage steps of different durations (2–50 ms) by microscopic observation of sarcomeres near the fiber surface in the voltage-clamped segment of muscle fiber. The Strength-Duration curve thus obtained in Na-free saline (+TTX) resembles that found in TTX-poisoned frog muscle, but threshold for long (20–50 ms) pulses (i.e., rheobase) is near -25 mV , substantially more positive than in frog. Tetracaine (0.5 mM) reversibly inhibits contractile activation in scorpion, especially with brief voltage steps, and renders contraction impossible with a 2 ms pulse. In Na-free saline (+TTX) containing 5 mM Ca, contractile activation is always accompanied by a voltage-dependent inward current. Both contractile activation and inward current are rapidly (and reversibly) eliminated when calcium is omitted from the external solution. Cadmium (0.05 mM) similarly blocks contractile activation and reduces or eliminates inward current. Thus, contractile activation in scorpion and frog muscle are similarly tetracaine-sensitive, but in scorpion external Ca appears to play an important role. Whether this apparent difference reflects the simple T-tubular geometry in scorpion muscle or a fundamentally different mechanism of excitation-contraction coupling than that in vertebrate skeletal muscle remains to be established.

M-PM-F3 ASYMMETRIC CHARGE MOVEMENTS DURING T-TUBULAR UNCOUPLING IN FROG SKELETAL MUSCLE. Donald T. Campbell, Dept. Physiology & Biophysics, University of Iowa, Iowa City, IA.

Capacity transients and asymmetric charge movements were measured in frog muscle fibers using the Vaseline gap voltage clamp. Capacity transients elicited by stepping from -135 to -90 mV show a rapid phase that lasts 10 to 30 μs and is presumably due to charging of the surface membrane, and a slow phase that lasts several ms and is presumably due to charging of the T-system. When the ends of the fiber are cut in fluoride-containing solution, the amount of slowly charging capacitance declines gradually over a 30–40 minute period, to between 2–20% of its initial value (Campbell & Hahn, 1983, *Biophys. J.* 41:177a), suggesting that the electrical connection between surface and T-system membranes becomes progressively uncoupled. During the course of tubular uncoupling, the slow charge movements, thought to be involved in E-C coupling (Schneider & Chandler, 1973, *Nature*, 242:244–246), are progressively slowed and total charge declines. These results are consistent with the hypothesized tubular location of the slowly moving charge. By contrast, Na channel gating currents decline only slightly, and display relatively unchanged kinetics, suggesting that these fast asymmetric currents arise predominately from charge located in the surface membrane.

Although the mechanism of the tubular uncoupling is still being investigated, three observations suggest that it is caused by CaF_2 precipitating in the T-system. 1) Capacity transients and charge movements remain unaltered over time when the ends of a fiber are cut in solutions in which aspartate and EGTA are the predominant anions. 2) The rate and degree of uncoupling are enhanced by external solutions containing elevated Ca. 3) Rapid change of external solution from isotonic CsF to Ca-containing Ringer causes a rapid decrease in amplitude, and slowing in the kinetics, of the slow phase of capacity current. Supported by MDA and NIH (NS 15400).

M-PM-F4 ANTIPYRYLAZO III (Ap III) AND ARSENAZO III (Az III) CALCIUM TRANSIENTS FROM FROG SKELETAL MUSCLE FIBERS SIMULTANEOUSLY INJECTED WITH BOTH DYES. M. E. Quinta-Ferreira, S. M. Baylor & C. S. Hui. Depts of Physiology, University of Pennsylvania, and Biological Sciences, Purdue University.

The use of calcium-indicator dyes to monitor changes in myoplasmic free calcium during activity has led to different estimates of the time course of the Ca transient. For example, in response to an action potential, the Ca-dye signal from fibers injected with Ap III has an earlier peak and faster return to baseline than does the signal from Az III (Palade & Vergara, *J. Gen. Physiol.* 79, 679-707; Baylor, Quinta-Ferreira & Hui, *Biophys. J.* 44, 107-112). These results suggest that one of the dyes either does not follow Ca in a rapid and linear manner or has a pharmacological action that changes the free Ca waveform. In order to distinguish between these possibilities, we have measured Ca-dye signals from intact single fibers simultaneously injected with both dyes. Based on the differing spectral properties of the two Ca-dye reactions, the components of the total signal attributable to Ap III and Az III could be separated. In agreement with the results from fibers injected with either dye alone, the Ca-Ap III component is faster and does not summate in response to a brief high-frequency train of stimuli, while the Ca-Az III component is slower and does summate. However, the initial part of the rising phases of the two Ca-dye signals can be made to superimpose by appropriate scaling, suggesting that a portion of the Ca-Az III signal is kinetically rapid. Under the assumption that the Ca-Ap III signal tracks myoplasmic free Ca in a rapid and linear fashion, the Ca-Az III signal can be described as a linear combination of two waveforms: one that has the time course of free Ca and another that follows free Ca with an exponential delay of about 10 ms. This delay can explain the later peak and slower return to baseline of the Ca-Az III signal, as well as the increase in peak amplitude that is observed during repetitive stimulation.

M-PM-F5 EFFECT OF CAFFEINE ON MYOPLASMIC CALCIUM TRANSIENTS IN INTACT FROG SKELETAL MUSCLE FIBERS S. M. Baylor and M. E. Quinta-Ferreira, Dept. of Physiology, Univ. of Pennsylvania, Philadelphia, PA

Low doses of caffeine potentiate the muscle twitch with minimal effects on the action potential. Possible mechanisms of action include: (1) an increase in Ca release from the SR during activity; (2) an increase in resting leakage of SR Ca; (3) an inhibition of Ca uptake by the SR Ca pump. In order to distinguish among these possibilities, we have measured the effects of 2 mM caffeine on twitch tension and absorbance signals from the Ca-indicator dye Antipyrylazo III (Ap III). Intact single fibers from *Rana temporaria* were mounted at long sarcomere spacing (3.5 to 4.5 μm) in an H_2O Ringer's solution at 15-17°C, micro-injected with dye, and activated by action potential stimulation. Caffeine caused no change in Ap III absorbance in resting fibers nor in the spectral dependence of the Ca-Ap III transient in response to an action potential. However, caffeine (usually) caused a definite reduction in the rate of rise and peak amplitude of the Ca transient and significantly prolonged its falling phase. In no fibers did we observe a larger or faster calcium transient in the presence of caffeine. We conclude that in stretched, intact fibers the mechanism responsible for potentiation of the twitch response by 2 mM caffeine does not involve an increase in the peak rate of SR Ca release during activity. Instead, we postulate an elevation in the resting myoplasmic Ca (due to mechanism (2) or (3) above) in combination with a smaller release during activity (cf. Fig. 13 of Baylor, Chandler & Marshall, *J. Physiol.* 344). This conclusion stands in contrast to caffeine's reported effects on cut frog fibers (Delay, Ribalet & Vergara, *Biophys. J.* 41, 396a; Kovacs & Szucs, *J. Physiol.* 341, 559-578), where a potentiation of the mechanism linking T-tubular depolarization and SR Ca release has been proposed. Supported by NIH grant NS 17620.

M-PM-F6 DIFFERENTIAL EFFECTS OF 2,3-BUTANEDIONE MONOXIME (BDM) ON ACTIVATION AND CONTRACTION. Louis A. Mulieri and Norman R. Alpert. Dept. Physiol. & Biophys. Univ. of Vermont, Burlington, VT 05405.

We report results of a preliminary survey to determine if BDM can be used to selectively block cross-bridge tension and heat production during activation heat measurements. Bundles of fibers (35 to 50) from frog anterior tibialis muscle were studied at resting sarcomere lengths (S_r) of 2.3, 3, or 3.6 μm in Ringer solution at 15°C or 0°C. With 7.5mM BDM added, twitch tension was depressed 85% ($S_r=2.3$ and 3.0) while time to peak twitch tension decreased 25% ($S_r=3\mu\text{m}$) to 50% ($S_r=2.3\mu\text{m}$). Tetanic tension ($S_r=2.3\mu\text{m}$) was depressed 50% with an 85% reduction in rate of tension build-up. Mechanical V_{max} was depressed 35% (0°C) and curvature of the tetanic force-velocity relation was markedly increased. The downstroke of the latency relaxation (LR) was not altered except that a reduced rate of upstroke development caused it to be prolonged 120% at $S_r=2.3\mu\text{m}$ and 60% at $S_r=3\mu\text{m}$ resulting in an increased depth of latency relaxation (by 140% and 20%, respectively). The fast component of activation heat (A_p) was not altered by BDM ($S_r=3.6\mu\text{m}$). Since the downstroke of the LR (Mulieri, *J. Physiol.* 223, 1972) and A_p (Mulieri & Alpert, *Canad. J. Physiol. & Pharmacol.* 60, 1982) are believed related to Ca^{++} release from the SR and Ca^{++} binding to troponin, respectively, the present observations suggest 7.5mM BDM does not appreciably alter these processes. The reduction in tetanic tension, mechanical V_{max} , and rate of tetanic tension build-up suggests BDM does depress cross-bridge function (reduced cycling rate?) and hence is potentially valuable as a selective inhibitor of cross-bridges. Supported by L.A.M. and USPHS 1-P01-HL28001-02/P1.

M-PM-F7 THE EFFECT OF 2,3-BUTANEDIONE MONOXIME (BDM) ON THE RELATION BETWEEN INITIAL HEAT AND MECHANICAL OUTPUT OF RABBIT PAPILLARY MUSCLE. Edward M. Blanchard, Louis A. Mulieri, Norman R. Alpert. Dept. Physiol. & Biophys. Univ. of Vermont, Burlington, VT 05405.

BDM has negative inotropic effects on heart muscle yet the mechanism of action is unresolved. Inhibition of Ca^{2+} delivery to the contractile apparatus and/or direct inhibition of cross-bridge cycling are reasonable sites of BDM action. We measured the effect of BDM on the relation between initial heat and the twitch tension-time integral (TTI). If BDM acts as a selective inhibitor of cross-bridges, the relation between initial heat and twitch TTI should be linear with an intercept on the heat axis that represents the heat due to Ca^{2+} cycling (activation heat, H_A). Papillary muscles from the right ventricles of rabbits are mounted on a rapid, high-sensitivity thermopile, connected to an isometric force transducer, and stimulated at 0.2 Hz at 21°C in Krebs solution at the peak of the length-tension curve (L_o). Peak twitch tension was reduced to $7.8 \pm 0.7\%$ of control at 8mM BDM with 50% inhibition at 3mM BDM. The relation between initial heat (1.48 ± 0.1 mcal/g) and twitch TTI was linear for 0.2, and 4mM BDM but heat was disproportionately inhibited at higher concentrations of BDM. Extrapolation of the linear portion of the curve to zero TTI predicts an H_A which is 14% of initial heat at L_o or 0.21 mcal/g. Combination of 4mM BDM and 1.75X hyperosmotic mannitol-Krebs reversibly reduced twitch TTI to $6.6 \pm 2.7\%$ of control and reduced initial heat to 0.27 ± 0.03 mcal/g. This H_A value fell on the line predicted by the linear portion of the initial heat vs. TTI curve. The results are consistent with the concept that BDM selectively inhibits cross-bridges within concentration limits and indicate that BDM in combination with mannitol may permit accurate measurement of H_A in cardiac tissue at L_o . Supported by USPHS 28001-02/P1 and USPHS F3206577-01 postdoctoral fellowship to E.M.B.

M-PM-F8 PARTIAL IMMOBILIZATION OF MEMBRANE CHARGE PRODUCES BLOCK OF CALCIUM RELEASE IN FROG SKELETAL MUSCLE FIBERS. R.F. Rakowski and Marilyn R. James-Kracke, Department of Physiology and Biophysics, Washington University School of Medicine, St. Louis, MO 63110.

Membrane charge movement was measured in cutaneous pectoris muscle fibers of the frog, Rana temporaria using the three microelectrode voltage-clamp technique. Steady-state charge immobilization was measured by changing the holding potential (Rakowski, J. Physiol. 317: 129-148, 1981). Fibers were bathed in hypertonic Ringer's solution (350 mM sucrose) to prevent contraction. Calcium release was measured using the metalochromic dye arsenazo III. The absorbance change of the dye was measured using a three wavelength microscope photometer at 572, 632, and 653 nm. The inactivation of calcium release occurred at more negative holding potentials and was more steeply voltage-dependent than the inactivation of charge movement. Charge movement and optical data were fitted to $S/S_{\max} = 1/[1 + \exp((V_h - V)/k)]$ where V_h = the holding potential, S/S_{\max} = either the normalized value of the charge that remains mobile or the initial rate of the absorbance change during the first 15 msec of a test pulse to 0 mV. The charge immobilization parameters for the most complete set of data were $V = -51.8$ mV and $k = 14.0$ mV (6°C). The optical data from this fiber gave $V = -64.4$ mV and $k = 6.9$ mV. The discrepancy remained after correction for sub-threshold charge movement. At a holding potential of -40 mV approximately 60% of the total membrane charge remains mobile, but calcium release is abolished. These data suggest that the more steeply voltage-dependent Q_y component of charge movement is more likely to be directly associated with calcium release than the component of charge movement (Q_{β}) that remains mobile at a holding potential of -40 mV. Supported by NIH grant NS-14856 and the Muscular Dystrophy Association.

M-PM-F9 MEASUREMENTS OF FREE $[\text{Ca}^{2+}]$ IN HUMAN MALIGNANT HYPERTHERMIC MUSCLES. López J.R., Alamo L. Caputo C. Vikiński J., Ledezma D. Centro de Biofísica y Bioquímica, IVIC, Dept Anaestesiología del Hospital Universitario, UCV, y del Hospital J.M. de los Ríos, Caracas, Venezuela.

Malignant hyperthermia (MH) is a pharmacogenetic syndrome of skeletal muscle which is triggered most commonly by inhalation of anesthetic agents, usually halothane, or depolarizing muscle relaxants. Ca^{2+} selective microelectrodes have been used to determine the free myoplasmic $[\text{Ca}^{2+}]$ in human skeletal muscle obtained from patients that during anesthesia had developed early signs associated with MH. Intercostal muscle biopsies were performed under local anesthesia in 4 M.H. patients 15 days to 4 months after developing the M.H. crisis and in 3 control subjects. Each muscle fascicle was dissected free of adipose and connective tissues, and then placed in a temperature controlled bath (37°C) for electrophysiological measurements. The calcium sensitive microelectrodes were prepared as described previously (Lopez et al Biophys. J. 43:1-4 1983). We used only microelectrodes that showed a Nernstian response between pCa_3 and pCa_7 (30.5 mV per decade at 37°C). Membrane resting potential (V_m) and calcium potential (V_{Ca}) were obtained from superficial fibers and were considered only if the value of V_m was not lesser than -73mV and that the penetration of the second microelectrode (V_{Ca}) did not induce a depolarization larger than 5mV. The free cytosolic $[\text{Ca}^{2+}]$ was $0.38 \pm 0.1 \mu\text{M}$ ($M \pm \text{SEM}$, $n=18$) in muscle fibers obtained from malignant hyperthermic patients, while in control subjects it was $0.11 \pm 0.02 \mu\text{M}$ ($M \pm \text{SEM}$, $n=11$). These results suggest that this syndrome might be related to an abnormally high myoplasmic free resting calcium concentration probably due to a defective function of the Sarcoplasmic Reticulum. (Supported by CONICIT S1-1148)

M-PM-F10 CALCIUM REUPTAKE IN SKELETAL MUSCLE MEASURED USING CALCIUM-SENSITIVE DYES. B. Ribalet, M. Delay and J. Vergara, Dept. of Physiology, UCLA, Los Angeles, CA 90024.

The process of resequestration of released Ca^{++} by the sarcoplasmic reticulum (SR) was studied by monitoring Ca release elicited by two stimuli, separated by a variable time interval, in voltage-clamped cut frog skeletal muscle fibers. Comparisons were made between results obtained using the metallochromic Ca^{++} indicator dyes Arsenazo III (ArIII) and Antipyrilazo III (ApIII). For very short interstimulus intervals (about 2 ms), the peak absorbance change due to the second Ca release (above any persisting change due to the first release) is ca. 50% of the control release for both ArIII and ApIII. As the interstimulus interval is increased, the magnitude of the second Ca release returns to the control value in two phases, a rapid phase to a recovery of ca. 80% lasting about 100 ms for ApIII and 200 ms for ArIII, and a second, slower, phase that lasts over 1 min until 100% recovery of the Ca release relative to control. In the presence of low concentrations of caffeine, the first release of Ca is potentiated; however, a closely following second stimulus results in a smaller Ca release than occurs in the absence of caffeine. The percent of recovery of the second release reached at the end of the rapid phase is progressively reduced with increasing levels of caffeine. Subthreshold depolarizing prepulses do not affect the magnitude of Ca release, and hyperpolarizing and subthreshold depolarizing pulses applied between stimuli do not modify the second Ca release. The results of these experiments suggest a dye dependent effect on the rate of Ca uptake by the SR and are consistent with the possibility that the amount of Ca released by the SR is limited by the amount of Ca available. (Supported by USPHS (AM 25201), MDA (Project 2, JLNRC) and the Laubisch Fund.)

M-PM-F11 DELAYED RECTIFICATION IN THE T-SYSTEM OF FROG SKELETAL MUSCLE. J. Vergara, Dept. of Physiology, UCLA, Los Angeles, CA 90024.

Outward potassium currents were recorded from frog single muscle fibers voltage-clamped with the three vaseline-gap method. The potential change across the T-system membranes was simultaneously monitored optically using the absorbance change from the non-penetrating potentiometric dye NK2367 at 670 nm. The fibers were internally diffused with K or Cs containing relaxing solutions and externally perfused with Ringer with TTX. The effects of the delayed rectifier conductance on the time course and magnitude of the tubular membrane potential were studied in response to voltage clamp steps from -120 to +180 mV. In K diffused fibers, the absorbance signals showed an early rising phase, typical of the passive charging process of the T-system membranes, followed by a delayed decremental phase with a time course that closely resembled the kinetics of activation observed in the current records. Small and slow decremental phases were associated with small and kinetically slow K currents elicited by small depolarizing pulses. Large depolarizing pulses produced large K currents and pronounced decremental phases in the absorbance signals. In Cs diffused fibers the delayed rectifier conductance was blocked and there was no evidence of a decremental phase in the optical signals. The voltage dependence of the absorbance signals, measured at 40 ms after the onset of the voltage clamp pulses, showed a linear behavior in Cs diffused fibers but was non-linear in K diffused fibers. The results of these experiments suggest that there is a significant amount of delayed K conductance in the tubular membranes of skeletal muscle fibers. Supported by grants from USPHS (AM25201) and MDA (Project 2, JLNRC).

M-PM-F12 CHARACTERIZATION OF AN ELECTROGENIC Na PUMP IN RABBIT CEREBRAL ARTERIES USING A NEW CHOPPED VOLTAGE CLAMP. M. Chung and C.J. Cohen, Miles Inst. Preclin. Pharm., New Haven, CT.

We have modified a one microelectrode voltage clamp technique to facilitate studies of an electrogenic Na pump current (I_{pump}) in small branches of rabbit middle cerebral arteries ($d=50-150 \mu$). The cable properties of the arteries were determined by injecting constant current pulses and adjusting τ_m and λ to fit the time course of the voltage change. The arterial segments behave as linear cables with sealed ends and, at $E_m = -83 \text{ mV}$, $\lambda = 340 \mu$ and $\tau_m = 110 \text{ ms}$. Arterial segments 300-500 μ in length were voltage clamped with a microelectrode at the center. The cable analysis predicts that longitudinal variation of V was $<3 \text{ mV}$ during measurements of steady-state currents. When several nAmp of current are injected through a single-barrelled microelectrode, a prohibitively large voltage drop develops across the tip if the resistance $>50 \text{ M}\Omega$, as is required for the stable impalement of vascular smooth muscle cells. To circumvent this difficulty, double-barrelled microelectrodes were used. Chopping between current passing and recording modes minimized artifacts due to capacitive coupling between the barrels. The steady-state I-V is linear from -30 to -70 mV in the presence of $540 \mu\text{M Ba}$. Ba also reduces the sensitivity of the I-V to changes in K_0 and increases R_m from 24 to $90 \text{ k}\Omega/\text{cm}^2$. Thus, Ba makes it possible to follow changes in I_{pump} by measuring ΔE_m . Cells were loaded with Na by exposure to K-free solution with Ba. Addition of 8 mM K reactivated the pump. A transient hyperpolarization occurred that decayed with $\tau_1 = 170 \text{ s}$. The potential change was eliminated by $10 \mu\text{M}$ strophanthidin, indicating that it was due to Na pump activity. 200 nM nimodipine (a cerebrally-active vasorelaxant) did not alter the rate of Na pumping. I_{pump} at rest is $\approx 70 \text{ nA}/\text{cm}^2$, about one tenth the value of myocardium.

M-Pos1 INTERACTIONS OF ORGANIC Ca CHANNEL ANTAGONISTS WITH Ca CHANNELS IN ISOLATED FROG ATRIAL CELLS: TEST OF A MODULATED RECEPTOR HYPOTHESIS. A. Uehara and J.R. Hume. Department of Pharmacology and Toxicology, Michigan State University, East Lansing, MI 48824.

Tonic and frequency-dependent block of i_{Ca} in isolated frog atrial cells by D-600 (5×10^{-6} M), diltiazem (5×10^{-5} M) and nifedipine (3×10^{-7} M) was examined using a one-microelectrode voltage clamp technique. Trains of i_{Ca} were elicited by depolarizing voltage clamp pulses applied at .33 Hz from a holding potential of -90 mV before and following exposure to each of the antagonists. The percentage of total i_{Ca} block due to tonic inhibition was found to be correlated with the expected proportion of neutral drug form at pH 7.4 for each of the three antagonists (2% D-600, $pK_a = 8.6$; 24% diltiazem, $pK_a = 7.7$; 90% nifedipine, $pK_a = 1.0$). When extracellular pH was changed to 6.4, tonic inhibition of i_{Ca} by diltiazem, an antagonist with an intermediate pK_a was reduced to 3% and frequency-dependent inhibition was increased (97%). In additional experiments, the effects of each of these antagonists on i_{Ca} availability and i_{Ca} reactivation were examined. All three antagonists produce large hyperpolarizing voltage shifts in i_{Ca} availability and produce a second, slower exponential recovery phase. The kinetics of the slower drug-induced recovery process was fastest for nifedipine ($\tau = 500$ ms, $n=5$), intermediate for diltiazem ($\tau = 2200$ ms, $n=5$) and slowest for D-600 ($\tau = 15,000$ ms, $n=4$). Overall, these results provide direct evidence that a modulated-receptor hypothesis may account for the interactions of a variety of organic Ca channel antagonists with myocardial Ca channels. However, unlike local anesthetic interactions with Na channels, extracellular acidification fails to significantly modify the kinetics of the drug-induced slow i_{Ca} recovery process. Therefore, molecular weight and size of organic Ca antagonists, in addition to lipid solubility, may be important determinants of drug-channel dissociation rates. (Supported by NIH Grant HL-30143.)

M-Pos2 CONDUCTANCE AND KINETICS OF ELEMENTARY INWARDLY-RECTIFYING K^+ CURRENTS IN VENTRICULAR MYOCYTES. I. R. Josephson and A. M. Brown, Department of Physiology and Biophysics, University of Texas Medical Branch, Galveston, Texas 77550.

The time- and voltage-dependent properties of single channel and whole-cell inward-rectifying K^+ currents were studied in adult (freshly dispersed) and neonatal (primary culture) rat ventricular myocytes using the patch clamp technique. Inward rectification was evident in the single channel I-V ($K^+ = 150$ mM) at potentials negative to E_K (0 mV in 150 mM K^+). Outward currents in single channels were not detected positive to E_K (background noise of 0.3 peak-to-peak at 1 kHz low pass filter) although small outward whole-cell currents were present. The single channel mean open time (MOT) decreased with hyperpolarization. Burst-like behaviour with fast and slow exponential closed times also appeared at more negative potentials. The steady-state probability of channel opening (P_o) was determined from averaged patch clamp traces which were divided by the single channel patch current amplitude at the same potential. In the steady-state, P_o was decreased with hyperpolarization from E_K . This finding was consistent with the macroscopic steady-state current-voltage relationship which displayed a reduced conductance at negative potentials. In < 20% of the patches analysed two or more open levels were observed and these were not multiples of each other. The two classes were separable kinetically, having MOT's differing by 1-2 orders of magnitude. Transitions from the higher level directly to the closed state were observed and suggested state changes of a single open channel or cooperativity between two populations of inward rectifying K^+ channels.

Supported by NIH HL-25145 to A. M. Brown and NIH HL-06556 to I. R. Josephson.

M-Pos3 INTRACELLULAR PRESSURE INJECTION OF cGMP DEPRESSES CARDIAC SLOW ACTION POTENTIALS (APs). Gordon M. Wahler and Nick Sperelakis. Department of Physiology, University of Cincinnati College of Medicine, Cincinnati, OH 45267.

It has recently been demonstrated in our laboratory that intracellular injection of cyclic AMP (cAMP) transiently enhances the slow inward current in myocardial cells, presumably by phosphorylating the slow channels. To test the possibility that intracellular cGMP may also play a regulatory role in cardiac slow channel function, intracellular injections of cGMP were carried out in guinea pig papillary muscles (stimulated at 0.5 Hz at 37°C). The cells were depolarized to about -40 mV by superfusion with 25 mM K^+ -Tyrode's solution to voltage inactivate the fast Na^+ channels. Slow APs were elicited by electrical stimulation following the addition of 10 mM TEA-Cl and doubling the bath [Ca] (to 4.0 mM). Slow APs are dependent on the slow inward current carried through the voltage- and time-dependent slow channels. cGMP was injected intracellularly by application of pressure pulses (40 - 60 psi, 1 - 30 sec in duration) to the recording microelectrode, which contained cGMP (0.05 - 0.01 M Na^+ salt in 0.2 M KCl). Intracellular injection of cGMP resulted in a transient depression ($n = 14$) or abolition ($n = 2$) of the slow APs. The effect began at 1.0 - 2.0 min after the onset of the pressure pulse, and reached a maximum at 2.5 - 3.5 min. Full recovery of the slow APs was generally observed within 5 - 6 min (after the onset of the pulse). Repeating the injection of cGMP into the same cell again produced a similar transient inhibition of the slow APs. Thus, it appears that the intracellular cGMP level is capable of modulating the slow inward current in a direction opposite to that of cAMP. (Supported by N.I.H. grant HL-31942 and fellowship 1F32 HL-06736-01.)

M-Pos4 Effect of Thallium (Tl^+) on the Inwardly-Rectifying Background Conductance of Canine Cardiac Purkinje Strands. N. Mulrine & I. Cohen, Intr. by G. Gintant, Dept. Physiol & Biophys, SUNY, Stony Brook, NY 11794

The cardiac inward rectifier I_{K1} resembles the inward rectifiers in starfish egg and frog skeletal muscle; its conductance is a function of driving force, strongly depending on K^+ at negative potentials, and it is blocked by Ba^{++} , Cs^+ and Rb^+ . In starfish egg, the conductance in mixtures of K^+ and Tl^+ depend anomalously on the molar fraction of Tl^+ : the current through the inward rectifier is reduced when Tl^+ is partially substituted for K^+ , even though the current is larger in Tl^+ alone than in K^+ alone. To explain this effect, Ciani et al. formulated a model in which the ion selectivity and conductance of the inward rectifier depend on the activating cation, K^+ or Tl^+ . In order to assess the applicability of this model to I_{K1} , we examined the effect of Tl^+ on currents in canine Purkinje strands of narrow radius, cut short (2mm) to employ the two microelectrode voltage clamp technique. We constructed the current-voltage (I-V) relation from the instantaneous jump in current during hyperpolarizing pulses to -70 to -150 mV from holding potentials between -50 and -90 mV. We substituted equimolar quantities of Tl^+ for K^+ . At molar fractions of Tl^+ less than 0.5, the I-V relation was similar to that in pure K^+ . At higher molar fractions, the I-V relation was steeper than in pure K^+ . In the absence of K^+ , Tl^+ is more permeant than K^+ through the background inward rectifier. However detailed analysis of Tl^+ 's actions on I_{K1} has not been possible because of the unknown contributions of inward leak and pump currents to the instantaneous I-V relation in this potential range, and because Tl^+ also blocks the pacemaker current. Supported by HL20558. 1. Hagiwara, Miyazaki, Krasne & Ciani, 1977, JGP 70:269. 2. Ciani, Krasne, Miyazaki & Hagiwara, 1978, JMB 44:103

M-Pos5 ANALYSIS OF THE CHLORIDE-SENSITIVE COMPONENT OF TRANSIENT OUTWARD CURRENT IN RABBIT CARDIAC PURKINJE FIBERS. T.J. Colatsky and J. Goto, Div. of Exp. Therap., Wyeth Labs, Inc. and Dept. of Medicine, U. Penn., Philadelphia, PA.

The involvement of chloride ions (Cl^-) as charge carriers in the transient outward current (Ito) in cardiac Purkinje fibers (PF) has been questioned by recent studies demonstrating effects of Cl^- substitution on αCaO or gK. We have previously reported the existence of a component of Ito in voltage clamped rabbit PF which is rapidly inhibited by Cl^- removal (Circ., 66:II-234). Further characterization of this component was conducted by analysis of Cl^- -sensitive "difference" currents obtained by computer subtraction of membrane current records in NaCl and NaIsethionate Tyrode's solutions. Inactivation curves measured with 5 sec. prepulses were well fitted by the equation, $r = 1/(1 + \exp(V - V')/k)$, with $V' = -41 \pm 4$ mV and $k = 5.5 \pm 1$ mV (mean \pm SEM, $n=4$). Half-maximal activation occurred near -30 mV. Current-voltage relations obtained using difference tail currents elicited by repolarization at peak Ito ($t \approx 10$ msec) were linear within 30 mV of the estimated reversal potential of -68 ± 1 mV ($n=4$). A steady-state "window" current predicted by overlap between activation and inactivation curves was observed experimentally using slow ramp depolarizations. Ion-sensitive microelectrode measurements (performed by Dr. C.O. Lee) revealed that Cl^- substitution by isethionate lowered αCaO by 28%; however, reduction of external $CaCl_2$ from 2.7 to 1.35 mM for 30-45 min. did not appreciably alter Ito. Non-specific inhibitory effects of Cl^- removal on gK were excluded by the observation that the outward tails associated with delayed rectification were increased, not decreased, with isethionate. These data implicate Cl^- as charge carrier in Ito, and support the existence of a voltage-gated Cl^- channel in the intact rabbit cardiac PF.

M-Pos6 Cl^-/HCO_3^- EXCHANGE REGULATES INTRACELLULAR Cl^- ACTIVITY IN HYPOXIC RABBIT VENTRICLE. Scott W. N. Duncan and Clive Marc Baumgarten. Department of Physiology and Biophysics, Medical College of Virginia, Richmond, VA 23298.

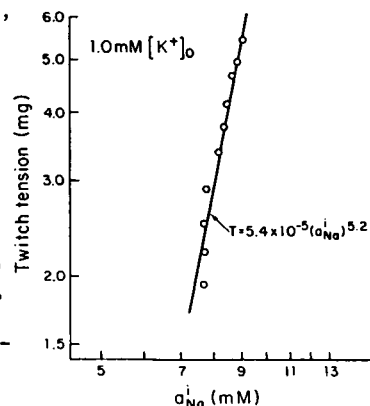
The effect of hypoxia on intracellular Cl^- activity (a_{Cl}^i) is unknown. In heart a_{Cl}^i is greater than expected from a passive distribution. Although Cl^-/HCO_3^- exchange is thought to contribute to Cl^- accumulation, removal of HCO_3^- from the superfusate has been reported not to cause a fall in a_{Cl}^i in oxygenated ventricle. Hypoxia may alter Cl^-/HCO_3^- exchange function and, therefore, a_{Cl}^i . These experiments assessed the importance of Cl^-/HCO_3^- exchange in regulating a_{Cl}^i under both normoxic and hypoxic conditions. Cl^- ion-selective microelectrodes were made with Corning 477913 liquid ion-exchanger. Right papillary muscles were superfused with HEPES-buffered or HCO_3^- -buffered Tyrode's solution. Under normoxic conditions, removal of HCO_3^- did not significantly change a_{Cl}^i (HEPES = 24.7 ± 2.0 mM, HCO_3^- = 19.7 ± 3.9 mM, $P > 0.2$, unpaired t-test). Following 90 min of hypoxia, a_{Cl}^i was not affected when HCO_3^- was present (O_2 = 19.7 ± 3.9 mM, N_2 = 20.3 ± 4.5 mM, $P > 0.2$, paired t-test). In contrast, in HCO_3^- -free media where Cl^-/HCO_3^- exchange is blocked, hypoxia caused a significant fall in a_{Cl}^i from 24.7 ± 1.9 mM to 20.3 ± 4.0 mM ($P < 0.005$, paired t-test). Similarly when Cl^-/HCO_3^- exchange was blocked with 100 μ M SITS in the presence of HCO_3^- , a_{Cl}^i fell significantly from 22.7 ± 3.5 mM to 19.8 ± 3.3 mM ($P < 0.01$, paired t-test). E_m was unaffected by all interventions. These results indicate an important role for Cl^-/HCO_3^- exchange in regulating a_{Cl}^i during hypoxia. On the other hand, the importance of the exchanger is less clear under normoxic conditions. (Supported by grants from NIH (HL-24847), Am Heart Assn (82-792) and EO and PD Sang Foundation. CMB is an Established Investigator of Am Heart Assn.)

M-Pos7 MODIFICATION OF INTRACELLULAR CALCIUM MOVEMENTS BY AMRINONE IN FERRET PAPILLARY MUSCLE. C.O. Malécot and B.G. Katzung, Dept. Pharmacology, University of California, San Francisco, CA 94143.

Electrical and mechanical effects of amrinone (A) on ferret right papillary muscles were studied in the single sucrose gap using microelectrode techniques. A was found to exert a positive inotropic effect in a dose-dependent manner (50 μ M-4 mM) when contraction was triggered by a free-running action potential. In voltage clamp conditions, A decreased the amplitude of the phasic tension at all voltages, although the inward current was increased. This dual effect of A on the phasic tension was also found with caffeine (C) 2 mM, in agreement with results reported by Goto et al. (1975) in dog papillary muscles. The descending staircase elicited in current clamp conditions after a transient increase in the frequency of stimulation can be fitted by a biexponential process in control conditions ($t_1=1.85$ sec, $t_2=27.12$ sec). A (2 mM) and C (2 mM) increased both t_1 and t_2 . A and C also decreased the ratio of post-rest to steady-state contraction, and the rest duration yielding peak force. The absolute amplitude of the first twitch after rest is almost the same with A as in drug-free conditions, but is decreased with C. The results suggest that A may modify intracellular Ca movements in addition to transmembrane Ca flux.

M-Pos8 RELATIONSHIP BETWEEN TWITCH TENSION AND INTRACELLULAR SODIUM ION ACTIVITY DURING POSITIVE AND NEGATIVE INOTROPY OF CANINE CARDIAC PURKINJE FIBERS W.-B. Im* and C.O. Lee, Department of Physiology, Cornell University Medical College, New York, N.Y. 10021.

Intracellular sodium ion activity (a_{Na}^i), twitch tension (T) and action potential of cardiac Purkinje fibers electrically driven at 1 Hz were measured simultaneously and continuously during exposures to different K^+ concentrations, $[K^+]_o$ (1.0, 2.0, and 8.1 mM), strophanthidin (5×10^{-7} - 10^{-6} M) and tetrodotoxin (10^{-6} - 5×10^{-6} M) and restoration back to normal Tyrode solution. T was plotted against a_{Na}^i and their relation was expressed by an equation of $T = \beta (a_{Na}^i)^\gamma$ as shown in the Figure which shows a relation between T and a_{Na}^i during exposure to 1.0 mM K^+ from 5.4 mM. In each experiment the data fit on a single line well and γ value was determined. During reduction of $[K^+]_o$ to 2.0 and 1.0 mM, the γ values were 4.4 ± 0.8 (mean \pm SD, $n=6$) and 4.0 ± 1.0 ($n=6$) respectively. During increase of $[K^+]_o$ to 8.1 mM, the γ value was 7.7 ± 1.9 ($n=6$). During exposure to and washout of strophanthidin, the γ value obtained was 6.1 ± 0.9 ($n=7$). Exposure to and washout of tetrodotoxin resulted in the γ value of 6.5 ± 0.5 ($n=4$). The action potential shape and diastolic potential of the fibers changed more or less depending on the experimental conditions. The results indicate that T of the fibers is a function of $(a_{Na}^i)^\gamma$ and quite sensitive to a_{Na}^i . (Supported by USPHS HL 21136).



M-Pos9 CURRENT AND VOLTAGE CLAMP STUDIES ON THE EFFECT OF COPPER IONS ON THE ELECTRICAL PROPERTIES OF FROG ATRIAL FIBERS - K.-S. Tan, Z. Jarmoc, and C.E. Challice, Departments of Pharmacology and Physics, The University of Calgary, Calgary, Alberta, Canada T2N 1N4.

Copper is an essential trace element in mammalian life, but excess intake can accumulate in the body, producing hepatic and neurological disorders. Penicillamine is used to relieve these conditions. The mechanism of these processes remains to be determined. In the present experiments 30 μ M Cu^{++} produced a decrease in amplitude of the action potential (AP), and a transient increase in duration which peaked at ~ 5 min. following introduction of the Cu^{++} . The longer the perfusion the shorter the duration. Washout with normal Ringer failed to restore the AP. Voltage clamp showed a decrease in slow inward current which was time and concentration dependent. 30 μ M Cu^{++} produced a transient increase in total outward current, also with maximum effect at ~ 5 min., with an associated decrease in membrane resistance. Continued perfusion produced a small increase in total outward current along with a decrease in membrane resistance, and a gradual increase in leakage current. At 50 μ M Cu^{++} , a small increase in total outward current and a gradual increase in membrane resistance were seen. For 20 μ M Cu^{++} , following washout, 0.1 mM penicillamine produced $\sim 90\%$ recovery of AP. < 0.75 mM allowed further decrease in amplitude; > 1.5 mM abolished AP. It is suggested that the observed decrease in AP amplitude and the biphasic changes in duration produced by Cu^{++} represent a combination of decrease in slow inward current and the changes in total outward current. The increase in leakage current is thought to represent the irreversible element in the effect of Cu^{++} . The mode of action of penicillamine is under investigation. Supported by NSERC, Canada.

M-Pos10 THE MEMBRANE POTENTIAL OF SINGLE ISOLATED HEART CELLS. H.J. Jongsma, A.C.G. van Ginneken and W.P.M. van Meerwijk. University of Amsterdam. Department of Physiology. le Constantijn Huygensstraat 20. 1054 BW Amsterdam. The Netherlands.

Single isolated heart cells beat spontaneously but very irregularly. Regular beating ensues only when a number of cells becomes interconnected. In the present communication we analyse the membrane potential variations in single isolated heart cells giving rise to this irregularity of beating. Whole cell recordings were obtained using the technique of Hamill et al. (1981). Transmembrane potentials with a maximum diastolic potential of -80 mV and an amplitude of 120 mV were measured in these cells. The duration of the action potential was very variable in some cells mainly because of differences in the duration of the plateau phase. Some of the spontaneously firing cells exhibited diastolic depolarization and some did not. Both kind of cells showed voltage fluctuations during diastole large enough to elicit an action potential. Therefore the property of diastolic depolarization is not necessary for these cells to behave like pacemaker cells. This finding explains why non-pacemaker heart cells are spontaneously active in tissue culture. Some evidence is presented to show that the voltage fluctuations causing the cells to be spontaneously active, are due to the opening or closing of one or a few ionic channels in the membrane of the relatively small cells. Aided in part by ZWO grant no: 132250. Ref.: O.P. Hamill, A. Marty, E. Neher, B. Sakmann, F.J. Sigworth (1981) Pflügers Archiv, 391: 85-100.

M-Pos11 INTERACTIONS BETWEEN TWO INHOMOGENEOUSLY COUPLED LAYERS OF CARDIAC TISSUE. R.W. Joyner, E.D. Overholt, B. Ramza, and R.D. Veenstra. Depts. of Physiology and Biophysics and Pediatric Cardiology, The University of Iowa, Iowa City, IA 52242.

Most of the Ventricular (V) endocardial surface is covered with a layer of Purkinje (P) cells which provide rapid spread of activation of the underlying V cells. We have experimentally shown that the P-V junctional region of papillary muscles is spatially inhomogeneous, with bidirectional conduction, bidirectional block, or unidirectional block between the P and V layers. We have extended our one dimensional simulations to a double layer of excitable cells with spatially inhomogeneous electrical coupling between the two layers. Our simulations show: a) homogeneous partial uncoupling can actually increase the common conduction velocity of the two layers, b) partial uncoupling at isolated junctional sites can produce successful P to V conduction at sites that would otherwise show P to V block, and c) inhomogeneous spatial distributions of coupling resistivity can simulate the observed spatial distribution of conduction pathways between the P and V layers of papillary muscles. Our theoretical spatial distributions of coupling resistivity which produce regional unidirectional block are in agreement with experimental indirect assessments of coupling resistivity between the P and V layer made by measuring the action potential duration difference for P and V cells at specific junctional and non-junctional sites. Our simulations indicate that partial electrical coupling may be a useful design feature of the heart to enhance the velocity and safety factor of ventricular activation, but further uncoupling with ischemia may provide a structural basis for arrhythmias.

M-Pos12 The antiarrhythmics Mexiletine and Disopyramide block the sodium current in single isolated rat ventricular cells. A. Yatani, Department of Physiology and Biophysics, University of Texas Medical Branch, Galveston, TX 77550.

The blocking effects of local anesthetics, Mexiletine and Disopyramide on sodium currents (I_{Na}) of enzymatically isolated rat ventricular cells were studied under voltage clamp conditions. A suction pipette was used for passing current and internal perfusion, and the membrane potential was measured by microelectrode. Potassium currents were blocked by replacing K^+ with Cs^+ in the internal and external solutions. The external Na^+ concentration was reduced to 40 mM and the temperature to 22°C to ensure good voltage control. When cells were stimulated infrequently (> 1 Hz), Mexiletine and Disopyramide produced qualitatively similar effects on I_{Na} . Both these agents decreased I_{Na} without changing the shape of the current-voltage curve. The inactivation curve of I_{Na} shifted to negative potentials. The drugs also produced lengthening of the recovery time constant and an additional use-dependent block of I_{Na} which depended on the frequency and duration of the voltage step. The use-dependent action of Mexiletine was greater than that of Disopyramide. The difference may be related to their molecular weight and lipid solubility.

M-Pos13 THE ELECTROPHYSIOLOGIC CHARACTERISTICS OF ISOLATED CANINE PURKINJE CELLS

K.W. Hewett, R.B. Robinson and B.F. Hoffman, Dept. of Pharmacology, Columbia University, NY

Free running Purkinje strands from 1-2 year old dogs were enzymatically disassociated with a 5 mg/ml collagenase solution. Transmembrane action potentials (AP) were recorded from single Purkinje cells (or occasionally chains of 2-3 cells) using 3 M KCl filled glass microelectrodes with tip resistances of 30-60 M-ohm. The cells were superfused with oxygenated physiologic saline solution warmed to 37°C. The signal was channeled through a high impedance electrometer and brief depolarizing pulses (< 1 mS and of minimal amplitude to reach threshold) were used to stimulate the cell at a basic cycle length of 1500 mS. AP characteristics were ($\bar{X} \pm \text{SE}$, n=6): maximum diastolic potential (MDP) = -89 ± 2.4 mV; AP amplitude = 129 ± 3.4 mV; dV/dt_{max} of the upstroke = 404 ± 91 V/S; AP duration at 90% repolarization = 281 ± 9.8 mS. These data are very similar to AP characteristics of the intact tissue. However, these cells appear to lack normal phase 4 depolarization. Typically the diastolic potential is flat, except for intermittent transient depolarizations of 5-10 mV which sometimes reach threshold. These depolarizations are most common in the least healthy cells (i.e. having the lowest MDP and dV/dt_{max}) and are not like classic phase 4 automaticity. Epinephrine (1 μM) and barium (0.03 mM) failed to induce phase 4 depolarization or pacemaker currents during clamp steps from -50 mV to -80 mV for 10 seconds using a single microelectrode voltage clamp. These results suggest that the electrophysiological integrity of the isolated Purkinje cell is for the most part intact. However, it must be determined whether the absence of a normal diastolic pacemaker current depends on the dispersion protocol or is an invariable characteristic of the isolated cell.

M-Pos14 SIMULATIONS OF Ca^{++} BUFFERING AND Ca^{++} EXTRUSION VIA AN ELECTROGENIC $\text{Na}^{+}/\text{Ca}^{++}$ EXCHANGER IN BULLFROG ATRIAL CELLS. D.L. Campbell, K. Robinson and W. Giles, Univ. of Texas Medical Branch, Galveston, Tx 77550 and Univ. of Calgary Medical School, Calgary, Canada T2N 4N1.

A computer program has been developed to simulate certain Ca^{++} buffering and extrusion processes in isolated bullfrog atrial myocytes. The experimentally recorded transmembrane current, $i_{\text{Ca}^{++}}$, served as the forcing function; intracellular Ca^{++} buffers (troponin, calmodulin) were included according to Robertson *et al.* (Biophys. J. 34: 559, 1981); and the Ca^{++} extrusion process was assumed to be an electrogenic $\text{Na}^{+}/\text{Ca}^{++}$ exchanger as proposed by Mullins (Am. J. Physiol. 236: C103, 1979). The effect of radial diffusion of Ca^{++} was modelled by alterations in the volume of distribution for Ca^{++} .

In response to an i_{Ca} elicited by a 100 msec voltage clamp pulse to 0 mV, the model indicates that: (1) Ca entry during i_{Ca} is sufficient to activate contraction in the absence of Ca^{++} induced Ca^{++} release; (2) both calmodulin and Ca-specific troponin sites rapidly bind Ca and are the major Ca^{++} buffers; (3) changes in free $[\text{Ca}]_i$ peak within 5-7 msec and rapidly decline thereafter; therefore, changes in E_{Ca} should not alter the inactivation gating kinetics of i_{Ca} ; and (4) during a typical diastolic interval (4 sec at -85 mV) the Na/Ca exchanger, as modelled ($r=3$ Na/1 Ca, $K_a=10$ μM), is able to remove completely the Ca that has entered. Thus, this model provides one plausible scheme for Ca^{++} regulation in a single atrial cell. At present, an ATP-driven Ca pump is not included in our model. These calculations represent a useful starting point in understanding Ca^{++} homeostasis in atrial cells.

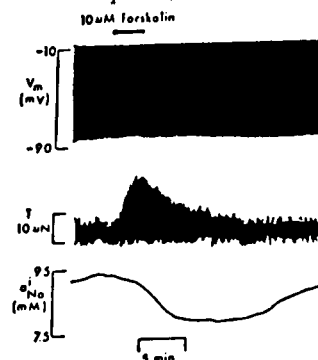
Supported by DHHS-HL-27454, AHA 81-835, and The Alberta Heritage Foundation.

M-Pos15 THE EXISTENCE OF TWO COMPONENTS OF TRANSIENT OUTWARD CURRENT IN ISOLATED CARDIAC VENTRICULAR MYOCYTES. K. Ito, J.L. Kenyon, G. Isenberg and J.L. Sutko. The Univ. Texas Hlth. Sci. Ctr., Dallas, TX 75235 and Univ. Saarlandes, D-6650 Homburg/Saar, Federal Republic of Germany.

Ryanodine (R), a putative inhibitor of SR calcium release, abolishes a component of transient outward current (TOC) in calf Purkinje fibers, which may be activated specifically by calcium released from the SR (Sutko & Kenyon, J. Gen. Physiol. 82:385, 1983). To determine if a R-sensitive current exists in ventricular muscle and contributes to species differences in action potential configuration, we examined the effects of R (1 μM) and 4-aminopyridine (4AP, 0.5 mM), which blocks a second component of TOC, on action potentials and contractions recorded from myocytes isolated from adult rat, cat and rabbit hearts. The cells were stimulated at frequencies of 0.2, 1 and 2 Hz. In rat cells, both R and 4AP slowed the rate of phase-1 repolarization; at the concentrations tested, 4AP was more effective than ryanodine. 4AP abolished the frequency dependence of the phase-1 rate, but R did not. R consistently abolished mechanical activity, while 4AP had a variable effect on this parameter. In cat cells, R was more effective than 4AP at slowing the phase-1 rate, abolishing the notch. R significantly reduced mechanical activity, while 4AP frequently increased it. In rabbit cells, phase-1 was often not clearly defined. APD20 was highly frequency dependent and was not consistently affected by R, which was also less effective in reducing mechanical activity, than in rat or cat cells. 4AP increased APD20 and potentiated mechanical activity. In preliminary voltage clamp experiments, R reduced TOC in rat and cat cells. These results suggest that two components of TOC are present to differing extents in ventricular myocardium from these species and that one component may be activated specifically by SR calcium.

M-Pos16 EFFECTS OF FORSKOLIN ON INTRACELLULAR SODIUM ACTIVITY AND ELECTROMECHANICAL PROPERTIES IN SHEEP CARDIAC PURKINJE FIBERS. S.-S. Sheu, Departments of Pharmacology and Physiology, University of Rochester Medical Center, Rochester, New York 14642.

The cellular mechanism of actions of cyclic AMP in producing inotropic and chronotropic responses on cardiac muscle still remains obscure. This is due to, in part, the lack of a specific agent that can increase intracellular cyclic AMP level without evoking multiple side effects. Forskolin, a diterpene from an Indian medical plant, has demonstrated to have unique characteristics in activating cyclic AMP generating systems in a variety of cells. I have therefore studied the effects of forskolin on electrical and mechanical properties of sheep cardiac Purkinje fibers. Intracellular sodium activity (a_{Na}^i) was also measured with a Na-sensitive microelectrode. In preparations driven at 1Hz, 1-10 μ M of forskolin caused: 1) marked acceleration of phase 4 pacemaker depolarization and, in some instances, spontaneous activity, 2) elevation of the plateau to more positive potential, 3) significant increase of twitch tension, and 4) reduction of intracellular sodium activity. These results suggest that forskolin has interesting pharmacological actions on the cardiac muscle. It may be an extremely useful tool for investigating how intracellular cyclic AMP is able to modulate several physiological functions of cardiac muscle.



M-Pos17 ANALYSIS OF REPOLARIZATION CURRENTS IN CHICK EMBRYONIC HEART CELL AGGREGATES. Alvin Shrier¹, John R. Clay² and Richard M. Brochu^{1*}. ¹Dept. of Physiology, McGill University, Montreal, PQ, Canada H3G 1Y6 and ²Lab. of Biophysics, NINCDS, NIH at the MBL, Woods Hole, MA 02543. (Intr. by D.E. Goldman).

We have measured repolarization currents in aggregates of cells derived from the atria of 7-14 day old chick embryonic hearts using the two microelectrode voltage clamp technique. We have found two kinetically distinct potassium current components. One component is activated in the -55 to -30 mV voltage range (I_{x1}). The other component is activated between -20 and +20 mV (I_{x2}). The I_{x2} response to a 5 sec duration depolarizing step from a holding potential of -25 mV and the tail current upon return to -25 mV are both adequately fitted by a single exponential curve. The I_{x2} time constants as a function of voltage describe a bell-shaped curve having a maximal value of about 0.9 sec at $V=0$ mV. The I_{x2} current-voltage relation is approximately a linear function of driving force. The I_{x1} component is also described by a single exponential process with a maximal time constant of about 0.7 sec at -40 mV. The I_{x1} current-voltage relation inwardly rectifies and it has negative slope conductance for $V > -50$ mV. These preparations do not have a time-dependent pacemaker current. The I_{x2} component together with the slow inward component (I_{si}) underlie the plateau phase of the action potential. The I_{x1} component underlies the rapid repolarization phase of the action potential. We did not observe significant changes with development in either I_{x1} or I_{x2} during the 7-14 day incubation period. Supported by a grant to A.S. from the MRC, Canada.

M-Pos18 THE SIALIC ACID CONTENT AND THE ELECTROPHORETIC MOBILITY OF CULTURED BRAIN CELLS. V. Aleman, C. Argüello and E. Morales. "(Intr. by Dr. Jose Luis Saborio)". Lab. of Neurochemistry, Department of Neuroscience. CINVESTAV, Apdo. Postal 14-740, Mexico, D.F. 07000.

The electrophoretic mobility of a cell depends on the positive or negatively charged chemical groups located in the outer surface of the plasma membrane. It is known that sialic acid has an important contribution on the electrophoretic mobility of some cells such as erythrocytes, lymphocytes, etc. Glioblasts and neurons at the fourth and seventh day of culture showed the highest content in sialic acid: 18 and 16 nanomoles/mg of protein, respectively. At these days of culture, we determined the influence of the negative charge and in particular the effect of the carboxyl group from sialic acid on the electrophoretic mobility of rat astroblasts ($1.078 \mu\text{sec}^{-1} \text{V}^{-1}\text{cm}$), morphologically differentiated astrocytes (0.930), as well as chicken neurons (1.261). Electrophoretic mobilities were greater for neurons than for astroblasts. This effect was measured both in the control and neuraminidase treated cells. In both types of cells, neuraminidase treatment decreased the electrophoretic mobility in a statistically significant manner ($P < 0.001$); however, this change was greater in the case of neurons. The electrophoretic mobility of glioblasts transformed by a brain extract was higher than in control cells and again when these cells were treated with neuraminidase, their electrophoretic response decreased. When glioblasts and neurons were treated with phospholipase C, their electrophoretic mobility decreased (10 and 2.2% respectively) to a less extent than with neuraminidase. That neuraminidase treatment was effective in removing sialic acid, was tested by measuring the total sialic acid cell content before and after the enzyme treatment. In all cases there was a correlation between the amount of sialic acid released by the enzyme and the change in cells electrophoretic mobilities.

M-Pos19 DETECTING COOPERATIVITY IN NEURONAL POPULATIONS. George L. Gerstein, Donald H. Perkel and Judith E. Dayhoff, Dept. Physiology, Univ. Pennsylvania, Philadelphia, PA 19104

Recent advances in techniques for recording impulses from individual nerve cells allow simultaneous observation of substantial populations of neurons. In such a recording, a group of over 20 individual spike (impulse) trains (each from a different cell) can be obtained over the same period of time. In such multichannel data, it is important to detect cooperative behavior among groups of neurons; such cooperative behavior may relate to experimental and behavioral parameters. Traditional spike-train analysis techniques only detect pairs or triples of cooperating neurons. When larger numbers of neurons are recorded, the combinatorial possibilities make the computations impractical with traditional methods.

A new analysis method has been developed that detects, in a set of simultaneously recorded nerve cells, groups of cells that tend to fire together. The method does not require a priori knowledge of the identities of the neurons in such a "functional group". The strength of the cooperative behavior is estimated by the analysis results. More than one functional group can be detected at the same time.

The calculation is based on a gravitational clustering model. Each neuron is represented as a point in n -dimensional space. The impulse train of each neuron is converted into a time-varying "gravitational charge" for the corresponding point. Those points that represent functionally related neurons "gravitate" into clusters. The method has been implemented on a computer, and its effectiveness has been demonstrated on simulated spike-train data containing known functional groups.

M-Pos20 MATHEMATICAL MODELS FOR DIFFUSION IN CYLINDRICAL CELLS AND MEMBRANES. Charles Gravis* & Shinpei Ohki, Dept. of Biophysical Sciences, SUNY at Buffalo, NY 14214.

There are a number of models that have been proposed over the years for diffusion into various cylindrical geometries which have been used to represent, for example, experimental systems all the way from seminiferous tubules to tubular membrane (hollow fiber) enzyme reactors. Examination of the microanatomy of giant axons led to a consideration of these models for the purpose of selecting a model for particular application to diffusional uptake of local anesthetics (LA) into axons. One particular model was selected, a special case falling between these others. The model chosen is one of diffusion into a solid cylinder with a permeability barrier or resistance on its exterior, corresponding to the axonal membrane. The diffusion equation for this model was solved; however, the solution may also be derived as a special case from the more general works existing in the literature, such as those alluded to above. The values of the parameters, corresponding to the diffusion coefficient of the axoplasm and the permeability of the membrane to LA, that arise from the fit of this model to experimental data from axons will be presented; they compare favorably with values obtained from other models by investigators using different techniques.

M-Pos21 THE NOISE PRODUCED BY PATCH ELECTRODES: A MODEL. F. Sachs, Dept. of Biophysical Sciences, SUNY, Buffalo, NY USA, 14214.

Current techniques of single channel recording involve sucking a small bleb of membrane into the tip of a glass pipette. Three observations suggest that there is no chemical bond between the glass and the membrane. The resistance of this sealed tip can be on the order of tens of Gohms, which although large with respect to the open pipette resistance, is much less than that expected for a few square micra of bilayer. The noise recorded from a membrane-sealed patch electrode is greater than that expected from the equivalent source resistance, and finally, small amplitude, ionic channel events can be observed which charge and discharge on millisecond time scale, in the presence of other channel events that charge and discharge on a time scale limited by the instrumentation. These observations can be explained by a model for the patch electrode tip in which a finite length of the membrane bleb is closely apposed to the glass, but a high conductivity pathway (saline) exists between the glass and the membrane. The electrical equivalent of the above structure is a finite length lossy electrical cable. The input resistance of this cable is primarily a function of the glass-membrane spacing and the resistivity of the solution in that space. Thermal noise of the patch is proportional to the real part of the admittance, which increases with frequency due to shunting across the membrane capacity. For reasonable values of parameters, i.e., a space of 20Å, a space resistivity of 200 ohm-cm and a membrane capacitance of 1uF/cm², a bleb 5 micra in length with a diameter of 2 micra will produce Gohm seals and appropriate values of noise. The slowly charging channel currents can be explained by channels which are located between the membrane and the glass.

M-Pos22 A COMPARISON OF THE LIGHT SIGNAL FROM AEQUORIN WITH THE OUTPUT OF A CALCIUM ELECTRODE WHEN BOTH ARE IN A SQUID GIANT AXON. J. Requena, J. Whittembury and L. J. Mullins. Centro de Biociencias, Instituto Internacional de Estudios Avanzados (IDEA) Caracas, Venezuela, Universidad Peruana Cayetano Heredia, Lima, Peru and Department of Biophysics, University of Maryland School of Medicine, Baltimore.

Calcium-sensitive capillary electrodes (OD 140 µm) were filled with ETH 1001 and PVC. These electrodes had a Nernstian response to Ca to 100 nM and a substantially reduced slope between 10 and 100 nM. Such electrodes were introduced axially into squid giant axons previously injected with aequorin. The two indicators of axoplasmic [Ca] were compared both under resting conditions and following procedures that increased Ca entry into the axon. It was possible to stimulate the axon and record an increase in aequorin glow without any change in the Ca electrode reading. This finding presumably is an indication that the Ca increase is highly local and far from the electrode. Other procedures for Ca loading (Na-free solutions or high K solutions) resulted in an increased aequorin glow of some 50-fold before the Ca electrode began to respond. After the electrode responded, it followed the continually increasing aequorin response. Substances such as FCCP cannot be used to release stored Ca from mitochondria as they affect the Ca electrode; the application of CN which also releases stored mitochondrial Ca also showed that aequorin light emission increased substantially before there was any change in the Ca electrode. (Aided by grants BNS 76-19718 from the National Science Foundation.

M-Pos23 WATER AND PROTON INVOLVEMENT IN THE STRUCTURE AND FUNCTION OF BIOLOGICAL SYSTEMS AS REVEALED BY NON-DESTRUCTIVE TECHNIQUES.

V. Vasilescu, Eva Katona, Cornelia Zaci, Constanța Ganea and Mioara Tripsa, Department of Biophysics, Medical Faculty, Bucharest, Romania

Systematical studies on the mobility properties of water and water protons in several biological systems by various non-destructive techniques revealed at least 3 water molecule populations. As a conclusion the existence of a multicompartamental distribution of water in biological systems is pointed out. Sizes and properties of different water compartments are disclosed to be dependent on the state of system in physiological and pathological conditions.

Survey of experimental data concerning antagonism of different proton donors and acceptors as concerns their action on the excitable membrane structure and function, allows us to discuss physico-chemical and enzymatic mechanisms of these antagonisms.

Taking into account compartmental distribution of water and the antagonisms observed, mechanisms of anesthesia settling are examined.

M-Pos24 UNSTIRRED LAYERS IN SERIES WITH POROUS MEMBRANES: INFLUENCE ON THE OBSERVED WATER DIFFUSIONAL PERMEABILITY. J. Wietzerbin, F. Morin, J. Merot and M. Parisi. CEN Saclay, Dept. Biologie, Gif-sur-Yvette, 91191. FRANCE.

The observed diffusional permeability (W') for a solute crossing a membrane bounded by symmetric unstirred layers is given by

$$1/W' = 1/W + 2/W^0 \quad (1)$$

where W and W^0 are respectively the membrane and unstirred layers permeabilities for the solute. If D^0 is the diffusion coefficient in water of the tested molecule and d the unstirred layers thickness, assumed equal at both sides of the membrane, it follows $1/W' = 1/W + 2RTd/D^0$ (Ginsburg and Kachalsky, 1963) (2)

In "black box" conditions, the total surface (A) is generally considered as been the site for the permeation process. This is not the case when a small channel is open in a relatively large exposed area. In this situation equi-concentration points for the tested molecule will define an hemispheric shape around the channel, rather than parallel surfaces to the total membrane area. Then W' could be defined by

$$1/A W' = 1/a W_c + 2/a' W^{0*} \quad (3)$$

where a is the channel area, W_c the channel permeability, a' the hemispheric surface defined by the points where the concentration gradient around the channel vanished and W^{0*} is the equivalent permeability of the hemispheric volume in series with the channel and defined by a' . If we have a membrane having n channels sufficiently separated ones from the others to disregard interactions between the concentration profiles established around each channel, we will have:

$$W' = (1/a W_c + 2/a' W^{0*})^{-1} \cdot n/A \quad (4)$$

If we increase the channels density, we will arrive to the limite situation described in ec 1, where all the membrane surface permeability is changing. This analysis could be relevant in the case of biological membranes that change its water permeability by inserting channels that cover a small fraction of the total cell area.

M-Pos25 ELECTROPHYSIOLOGICAL PROPERTIES OF THE MACROPHAGE-LIKE CELL LINE J774.1. Paul Sheehy and Elaine K. Gallin, Physiology Departments, Uniformed Services University of Health Sciences and Armed Forces Radiobiology Research Institute, Bethesda, Maryland.

The macrophage-like cell line J774 has been extensively studied as a model of macrophage function. Electrophysiological properties of J774.1 cells were determined using intracellular microelectrodes containing either 3M KCl or K Acetate (80-150 Mohms). Cells exhibited a wide range of resting membrane potentials (-8 to -91 mV) averaging -50.8 ± 3 SEM ($n = 55$). The lower values of membrane potentials probably reflect microelectrode-induced cell damage. Average input resistances and time constants were $117 \text{ Mohms} \pm 13$ and $19 \text{ ms} \pm 3$, respectively. The specific membrane resistance, calculated from the time constant assuming a specific membrane capacitance of $1 \mu\text{F}/\text{cm}^2$, was 19 Kohms cm^2 . In some studies, cells were irradiated (2 krad, 500 rad/min, ^{60}Co) to block cell division. Irradiated cells remained phagocytic but more than doubled their size within 4 days, thus becoming better subjects for intracellular recordings. These cells had resting membrane potentials, input resistances, and time constants of $-60.1 \text{ mV} \pm 4$ (range -18 to -92, $n = 26$), $94.5 \text{ Mohms} \pm 15$ and $27 \text{ ms} \pm 6$, respectively. Many irradiated and control cells exhibit nonlinear I-V relationships characterized by prominent inward rectification and a high resistance or unstable region in the range of -60 to -40 mV, similar to that previously reported in normal mouse macrophages (Gallin, 1982). Addition of BaCl_2 eliminated both the inward rectification and the high resistance region. Spontaneous slow hyperpolarizations associated with an increase in conductance similar to those previously noted in primary macrophage cultures were seen in a few J774.1 cells. These data indicate that J774.1 cells exhibit electrophysiological properties similar to those of primary cultures of mouse macrophages, and may thus serve as a useful model for studies correlating macrophage effector functions with identified membrane ionic conductances.

M-Pos26 ANALYSIS OF A CANONICAL SET OF PATCH CLAMP CONFIGURATIONS WITH COMPENSATION OF PIPETTE RESISTANCE (R_p) AND FEEDBACK RESISTANCE (R_f).

Ronald Millecchia and Gunter N. Franz. Dept. Physiology, West Virginia University Medical Center, Morgantown, WV 26506.

The clamps studied were a canonical set of single-amplifier clamps (Franz and Frazer, *Bioph. J.* 37: 73a, 1983) of the inverting ("I") type (e.g. Zilberter, Timin, Bendukidze, and Burnashev, *Pflugers Arch.* 394: 150-155, 1982), the non-inverting ("N") type (eg. Hamill, Marty, Neher, Sakmann, and Sigworth, *Pflugers Arch.* 391: 85-100, 1981), and a novel bootstrap ("B") type. This set of clamp circuits was applied to two common patch-clamp preparations, the isolated membrane patch and the whole-cell preparation. Open-loop and closed-loop responses of idealized circuits and circuits with parasitic elements were determined. We also investigated the effect of current feedback for the compensation of (1) pipette resistance (R_p) and (2) pipette and feedback resistance (R_f). Compensation criteria were developed for "incomplete" (R_p) and "complete" (R_p , R_f) compensation (Franz and Frazer, *Bioph. J.* 41(2, pt. 2): 399a, 1983). We present formulas adapting these criteria to the presence of parasitic elements and practical current measurement methods. "Complete" compensation significantly improves clamp fidelity.

M-Pos27 THE EFFECTS OF PARASITIC CIRCUIT ELEMENTS AND AMPLIFIER CHARACTERISTICS ON STABILITY AND FIDELITY OF GAP VOLTAGE CLAMPS.

Gunter N. Franz, Ronald Millecchia, and David G. Frazer. Department of Physiology, West Virginia University Medical Center and Lab. Investig. Branch, Div. of Respir. Dis. Studies, NIOSH/CDS/PHD Dept. of Human Health Services, Morgantown, WV 26506.

We investigated three types of circuits taken from a canonical set of clamp schemes (G.N. Franz and D.G. Frazer, *Bioph. J.* 37 (2, Pt. 2): 73a, 1982), i.e. "inverting" and "non-inverting" clamps in double- and triple-gap versions, and triple-gap "bootstrap" clamps. We present formulas and frequency response plots describing the effects on open-loop gain (stability) and closed-loop response (fidelity) of the following types of parasitic elements: seal or gap admittance, amplifier input capacitance, stray capacitance, and membrane admittance in the ancillary B-pool of triple-gap clamps. Requirements for amplifier characteristics ensuring stability and acceptable fidelity in the presence of parasitic circuit elements are presented.

M-Pos28 POLYMER-INACCESSIBLE SPACE AS A MEASURE OF THE VOLUME CHANGE DURING CHANNEL OPENING AND CLOSING: VDAC CHANNELS. J. Zimmerberg and V. A. Parsegian, Physical Sciences Lab., DCRT, NIH, Bethesda, MD 20205

Models of channel conductance control assume either site blockage at one point in an ion's path or a general closing down of the channel space by pore molecule rearrangement. These two classes of models suggest qualitatively different changes in channel volume (V) upon closing, i.e., in $\Delta V = V_{\text{open}} - V_{\text{closed}}$.

To find ΔV for the VDAC (voltage dependent anion channel), we put impermeant polymer on both sides of VDAC-containing bilayer membranes (M. Colombini, 1983. *J. Membr. Biol.* 74:115-121) to exert an osmotic pressure π to create an additional work $\pi\Delta V$ against channel opening. For VDAC, the probability that a channel is in the open vs. the closed state is, as a function of the transmembrane voltage ψ , of the form $(n_o/n_c) = A \exp(-(b|\psi|)/kT)$ (S. J. Schein, M. Colombini, and A. Finkelstein, 1976. *J. Membr. Biol.* 30:99-120). In the presence of osmotic stress, this ratio is modified to $\exp[-(b|\psi| + \pi\Delta V)/kT]$. The volume change ΔV is then obtained by comparing different transmembrane voltages ψ for equivalent conductance levels with different applied osmotic stress π .

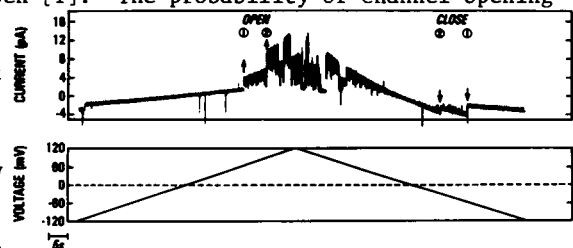
The ΔV we measure for VDAC supports a model with large changes in channel volume rather than gating control at a specific point.

We are applying this method of measurement to other biological channels in both cellular and reconstituted membranes.

M-Pos29 TETANUS TOXIN CHANNELS IN GANGLIOSIDE CONTAINING LIPID BILAYERS ARE VOLTAGE DEPENDENT

H. Borochoy-Neori, T. Delbruck, E. Yavin and M. Montal (Intr. by R.E. Greenblatt), Depts. of Biology and Physics, University of California at San Diego, La Jolla, CA 92093

The interaction of tetanus toxin (TT) with gangliosides (G) produces ionic channels in lipid bilayers which are cation selective and preferentially open [1]. The probability of channel opening (P) depends on the applied voltage (V) (Figure). P is significant only at $V > 50\text{mV}$ and increases with V . Once activated, the TT channel remains temporarily active at negative V : A switch from positive to negative V promotes channel closing with a relaxation time in the range of seconds. Channel re-opening upon a reverse polarity switch is not instantaneous. Thus, negative V inactivates the TT channel. Inactivation may result from voltage induced conformational change or from the depletion of protein from the bilayer. Our present data favor the first mechanism. Thus, TT forms a voltage dependent, cation selective and ganglioside specific channel. This channel may account for some aspects of the known action of TT *in situ*, i.e. disinhibition of neuronal transmission. Supported by NIH. [1] Borochoy-Neori, et al. (1984) *Biophys. J.* 45, January.



Legend: Membrane currents through a G-containing asolectin bilayer treated with TT: Response to a continuously cycled V from -120mV to 120mV . Conditions: 0.5M NaCl , 10mM Hepes , $\text{pH } 7$. The compartment *trans* to TT is defined as being at zero potential.

M-Pos30 THE EFFECT OF HIGH PH, LOW IONIC STRENGTH AND EXTERNAL Ca^{++} CONCENTRATION ON THE K^{+} PERMEABILITY OF HELA CELLS: SINGLE CHANNEL AND MEMBRANE POTENTIAL MEASUREMENTS. C. Simoneau*, R. Sauvé and G. Roy. Department of Physiology, Univ. of Montreal, Montreal, Canada, H3C 3J7.

We have investigated using the extracellular patch clamp method and transmembrane potential measurements with standard 3M KCl microelectrodes, the effect of external pH, calcium concentration and low ionic strength on the ionic permeability of HeLa cells. At high external pH (9.0) or low ionic strength it was found that the resting potential of these cells shifted from its normal average value of -38mV to -70mV. This hyperpolarization was not observed in the absence of external Ca^{++} but could be induced at normal pH (7.2) if 10 mM or more of Ca^{++} was present in the external medium. Quinine and Ba^{++} were effective in abolishing all pH or Ca^{++} induced hyperpolarizations. When patch electrodes filled with normal saline at pH 7.2 or pH 9 were used in the cell-attached configuration, outward K^{+} current jumps could in both cases be clearly detected. From these experiments we were able to show that an increase in external pH does not modify the channel I/V characteristics, but increases substantially, P_o , the channel probability to be open. Moreover the I/V curves obtained at both pH were not inward rectifying as those reported for the K^{+} currents measured in HeLa cells with patch electrode filled with various KCl solutions (Sauvé et al., 1983). Outside out experiments were also carried out with patch electrodes containing (in mM) 150 KCl + 1 CaCl_2 buffered at pH 7.2. The external medium was perfused with salines at pH 9 with (1.8 mM) and without Ca^{++} . We could observe a systematic increase in single channel activity whenever Ca^{++} was present in the external medium. It may thus be concluded from these results that HeLa cells have a K^{+} channel which can be activated at high external Ca^{++} concentration. Higher external pH increases the interaction of Ca^{++} on this particular channel. (J. Mem. Biol. 74-41).

M-Pos31 GAP JUNCTIONS: TWO VOLTAGE DEPENDENT GATES IN SERIES ALLOW VOLTAGE INDUCED STEADY STATE

CYCLING AROUND A CIRCULAR REACTION SCHEME. M.V.L. Bennett, D.C. Spray, Einstein Col. Med., Bx. NY 10461

Gap junction conductance (g_j) between amphibian blastomeres is decreased by transjunctional voltage (V_j) of either sign. Effects of sudden reversal of V_j suggest that two gates are in series (Harris et al., J. gen. Physiol. 77:95, '81). Series gates allow a single channel to exist in four states, both gates open, either gate closed and both gates closed, with the diagrammed circular reaction scheme where O is open, C is closed and the subscript is one or the other gate. We assume that all of V_j acts on a closed gate in series with an open gate and that $V_j/2$ appears across each of two closed gates in series or two open gates in series (the polarity being opposite for series gates). Qualitatively, V_j of sign that opens gate 1 and closes gate 2 drives the system towards the lower state $O_1 C_2$. In the upper left reaction, opening of gate 1 is driven by the entire V_j and closing of gate 1 by $V_j/2$. The reactions of gate 1 on the lower right are driven by smaller voltages, because gate 2 in series is closed. The voltages are $V_j/2$ for opening and zero for closing. Corresponding changes in gate 2 on the lower left and upper right are similarly less affected by V_j on the upper right where gate 1 in series is closed. Thus V_j moves the channels towards $O_1 C_2$ on both sides of the reaction scheme, but less strongly on the right where forward rates are less increased and back rates are less decreased. Calculations from approximate reaction rates (ibid.) for V_j opening gate 1 and closing gate 2 show that, in steady state, counter-clockwise transitions exceed clockwise transitions by c.5%. Similar but possibly larger effects are predicted for squid blastomeres where V_j increases g_j that has been lowered by increased cytoplasmic acidity. The results do not contradict microscopic reversibility. Although cycling is dissipative, it is driven by the applied voltage.

M-Pos32 VOLTAGE-GATED CHLORIDE-SELECTIVE CHANNELS IN CULTURED CHICK SKELETAL MUSCLE. J.A. Steele Department of Physiology, University of Alberta, Edmonton, AB T6G 2H7.

Chloride currents were recorded under voltage clamp from cultured chick skeletal muscle using the whole-cell patch clamp technique. Small diameter myoballs (10-25 μ) were grown by including 10^{-8} M colchicine in the media on day 2 of the culture. Suction electrodes were pulled from Radnoti microstar capillary tubing and filled with 20mM TEA, CsCl solutions (2-5 mO). 10^{-7} M TTX and 1.0mM Cd^{++} were added to the bath. During step depolarizations from -60mV, an inward current developed slowly (time to steady-state of 300 ms or more at -25mV). The current did not decline under maintained depolarization. Decline of the current upon repolarization to -60mV was slow with a half-time of 0.8 to 2 sec and complete. The current trace was flat at the reversal potential indicating successful block of other currents. Alterations in Cl^{-} concentrations (partial replacement with $\text{CH}_3\text{SO}_4^{-}$) resulted in shifts of the reversal potential which followed the values predicted by the Nernst relation. The current was blocked reversibly by SITS (2mM) and SCN^{-} (5mM) and blocked irreversibly by DIDS (10 μ M). Current density ranged from 3 to 30 $\mu\text{A}/\text{cm}^2$. Single channel events were recorded in outside-out excised membrane patches. Single channel conductance was ~ 30 pS (symmetrical 150mM Cl^{-}). Channel density was calculated to be less than one channel per square micron. The chloride channels are responsible for depolarizing the membrane during the long duration action potentials (10-20 sec) present in embryonic muscles during the last week of *in ovo* development.

Supported by Alberta Heritage Foundation for Medical Research.

M-Pos33 ION CHANNEL PHENOMENOLOGY RECONSTITUTED FROM LIVER GAP JUNCTION PREPARATIONS.

E. C. Lynch, A. Harris and D. Paul, Marine Biological Laboratory, Woods Hole, Mass.

Morphologically pure gap junctions, isolated by the procedure of Fallon and Goodenough¹, (with the addition of DFP to the detergent solutions), were reconstituted into liposomes and exposed to planar bilayers. We observed, under voltage clamp conditions in Ca^{+2} free ionic solutions, unit ion channels (150-220 pSiemens in .1M NaCl) that were voltage dependent and very poorly cation selective; ($p[\text{Na}^+/\text{Cl}^-] < 2.0$) and ($p[\text{Na}^+/\text{K}^+] = 1.0$). These channels were introduced into the membrane by potential pulses (± 80 -150 mV) and exhibited lifetimes on the order of seconds to minutes. Under certain conditions (pH, ionic strength, symmetry of protein addition), this "singlet" appeared to associate in the membrane to form a functional conducting "triplet" (500-650 pSiemens in .1M NaCl) that exhibited an increased channel lifetime (many minutes to hours) and an increased sensitivity to voltage ($V_o = \pm 40$ -60 mV), with units exhibiting open to closed transitions in steps of three. "Triplets" exhibited a permselectivity similar to that of the "singlet". Macroscopic conductances introduced into the membrane bathed by Mg, EGTA solutions indicated that the channel was permeable to the MgEGTA^{-2} complex (M.W = 404). Thus, we have demonstrated, in preparations of liver gap junctions, a voltage dependent, poorly ion selective channel of large conductance, which can associate into functional triplets and is also permeable to large multivalent ions. The relationship that this conducting unit bears to the physiologic entity of the gap junction (which is a low resistance path across two bilayer membranes in apposition) remains to be clarified.

(Supported by the Marine Biological Laboratories, Woods Hole, Mass. 02543)

¹Fallon, R.F., and Goodenough, D.A. (1981). J. Cell Biol. 90 521-526.

M-Pos34 COLICIN E1 CHANNELS AT LOW pH GATE IN MILLISECONDS AND INACTIVATE. Stephen Slatin and Alan Finkelstein, Albert Einstein College of Medicine, Bronx, N.Y. 10461

The E1 group (E1, A, K, Ia...) of colicins are proteins which form channels in planar lipid bilayers. The sequence of colicin E1 is known, and the channel-forming part of it is wholly contained in the C-terminal 152 amino acids. The macroscopic conductance induced by colicin E1 is both voltage and pH dependent. At low pH (3.5) several interesting properties of this conductance manifest themselves which are not seen at higher pH (>4.5): 1) The off rate kinetics occur on a time scale of milliseconds, whereas the on rates remain on a time scale of seconds. 2) All of the voltage dependence of the steady state conductance occurs between ± 30 mV; outside of this range all channels are either on ($V > 30$ mV) or off ($V < -30$ mV). [Potentials refer to the side to which colicin is added.] 3) For large positive voltages (>80 mV), channels turn off after first turning on, i.e., they inactivate. At +200 mV, the inactivation occurs in a few milliseconds. Inactivated channels are clearly not in the usual off state, since they do not turn on again with the same kinetics. These results imply that at pH 3.5 colicin E1 behaves much like voltage gated channels of excitable tissue.

(Supported by NIH GM 29210 and 5T32NS07183)

M-Pos35 EFFECTS OF HISTIDYL MODIFICATION ON THE CHANNEL PROPERTIES OF THE C-TERMINAL TRYPTIC PEPTIDE OF COLICIN E1. F.S. Cohen, L.J. Bishop, W.A. Cramer. Rush Medical College, Department of Physiology, Chicago, Illinois and Purdue University, Department of Biological Sciences, W. Lafayette, Indiana. Introduced by C.L. Schauf.

Colicin E1 is a water-soluble bactericidal protein with a known amino acid sequence, M.W. = 57,279, that forms voltage-dependent channels in planar bilayer membranes. The channel-forming domain has been found to reside in a C-terminal 187 amino acid tryptic fragment, M.W. = 20,000, that contains 2 histidyl residues which have been reacted in solution with diethylpyrocarbonate (DEP). The opening and closing of channels as a function of voltage, determined by measurement of macroscopic current at pH 4 or 6 in membranes made from asolectin, was not affected by histidyl modification. The requirement of a trans-negative membrane potential for macroscopic current, and the increase in the rate of channel opening at pH 4 relative to 6, was the same with control and DEP-modified fragment. For both polypeptides, when trans-positive potentials were applied, channels close at a faster rate at pH 4 compared to 6. The properties of the conducting channels were, however, affected by the chemical modification. The reversal potentials were 37 mV and 24 mV (Na^+ over Cl^-) for the 20 kDa fragment and the modified protein, respectively, in 1 M NaCl vs. 0.1 M NaCl, pH 6.0. The single channel conductance of the 20 kDa fragment is 20 pS for +30 mV, whereas for the modified protein it is 8 pS for -30 mV (trans-negative) and 13 pS for +30 mV in 1 M NaCl, pH 6.0. This rectification suggests that the bulky N-carboxy-histidyl residues, which reduce the single channel conductance, are located toward the cis side. (Supported by NIH grants GM-31039 and GM-18457).

M-Pos36 CHEMICAL MODIFICATION OF SPECIFIC HISTIDYL AND CYSTEINYL RESIDUES IN THE CHANNEL FORMING DOMAIN OF COLICIN E1. L. J. Bishop, V. L. Davidson, and W. A. Cramer, Department of Biological Sciences, Purdue University, W. Lafayette, IN 47907 (Intro. by T. Baker)

A 20 kDa tryptic fragment of colicin E1 contains the channel forming domain of the molecule. Modification of the two histidyl residues in the 20 kDa fragment by the addition of a carbethoxy group with diethylpyrocarbonate (DEP) results in a 2-3 fold increase in activity as assayed by Cl^- efflux from asolectin vesicles. Specificity of the modification for the 2 His residues was documented by spectrophotometric analysis and complete reversibility by incubation with NH_2OH of DEP-induced alterations of activity. The increase in activity was not due to increased binding of modified fragment to vesicles. The modified protein exhibited the same pH dependence for activity as the unmodified fragment. The activity of the unmodified fragment increased 2-3 fold as the K^+ -diffusion potential was changed from +45 mV to -60 mV (trans-negative). This voltage-dependence was not observed with the modified fragment, possibly due to the increase in conductance of the modified fragment at trans-positive potentials facilitating a more rapid Cl^- efflux.

The reactivity of the sole cysteine in colicin, residue 505, was tested with 5,5'-dithiobis-2-nitrobenzoic acid (DTNB), and the -SH reactive fluorescence probe 3-(4-maleimidylphenyl)-7-diethylamino-4-methylcoumarin. Cys 505, 17 residues from the C-terminus, was not accessible in the native protein, but 100% modification was possible in 8M urea. The *in vitro* activities of colicin and the fragment, and the *in vivo* activity of colicin, were not significantly altered by DTNB, indicating that Cys 505 is not critical for activity. (Supported by NIH grant GM-18457.)

M-Pos37 A MODEL FOR THE ACIDIC pH REQUIREMENT OF COLICIN E1 ACTION ON ARTIFICIAL MEMBRANE VESICLES. V. L. Davidson and W. A. Cramer, Department of Biological Sciences, Purdue University, W. Lafayette, IN 47907 (Introduced by M. G. Rossmann)

The bactericidal protein, colicin E1, requires a low pH to form ion channels in artificial membranes. This effect resembles the pH dependence in vitro of the action of diphtheria and tetanus toxins, and suggests that an explanation of this pH effect may reflect a general molecular mechanism for insertion of these proteins into membranes. Binding to asolectin vesicles by colicin E1 and a 187 residue C-terminal tryptic fragment of the colicin which contains in vitro activity was assayed by trapping vesicles on membrane filters after incubation with [³H] leucine-labeled colicin and fragment. For colicin, maximal binding was observed at pH 4.0, little binding was seen at pH > 5.5, and the effective pK for binding was ~4.6. The pH titration curve for binding corresponds very closely to that for colicin activity assayed by monitoring colicin-induced Cl⁻ efflux from vesicles. A pH titration curve for binding of the C-terminal fragment also corresponded with that for in vitro activity of the fragment, and was shifted downward approximately 1.0 pH unit, with an effective pK < 3.8, relative to that for the colicin. The fragment exhibits time-dependent binding at pH values above the optimum pH. Bound colicin was not displaced from the vesicles by washing with up to 2.0M NaCl, suggesting that at least part of the protein has inserted into the membrane. These data imply that one or more carboxyl residues must be protonated for effective binding and insertion into the membrane. (Supported by NIH grant GM-18457).

M-Pos38 BROWNIAN DYNAMIC SIMULATION OF ION MOVEMENT THROUGH CHANNELS. Peter Gates, Kimbal Cooper, Eric Jakobsson, Department of Physiology and Biophysics, University of Illinois, Urbana, IL 61801.

Diffusion of Ions through single-file selective channels can be simulated by the method of Brownian dynamics. The differential equation describing the ion movements in the channel is the microscopic stochastic analogue of the Nernst-Planck equation, i.e., the Langevin equation. It is less obvious how to calculate correctly the process by which ions enter the channel from the bath. The algorithm is tested by requiring it to conform to equilibrium constraints.

We present an entry algorithm that we have not been able to prove wrong on thermodynamic grounds. In particular, the algorithm gives zero net flux at the Nernst potential and distributes ions properly according to the Boltzmann relationship in fields produced by inserting a stationary charge in the channel. In this algorithm entering ions "see" the electrostatic force associated with ions in the channel but the ions in the channel do not "see" a force associated with ions in the bath due to shielding by counter ions. Various flux and ion distribution calculations are presented using this method of calculating entrances. We are at present considering the problem of taking into account image and membrane channel structural charges, for which the Brownian dynamic method is inherently more accurate than either bulk electrodiffusion or Eyring rate theory. This work has been supported by the Bioengineering Program, the Department of Physiology and Biophysics, the Research Board of the University of Illinois, and by the Cellular and Molecular Biology Training Grant No. PHS 5T32 GM07283.

M-Pos39 PROTON/HYDROXIDE TRANSPORT THROUGH LIPID BILAYER MEMBRANES. John Gutknecht, Physiology Department, Duke University, and Duke University Marine Laboratory, Beaufort, NC 28516.

Six recent studies of H/OH permeabilities of phospholipid bilayers have reported values ranging from 10^{-9} to 10^{-4} cm/sec. The purpose of the present study is to explain this large discrepancy and elucidate the mechanism(s) of H/OH transport through lipid bilayer membranes. Planar lipid bilayers were formed from decane or tetradecane solutions of natural or synthetic phospholipids, e.g., bacterial phosphatidylethanolamine and diphytanoylphosphatidylcholine. A pH electrode and electrical conductance techniques were used to measure H/OH fluxes over a wide range of pH. At low pH and high $[Cl^-]$, large nonconductive proton fluxes were produced by the diffusion of molecular HCl, which has a permeability coefficient of about 2 cm/sec. At physiological pH and low $[NaCl]$, the membranes behaved electrically as pH electrodes, and H/OH conductances ranged from 1–100 nS/cm². These conductances can be converted to apparent H/OH permeabilities ranging from 10^{-6} to 10^{-4} cm/sec at pH 7, which falls within the range of values reported for various biological membranes. H/OH conductance is maximum at pH 7–9 and decreases about 10-fold from pH 8 to pH 2. Thus, the calculated H^+ permeability decreases from about 10^{-4} cm/sec at pH 8 to 10^{-11} cm/sec at pH 2, which partly explains the wide range of published values of P_{H^+} . Several models have been proposed to explain the high H/OH conductance through bilayers: (1) proton jumping along linear aggregates of hydrogen bonded water molecules (2) H/OH conductance induced by residual organic solvents such as $CHCl_3$ and (3) carrier mediated proton transport by weakly acidic, lipophilic contaminants in the phospholipids. Although the mechanism(s) of H/OH conductance are not known, all of the available data are consistent with the proton carrier model. (Supported by NIH grant GM 28844.)

M-Pos40 CARRIER AND CHANNEL KINETICS IN UNILAMELLAR LIPID VESICLES. L.M. Loew, L. Benson and M. Bridge, Dept. of Chemistry, State University of New York, Binghamton, New York 13901.

The facilitated transport of ions across cell membranes can involve a variety of kinetically limiting processes depending on the ion, the membrane, the mechanism of transport and the experimental protocol. We have developed a method utilizing a voltage sensitive probe for monitoring the ionophore mediated decay of a diffusion potential across large unilamellar vesicles. By calibrating the dye response to variations in ionic ratios and by determining the entrapped volume of the vesicles, one can translate the rate of change of fluorescence into an ion flux. Over a 500-fold concentration range of monensin it was found that the flux was linear in the K^+ concentration gradient but not strictly linear with ionophore concentration. Under these conditions the maximal observed transport rate was 100 ion/(monensin·sec). For ionophores where the actual ion transport is not kinetically limiting, it is useful to calibrate the dye fluorescence with respect to the proportion of vesicles retaining a potential. This can allow the method to monitor the insertion of functional ion transport units into the membrane and is appropriate for gramicidin. We have found that the rate of appearance of gramicidin channels follows a single exponential indicating that binding sites are in excess; with $10^{-8}M$ gramicidin the rates have time constants in the range of 1–2 sec and are determined with a stopped-flow fluorometer. These results suggest that dimerization of monomers to form functional gramicidin channels is the limiting step. The rate of insertion of the monomeric peptide into the membrane must therefore be faster and can be bracketed between $10^8 M^{-1} sec^{-1}$ and $10^{11} M^{-1} sec^{-1}$; the latter is the expected diffusion limit for large unilamellar vesicles. (Supported by USPHS Grant GM25190 and a NIH RCDA, CA 677, to LML.)

M-Pos41 EFFECT OF SUBSTRATE AND INHIBITOR ON SULFHYDRYL MODIFICATION OF GLUCOSE TRANSPORT PROTEIN, BAND 4.5. Jimmy J. Chin, Edward Jung and C.Y. Jung, Department of Biophysical Sciences, SUNY/AB and V.A. Med. Center, Buffalo, NY 14215

Effects of sulphydryl specific fluorescence tagging reagents 5-iodoacetamidofluorescein (IAF) and 1,5-IAEDANS (IAE) on cytochalasin B (CB) binding activity of glucose transport protein, Band 4.5, isolated from human RBC were studied. Band 4.5 protein was incubated with IAF or IAE overnight, then washed before measuring CB binding and fluorescence.

IAF tagging of Band 4.5 protein inactivates the CB binding. The rate of this inactivation is shown to be dependent on the presence of transport substrate or inhibitor during the reaction of IAF: With D-glucose present, the inactivation rate is approximately twice that in the presence or absence of L-glucose (control). With CB present, however, the inactivation rate is approx. 1/2 that of the control. The effects of glucose and CB on IAF tagging measured by fluorescence correspond to those on the inactivation of CB binding referred to above.

IAE tagging of Band 4.5 protein does not inactivate the CB binding activity in the presence or absence of D-glucose or CB. Pretagging with IAE prevents both the IAF inactivation of CB binding and its modulation by substrate and inhibitor. The IAE pretreatment also abolishes the D glucose-induced increase in IAF tagging without affecting its CB-induced reduction.

It is suggested that the sulphydryl group tagged with IAE under the present conditions plays an important role in the D glucose -induced IAF inactivation of CB binding .
(supported by NIH grant AM13376)

M-Pos42 CHARACTERIZATION OF THE POTASSIUM-DEPENDENT-CONDUCTANCE-INCREASE ASSOCIATED WITH VESICLE-TO-PLANAR-LIPID-BILAYER FUSION MANIPULATIONS. D.F. Hastings and S.M. Dawson*, Dept. of Physiology and Pharmacology, University of South Dakota School of Medicine, Vermillion, SD 57069.

Osmotic gradient catalyzed fusion of sealed and unsealed membranes to planar lipid bilayers yields preparations containing many unusual conductance phenomena, which often appear to be pharmacologically "active". In an effort to separate native membrane phenomena from fusion induced phenomena, we studied the K^+ stimulated potassium conductance, which occurs during the KCl osmotic fusion manipulations. Rather than relying on voltage-clamped current measurements to infer conductance changes, we used current-voltage curves to monitor: conductance, capacitance, voltage at zero-current, current at zero-voltage, ionic selectivity, and channel opening and closing events. All experiments were performed in the presence of 100 mM Na^+ as the Na_2SO_4 salt, 5 mM Tris MOPS pH 7.3. KCl and $CaCl_2$ were added as required. In the absence of membranes, placing a K^+ gradient across a [PE:PS::70:30] 20 mg/ml n-decane bilayer caused an increase in membrane conductance and a shift of the zero-current potential toward E_K . The K^+ selectivity of the induced conductance was $t_K > 0.8$. The conductance increase was saturatable and dependent upon the absolute K^+ concentration with a $K_{1/2} = 7$ mM and $\text{Log}(G_{\text{max}}) = -6.8 \pm 0.3(9)$ $S \cdot \text{cm}^{-2}$ as compared to control values of $\text{Log}(G_m) = -8.0 \pm 0.4(19)$ $S \cdot \text{cm}^{-2}$. The time course of the conductance changes in response to step changes in voltage exhibit a biphasic current phenomena. Survey of the lipid composition which exhibit this phenomenon revealed: PS \gg PE, $>$ PI = PC = no response. The PE samples contained more than 50% plasmalogens. Removing the plasmalogens did not prevent the response. This work was supported by grants from the Eagles Art Ehrman Cancer Fund and USPHS #NS-19077.

M-Pos43 STRUCTURAL TRANSITIONS IN RECONSTITUTED CYTOCHROME C OXIDASE-DIMYRISTOYL PHOSPHATIDYLCHOLINE VESICLES. C. Rigell and E. Freire. Department of Biochemistry, University of Tennessee, Knoxville, TN 37996-0840

The thermotropic behavior of reconstituted cytochrome c oxidase-dimyristoyl phosphatidylcholine (DMPC) vesicles has been studied using high sensitivity differential scanning calorimetry. We have been able to identify three different structural transitions: 1) A transition centered at 17°C corresponding to a metastable configuration which arises from prolonged incubation in the cold. This transition disappears after passage of the sample through the main phospholipid phase transition and is absent in samples containing a protein:lipid ratio higher than 1:800. 2) The phospholipid main gel-liquid crystalline transition centered at 24°C. This transition becomes progressively broader and skewed towards the low temperature end as the protein:lipid molar ratio increases; also the enthalpy change and the transition temperature of this transition decrease monotonically upon increasing the protein:lipid ratio. Analysis of the dependence of the enthalpy change on the protein:lipid ratio indicates that cytochrome c oxidase prevents 99 ± 5 phospholipid molecules from undergoing the gel-liquid crystalline transition. 3) A broad high temperature transition centered at 60°C. This transition has been assigned to a conformational transition of the cytochrome c oxidase molecule itself as indicated by additional tryptophan fluorescence measurements and heme a absorption parameters. (Supported by NIH Grant GM-30819.)

M-Pos44 STABILITY AND ELECTRICAL PROPERTIES OF BILAYER LIPID MEMBRANES (BLM) IN THE PRESENCE OF MICROTUBULES. P.M. Vassilev, M.P. Kanazirska, and H. Ti Tien, Department of Physiology, Michigan State University, East Lansing, MI 48824.

Microtubules were found to be important for the maintenance of cell shape, generation of action potentials and for other cytoskeletal and electrical events in membranes. It should be valuable to study the influence of these cytoskeletal structures on the stability and the electrical properties of bilayer lipid membranes (BLM) in order to elucidate the mechanisms of their involvement in physiological processes. The electrical properties of BLM made from rat brain tubulin (T), polymerized in vitro, were compared. When added to one of the sides of BLM, T caused a slow decrease of resistance from $1-2 \times 10^8 \Omega$ to $5 \times 10^7 \Omega$. The membranes were unstable and broke in about 30 min at an applied potential of 10 mV. The resistance of BLM in the presence of T at both sides was $10^8 \Omega$ at 10mV applied voltage. In this case the membranes were very stable, the dielectric breakdown being observed in the range of 100-160 mV. The membranes remained stable for several hours. It was found also that T may induce some changes of the current-voltage characteristics of BLM. These results and our earlier findings (Biosci. Rep., 2, 12, 1982) showing microtubule orientation in very low electric fields (in the range of tens of mV) may serve as a basis for further studies on the relationships between the electric properties of membranes and microtubules, which may be suggested to play an important role not only for the maintenance and generation of nerve membrane potentials, but also for propagation and integration of nerve signals and other processes of information transfer and processing in the cells. Such investigations are now underway in this laboratory. (Supported by NIH grant GM-14971)

M-Pos45 TRANSMEMBRANE POTENTIALS IN BILAYER LIPID MEMBRANES (BLM) INDUCED BY CALCIUM CHANNEL AND BETA-ADRENERGIC BLOCKERS. Xia chang Shen, Biao Shi, and H. Ti Tien, Department of Physiology, Michigan State University, East Lansing, MI 48824.

Insight into the mechanism of interaction of calcium antagonists and other membrane-active drugs with biomembranes may be obtained by model membrane studies. An investigation of the potentials induced by calcium blocker (verapamil, diltiazem, nifedipine) and β -adrenergic blockers (propranolol, sotalol, labetalol, loprorenol, transcor) on BLM has been carried out in order to elucidate the mechanisms of interaction between simple lipid membranes and these drugs. After the addition of the drug, a potential was usually developed across the BLM. The sign of potentials of the side, to which the drug was added, was negative. The magnitude of potentials was found to be dependent on the concentrations of the drug, pH, ionic species and strength of the bathing solution, the composition and concentration of the membrane forming solution. Dose response curves show the difference in the intensity of interaction between the membrane and the drugs. The pH curve for verapamil shows clearly the potential change as a function of H^+ ion concentrations. For most cases, the potentials induced by the addition of drugs to solutions containing $CaCl_2$ were much less than those containing $NaCl$. Furthermore, in solutions containing both $CaCl_2$ and $NaCl$, the drug-induced potentials showed no significant change when the salt concentration was varied from 0 to $10^{-1}M$, but it decreased dramatically from $10^{-1}M$ to $1M$. The results obtained may provide insight into the membrane-drug interaction. The BLM used in this study lacks specific receptors. In future studies, we plan to incorporate receptor proteins and repeat the experiments so that the membrane-drug interaction may be clearly delineated. (Supported by NIH grant GM-14971)

M-Pos46 COVALENT LINKAGE OF A SYNTHETIC PEPTIDE TO A FLUORESCENT PHOSPHOLIPID AND ITS INCORPORATION INTO SUPPORTED PHOSPHOLIPID MONOLAYERS. Nancy L. Thompson, Adrienne A. Brian and Harden M. McConnell. Chemistry Department, Stanford University, Stanford, CA 94305.

In the course of a biophysical study of cellular and molecular membrane recognition, we have synthesized fluorescent peptide-lipid conjugates. Peptides with 10-11 amino acids are linked through a single lysine residue to the head group of phosphatidylethanolamine, fluorescently labeled on one acyl chain, using homobifunctional disuccinimidyl crosslinking reagents. Peptide-lipids can be further derivatized with the hapten dinitrophenyl. Purified peptide-lipids have been incorporated into dimyristoylphosphatidylcholine monolayers at the interface of air and phosphate-buffered saline, at concentrations of up to 11 mole %. For equal average molecular areas, monolayers containing peptide-lipids have higher surface pressures than pure lipid monolayers; for equal surface pressures, peptide-lipid monolayers have higher average molecular areas than pure lipid monolayers. When the peptide-lipid monolayers are transferred to hydrophobic glass slides, the fluorescence appears uniformly distributed. Fluorescence recovery after photobleaching measurements indicate that peptide-lipids diffuse in the monolayer with coefficient $1.5 \times 10^{-9} \text{ cm}^2/\text{sec}$, which is much smaller than that of typical lipids in fluid membranes. In addition, the diffusion coefficient of peptide-lipids decreases with increasing peptide-lipid concentration. We conclude that the peptide portion of the peptide-lipid associates with the lipid monolayer and/or that peptide-lipids oligomerize. This work was supported by Damon Runyon-Walter Winchell Cancer Fund Postdoctoral Fellowship DRG-593, American Cancer Society (CA Div.) Senior Postdoctoral Fellowship S-4-83, and NIH Grant 5R01 AI13587.

M-Pos47 SINGLE-CHANNEL STUDIES ON THE GATING OF BATRACHOTOXIN (BTX)-MODIFIED SODIUM CHANNELS IN LIPID BILAYERS. L.B. Weiss, W. N. Green and O.S. Andersen. Department of Physiology and Biophysics, Cornell University Medical College, New York, N.Y. 10021.

Voltage-dependent sodium channels from canine forebrain synaptosomes were incorporated into planar lipid bilayers following a procedure similar to that of Krueger et al. (*Nature*, **303**:172 [1982]), where inactivation is removed pharmacologically with BTX ($0.16-0.41 \mu M$). The membrane-forming solutions were 4:1 mixtures of phosphatidylethanolamine and phosphatidylcholine in *n*-decane. The gating characteristics were studied in symmetric solutions of $NaCl$ ($0.05 M < [Na^+] < 2.5 M$, $pH=7.4$, $22-24^\circ C$). The potential (V) was referenced to the aqueous solution facing the BTX-binding site. Open channels exhibited brief closing transitions at all potentials. The frequency and duration of the brief events increased as V decreased, and the time-averaged membrane conductance equalled the conductance of the unmodified bilayer around -130 mV (in $0.5 M NaCl$). Channel gating was studied as the time-averaged (fractional) open time (f_o) as a function of V . The relation between f_o and V was sigmoidal, with an apparent gating charge of 4-5 elementary charges at all concentrations tested. The midpoint potential V' varied considerably, between -75 mV and -95 mV in $0.5 M NaCl$. The variation in V' reflects, at least in part, the existence of several states in the gating machinery as extended records on single sodium channels reveal that f_o may undergo abrupt transitions (e.g. between 0.6 and 0.95 at -80 mV in $0.5 M NaCl$). Decreases in $[NaCl]$ were associated with a shift in V' to more negative potentials, about -105 in $0.1 M NaCl$. These variations in V' may reflect changes in surface potentials as well as the spontaneous variations in the gating characteristics seen at constant ionic strength.

M-Pos48 VOLTAGE- AND Na^+ -DEPENDENT TETRODOTOXIN (TTX) BLOCK OF BATRACHOTOXIN (BTX)-MODIFIED SODIUM CHANNELS. W.N. Green, L.B. Weiss and O.S. Andersen. Department of Physiology and Biophysics, Cornell University Medical College, New York, N.Y. 10021.

Voltage-dependent, BTX-modified sodium channels from canine forebrain synaptosomes were incorporated into planar lipid bilayers as described in the preceding abstract. When TTX was added to the 'extracellular' aqueous phase very long-lasting blocks of the channels were observed. The degree of this TTX-induced block was estimated from the fractional closed time, and exhibited a simple saturating behavior as a function of [TTX]. The [TTX] for 50 % block (K_D) varied as a function of $[\text{Na}^+]$ and potential (V). K_D was 10–20 nM in 0.05 M NaCl (pH=7.4, +60 mV, 22–24 °C), while it was 100–200 nM in 0.5 M NaCl, and about 900 nM in 2.5 M NaCl. The V -dependence of the TTX-induced block was 60–70 % ($-60 \text{ mV} < V < 60 \text{ mV}$), independent of $[\text{Na}^+]$ (0.05 M $< [\text{Na}^+] < 2.5 \text{ M}$). The block increased as the 'intracellular' aqueous phase was made more negative relative to the 'extracellular' solution. The V -dependence of the rate constants for block and unblock of the channels was about 30 % for both. The unblock rate constant varied weakly with $[\text{Na}^+]$, between about 0.1/s in 0.05 M and about 0.3/s in 2.5 M NaCl at +60 mV. The V -dependences of saxitoxin (STX)-induced block, and of the rate constants for block and unblock, were similar to those seen with TTX (see also Krueger et al., *Nature*, 303:172 [1982]), despite the different net charge carried by TTX (+1) and STX (+2). If STX and TTX bind to the same site in the sodium channel, one may conclude that the V -dependence of the block cannot reflect the electrical distance between the 'extracellular' aqueous phase and the binding site.

M-Pos49 EFFECTS OF OCTANOL ON SINGLE SODIUM CHANNELS IN BILAYERS. B.W. Urban, W.N. Green, L.B. Weiss and O.S. Andersen. Depts. of Anesthesiology and Physiology, Cornell University Medical College, New York, N.Y. 10021.

Voltage-dependent, BTX-modified sodium channels were incorporated into bilayers (see preceding abstract) made from a lipid solution containing phosphatidylethanolamine and phosphatidylcholine (4:1) in decane. The electrolyte of one compartment was subsequently exchanged for the same electrolyte containing also octanol (0.2 saturated), without breaking the bilayer (symmetrical 0.1, 0.5 or 1M NaCl and 10mM phosphate buffer, pH 7.4). At +60mV applied membrane potential, transitions to and from closed states became much more frequent for the octanol exposed channel, and the fractional closed time increased from less than 0.02 to 0.06 (0.5M NaCl, -60mV potential applied to the intracellular side of the sodium channel, T=22–24°C). Octanol could furthermore induce long channel closures (of the order of tens of seconds) or cause apparently permanent loss of conducting sodium channels. Such loss could not be reversed when the octanol containing electrolyte was replaced again with the control solution (30 to 60 minutes observation time), while the other effects were fully reversible within a few minutes. The single channel current amplitudes were not affected (to within $\pm 5\%$) at all three NaCl concentrations tested. The results did not depend on which compartment (with respect to sodium channel orientation) held octanol, and the concentration of octanol was comparable to that used in previous voltage-clamp studies of sodium currents (Haydon and Urban [1983], *J. Physiol.*, 341, 411–427). Octanol appears to induce an additional non-conducting state of the sodium channel (as ordinary inactivation has been eliminated by BTX) and/or interfere with BTX-binding.

M-Pos50 IN VIVO INDUCTION OF CYTOTOXIC T LYMPHOCYTES BY HERPES SIMPLEX VIRUS ANTIGENS AND MDP INCORPORATED INTO LIPOSOMES. Maria C. Correa-Freire, Hal S. Larsen, Francoise Audibert, Richard J. Courtney, Leaf Huang and Barry T. Rouse. University of Tennessee, Knoxville, TN and Institut Pasteur, Paris.

In vivo induction of cytotoxic T lymphocytes (CTL) which can recognize herpes simplex virus (HSV) infected cells was obtained upon injection of antigen bearing liposomes into the food pads of C₃H mice. Purified HSV glycoproteins (gp) were reconstituted into unilamellar liposomes along with either the water soluble adjuvant muramyl di-peptide (MDP) or its lipid soluble derivative glycerol mycolate MDP (gmMDP). The phospholipid compositions studied were a 1:1 mixture of PS:PE and PC:Chol; a 6:3:1 mixture of PC:Chol:Sterylamine and a 5:2.5:2.5 mixture of PS:PC:Chol. The total glycoprotein concentration injected per mouse was either 0.5, or 10 μg . The total MDP concentration per injection was .011 μM . Ten days after the initial challenge the mice were bled and injected a second time with the same liposome preparation. In some cases, due to the low levels of antibody production, a third and final injection was given. Mice were sacrificed 10 days after the final injection, the lymph nodes were removed and set up in a 5 day mixed lymphocyte culture; antibody production was monitored by RIA. Our results indicate that the degree of CTL production is dependent on the phospholipid composition of the liposomes and the type of adjuvant used. Maximum immunogenic effect was observed with negatively charged liposomes. PS:PE:gp liposomes elicited maximum response when gmMDP was incorporated in the bilayer; PS:PC:Chol:gp liposomes elicited maximum CTL production when MDP was trapped in the aqueous compartment of the liposomes. This research was supported by NIH grants A1 14981, 5 T32 A108123, and CA 24564.

M-Pos51 KINETIC FACTORS DETERMINE VESICLE SIZE AND PERMEABILITY. Masahara Ueno, Charles Tanford, and Jacqueline A. Reynolds, Dept. of Physiology, Duke Univ. Med. Ctr., Durham, N.C. 27710.

We have extended the method of Mimms et al. (Biochemistry 20, 833, 1981) for formation of unilamellar vesicles from mixed micelles of egg lecithin and octyl glucoside to allow for: (1) use of other nonionic detergents with a much lower cmc than octyl glucoside; (2) variation in the time course of detergent removal. The results show that spontaneous vesiculation begins at a molar detergent/lipid ratio of about 2:1. Initially formed vesicles are small, but the size increases slowly thereafter provided that detergent is not removed too quickly; vesicle size remains fixed when the molar detergent/lipid ratio falls below about 1:1. Detergent removal thereafter is kinetically biphasic, suggesting that removal from the inner monolayer of the vesicle membrane is much slower than removal from the outer monolayer. In the case of C₁₂E₈ (cmc < 10⁻⁴M) it is difficult to reduce the molar detergent/lipid ratio below 0.25 even over a period of several days. This residual detergent (presumably all in the inner leaflet) has surprisingly little effect on anion permeability but increases the rate of Na⁺/choline⁺ exchange by about 3 orders of magnitude, i.e. the net result is loss of the normal discrimination between anions and cations of pure lipid vesicles. All preparations, regardless of residual detergent level, were found to contain only unilamellar vesicles: no multilamellar liposomes or other lipid aggregates were present. This work was supported by NIH grants HL-30049 and AM-04576, and by NSF grant PCM-82-16109.

M-Pos52 ION CHANNELS INDUCED IN PLANAR LIPID BILAYERS BY THE PATHOGENS YERSINIA ENTEROCOLITICA, YERSINIA PESTIS AND ENTEROINVASIVE E. COLI.
Eileen C. Lynch, The Rockefeller University, N.Y., N.Y. 10021

Certain species of enteric pathogens can cause ulcerative lesions and invade epithelial cells in droves. Bacterial induced membrane permeability changes have been correlated with the cellular invasive potential of the Neisserial pathogens N. meningitidis and N. gonorrhoeae,^{1,2} the pathogens etiologic in the diseases of gonorrhea and bacterial meningitis.

Surmising that enteric pathogens with a high cellular invasion potential might also produce substances that would mediate membrane permeability changes, we exposed planar lipid bilayers to these bacterial cells and observed the spontaneous incorporation of ion permeable channels into the artificial films. The size of the unit channel, its ion selectivity, and voltage dependence was characteristic for each bacterial species that was examined. The magnitude of the permeability change imparted to the model membrane by the transferred bacterial channels was well correlated with the cellular invasive potential of each species. Non invasive E. coli controls were not observed to transfer ion channels or other permeability defects into the model membranes.

We propose that microbial channel transfer may be a pathogenic mechanism of general significance: the transfer of bacterial derived ion channels into the appropriate plasma membrane compartment may be a general relay signal for the initiation of phagocytotic uptake of the bacterium into the host epithelial cell.

(Supported by the Winston Fellowship Foundation)

¹ E. C. Lynch, M. Blake, E. Gotschlich, and A. Mauro, Biophys. J. 41 (1983) 62a.

² E. C. Lynch, et al., Biophys. J. (1983), in the press.

M-Pos53 POLYHISTIDINE MEDIATES AN ACID ENHANCED FUSION OF NEGATIVELY CHARGED LIPOSOMES. Chen-Yen Wang and Leaf Huang, Dept. of Biochemistry, Univ. of Tennessee, Knoxville, TN 37996-0840.

Polyhistidine facilitates the fusion of negatively charged liposomes prepared by sonication. Liposome fusion was demonstrated by (a) negative stain electron microscopy, (b) gel filtration and (c) dilution of fluorescent phospholipids. Liposome fusion required the presence of polyhistidine; histidine at equivalent concentration had no effect. Low level of liposome fusion was detectable at pH 7.4, but it was greatly enhanced when the pH of medium was reduced below 6.5. Acidic phospholipid is necessary for fusion, although phosphatidylglycerol and phosphatidic acid showed the highest activity. The presence of phosphatidylethanolamine (PE) enhanced the fusion competency of liposomes, while the presence of phosphatidylcholine and sphingomyelin lessened such activity. For liposomes made of PE:PS (1:1), fusion at pH 5.2 and at a 2.5 $\mu\text{g/ml}$ of polyhistidine concentration resulted in an increase in the average liposome diameter from 296 to 2400 Å, indicating multiple rounds of fusion had occurred. Liposome fusion was not very leaky as revealed by the release of an encapsulated dye, calcein. For PE:PS (1:1) liposomes, about 10% of dye leakage was observed for up to about 30% liposome fusion and about 45% leakage at 80% liposome fusion. Since polyhistidine becomes a strong polycation at acidic pH, fusion of liposomes may be a direct result of bilayer phase separation induced by the binding of polyhistidine to the negatively charged lipids. Therefore, the phenomenon is similar to the fusion of negatively charged liposomes induced by other polycations at neutral pH. Supported by NIH grant CA 24553.

M-Pos54 EFFECT OF H^+ ON THE STABILITY AND Ca^{2+} -INDUCED FUSION OF LIPOSOMES CONTAINING ACIDIC LIPIDS. H. Ellens, J. Bentz and F.C. Szoka, Departments of Pharmacy and Pharmaceutical Chemistry, School of Pharmacy, University of California, San Francisco, CA 94143.

We studied the effect of H^+ on the stability of lipid vesicles (diameter $\sim 0.1 \mu\text{m}$) composed of phosphatidylethanolamine (PE) and cholesterylhemisuccinate (CHEMS) and of phosphatidylserine (PS). The PE/CHEMS liposomes are stable at neutral pH and they aggregate and leak in buffers below pH 5.5. The mechanism of leakage was investigated by measuring the release of encapsulated p-xylylene-bis-pyridinium bromide (DPX) and 1-aminonaphtalene 3, 6, 8-trisulfonic acid (ANTS). DPX quenches the ANTS fluorescence in the liposomes. Leakage leads to a relief of the quenching and a continuous increase of fluorescence, which is a direct measure of the extent of leakage. The fluorescent signal from ANTS is insensitive to pH between 4.0 and 7.5. Analysis of the kinetics of release demonstrates that following protonation of the CHEMS the liposome bilayer remains stable until it comes into contact with another bilayer. Likewise, when PS vesicles are injected into a buffer below pH 2.5 the vesicles aggregate and leak and interbilayer contact enhances the release of contents. The PE/CHEMS vesicles can be induced to fuse with Ca^{2+} . The fusion is measured by the mixing of aqueous contents using a new fusion assay which is insensitive to pH between pH 4.0 and 7.5: ANTS in one population of vesicles and DPX in the other. Here fusion results in quenching of ANTS fluorescence. The Ca^{2+} induced fusion of PE/CHEMS is completely inhibited by H^+ below pH 5.5. The Ca^{2+} -induced fusion of PS vesicles is not affected by H^+ at or above pH 4.0. Supported by NIH grants GM-29514 (FCS) and GM-31506 (JB).

M-Pos55 OSMOTIC EFFECTS ON INTERVESICLE LIPID MIXING. Ruby I. MacDonald, Dept. of Biochem., Mol. Biol. and Cell Biol., Northwestern University, Evanston, IL 60201.

Large liposomes appear and an increase in light scattering is seen when sonicated, fluid phase phosphatidylcholine vesicles are treated with high molecular weight, carbohydrate polymers and subsequently diluted with hypotonic buffer. A convenient measure of liposome growth under these conditions is the change in fluorescence energy transfer between dansylphosphatidylethanolamine and dioctadecylindocarbocyanine on exposure of the vesicles to polymer. Dextran of 167,000 M_r begins to cause lipid mixing at a concentration of 30% (w/w) and can effect up to 80% mixing at concentrations of 40 to 50% (w/w). If the vesicles are sequestered from dextran by their inclusion in a dialysis bag, dextran can still cause lipid mixing in the same concentration ranges as are effective when dextran and the vesicles are in contact. Presumably, the polymer can destabilize the bilayers of vesicles by dehydrating them without actually interacting with them. The addition of hypertonic NaCl or KCl solutions to the vesicles, exposed either directly or indirectly (i.e., by dialysis) to dextran, partially inhibits lipid mixing. Thus, lipid mixing may proceed both during dehydration (e.g., by collapse of vesicles leading to bilayer discontinuities and reannealing between vesicles) and during rehydration (e.g., by osmotic inflation of vesicles into each other so that they fuse). These possibilities may be distinguished by means of experiments on dextran-induced lipid mixing among vesicles of dipalmitoylphosphatidylcholine, which occurs at or above, but not below, its phase transition temperature. As expected from the work of others, the high molecular weight dextran used in these experiments was less "mixogenic" per weight than various low molecular weight preparations of polyethylene glycol.

M-Pos56 A MODEL SYSTEM FOR NEUROTRANSMITTER RELEASE. M.S. Perin and R.C. MacDonald, Northwestern University, Evanston, Illinois 60201 U.S.A.

We are developing an assay for the fusion of synaptic vesicles with planar bilayer membranes, potentially reconstituted with presynaptic membrane components, with the aim of understanding certain aspects of neurosecretion. Synaptic vesicles, loaded with partially self-quenched concentrations of the fluorescent dye, calcein, are visible under the fluorescence microscope for several minutes before bleaching. On sudden release of their contents, they exhibit bright flashes of fluorescence which will be the basis for detection of fusion. Brain synaptic vesicles are loaded with calcein by freeze and thawing in 0.150 M calcein during which process the vesicles increase in volume 50-100X. Prototype experiments have been begun with purely lipid membranes. BLM's, formed on a horizontal aperture mounted on a microscope slide, are observed by phase contrast and incident fluorescence microscopy. LUV's (soy phospholipid:phosphatidylserine, 80:20) adhere to decane-based BLM's (PS:soy PL, 80:20) under the influence of 10mM calcium ion. Vesicles aggregate in the plane of the membrane and, for reasons unknown, accumulate on lenses and the torus. Sometimes calcein is observed to be abruptly discharged into aqueous droplets in the lenses or the torus. When stressed osmotically by the addition of a solution containing a permeant solute, some bound vesicles release calcein in flashes. Distinction between "secretion" and non-productive lysis will be made by asymmetrically adding cobalt ion, which at low concentrations effectively quenches calcein fluorescence, as well as by taking advantage of the sharp maximum in the plane of focus of incident fluorescence illumination.

M-Pos57 DYNAMIC MORPHOLOGY OF CA-INDUCED INTERACTION OF PHOSPHOLIPID VESICLES COMPOSED OF PHOSPHATIDYLSERINE (PS) AND DIOLEYLPHOSPHATIDYLETHANOLAMINE (DOPE). N.F. Fuller and R.P. Rand, Biological Sciences, Brock University, St. Catharines, Canada, and B. Kachar, NIH, Bethesda USA.

We have attempted to directly observe the processes by which uni- and multilamellar phospholipid vesicles combine, under the influence of added divalent cations, and eventually produce the largely dehydrated, multilamellar phase. We observe vesicles by freeze-fracture electron microscopy at times down to about 100 milliseconds after adding CaCl_2 . The earliest images include interacting vesicles that have been in contact for all times less than 100 ms. We reported (Biophys.J.41:359a, Can.J. Biochem.Cell Biol.inpress) that pure PS vesicles form large, flat, smooth, double-bilayer diaphragms as adhering vesicles flatten against each other with an energy far in excess of that capable of rupturing bilayers. Video light microscopy of multilamellar vesicles showed that 60% of diaphragms rupture, resulting in fusion, and that 40% of extra-diaphragm areas rupture, precluding fusion. We have carried out similar experiments with vesicles composed of DOPE/PS mixtures of ratios 1/1, 3/1, and 10/1. X-ray diffraction shows the end states of these vesicles after Ca addition to be a PS-Ca lamellar phase and a DOPE hexagonal phase. Freeze-fracture images of the earlier stages (seconds) show: (1) the formation of large, smooth, double-bilayer diaphragms, (2) prominent long, curved, line defects on the surfaces of cleaved bilayers, interpreted as fusion of the outer monolayers at the circumferences of the diaphragms, (3) no evidence of "pits and particles", even on large diaphragms presumably composed of DOPE/PS 10/1. Only at later stages and after collapse of the vesicle system does lipid segregation become evident. We are attempting to estimate the fusion/rupture ratio in these lipid mixtures by video microscopy.

M-Pos58 EFFECTS OF POLYAMINES ON THE AGGREGATION AND FUSION OF MODEL MEMBRANE VESICLES.

P. Meers, F. Schuber*, K. Hong and D. Papahadjopoulos. Cancer Res. Inst. and Dept. of Pharmacology UCSF, San Francisco, CA 94143, and *Laboratoire de Chimie Enzymatique (ERA 487), Institut de Botanique, Université Louis Pasteur 67083, Strasbourg, France.

The polyamines, spermine (SP), spermidine (SPD) and putrescine (PT), are present at relatively high levels in rapidly growing and secretory mammalian cells. The possible importance of polyamines in the regulation of secretion and membrane turnover was investigated by testing the effects of polyamines on the fusion of model membrane systems. Large unilamellar vesicles (LUV's) with terbium or dipicolinic acid (DPA) entrapped were used to measure fusion based on the generation of a highly fluorescent Tb-DPA complex upon mixing of vesicle contents. Aggregating concentrations (15 μM and up) of SP and SPD decreased the calcium threshold and increased the rate of calcium-induced fusion for vesicles composed of phosphatidic acid (PA), phosphatidylserine (PS), or mixtures of PA and phosphatidylcholine (PC), but did not cause fusion alone. These effects were dependent on preincubation time with the polyamines and were correlated with the slow aggregation of vesicles. LUV's composed of mixtures of acidic phospholipids and cholesterol with high proportions of phosphatidylethanolamine were fused by SP or SPD alone. PT had no effect on the aggregation or fusion of vesicles. In order to ascertain the amount of polyamine needed to induce aggregation and/or fusion, binding of polyamines to vesicles was measured by equilibrium dialysis with ^{14}C labelled polyamines. SP and SPD exhibit apparent 1:1 binding constants to PA vesicles of approx. $5(10^4)$ and $5(10^5)$ respectively. (supported by NIH grants GM 26369 and GM 28117)

M-Pos59 POLYCATION INDUCED FUSION OF ACIDIC LIPID CONTAINING VESICLES: pH AND CHARGE DEPENDENCE. Anne Walter, Daniel Margolis, and Robert Blumenthal, LKEM, NHLBI and LTB, NCI, Bethesda, MD 20205.

Polylysine-induced fusion of PC vesicles containing 10% or more acidic lipid was examined as a function of pH, fraction of acidic lipid, positive to negative charge ratio and degree of polylysine polymerization. Fusion between small unilamellar phospholipid vesicles was followed by the decrease in energy transfer efficiency between two lipid fluorescent probes, NBD-PE and rhodamine-PE (each 1% of the total lipid) as fluorescently tagged vesicles fused with unlabeled vesicles. The kinetics of lipid mixing suggest that a polylysine molecule involved in a fusion event is not immediately available for subsequent fusions. Fusion increased at a low pH corresponding to the pK_a of the negatively charged group on the phospholipids (PS, PI, PG, or DPG). Decreasing the mole fraction of acidic lipids decreased the fusion at a given pH. Maximal fusion occurred when the polylysine charge to lipid charge ratio was nearly 1:1 over a large range of polylysine sizes. Fusion was inhibited when (1) protein:lipid charge ratios were higher than 1, (2) when lysine polymer size was very large (e.g. 500 bases) and (3) when polymers contained too few bases. We interpret these data in a model for fusion in which polylysine binds to negative charges on two apposing vesicles forming a crossbridge leading to subsequent fusion when adjacent charges are neutralized by binding or protonation. Excess positive charge is inhibitory due to electrostatic repulsion; large polymers cannot bind completely to a single vesicle. The reduced fusion of small polymers may indicate that polylysine-lipid interactions are cooperative. Apocytocytome c, a basic protein containing 19 lysine residues, has similar fusogenic properties.

M-Pos60 pH- DEPENDENT FUSION INDUCED BY RECONSTITUTED VESICULAR STOMATITIS VIRUS GLYCOPROTEIN.

O. Eidelman, R. Schlegel, T. S. Tralka and R. Blumenthal. N.I.H., Bethesda, Md. 20205.

Purified G-protein from Vesicular Stomatitis Virus was reconstituted into egg PC vesicles by detergent dialysis of octyl glucoside. A homogeneous population of reconstituted vesicles could be obtained, provided the protein to lipid ratio was high (~0.3% protein) and the detergent removal was slow. The reconstituted vesicles were assayed for fusion activity using electron microscopy and fluorescence energy transfer. The fusion activity mediated by the viral envelope protein was dependent upon pH, temperature and target membrane lipid composition. Incubation of reconstituted vesicles at low pH with small unilamellar vesicles containing negatively charged lipids resulted in the appearance of large cochleate structures, as shown by electron microscopy using negative stain. This process did not cause leakage of vesicle-encapsulated aqueous marker. The efficiency of resonance energy transfer between two non-exchangeable fluorescent lipid probes was used to estimate fusion rates. The rate of fusion was pH dependent with a pK of ~4, and the apparent energy of activation for the fusion was 16 ± 1 kcal/mol. G-protein-mediated fusion showed a large preference for target membranes which are negatively-charged at neutral pH. The fusion rate was enhanced 120 fold over pure PC with PA/PC (1:1) target membranes, 20 fold with PS/PC (1:1), and 2 fold with PI/PC (1:1). PE/PC (1:1) showed no enhancement, and neither did inclusion of 36% cholesterol in any of the lipid compositions. These reconstituted vesicles provide a system to study the mechanism of pH-dependent fusion induced by a viral spike protein.

M-Pos61 ACID INDUCED FUSION OF LIPOSOMES WITH INNER MEMBRANES OF MITOCHONDRIA. L. Huang, Dept. of Biochemistry, Univ. of Tennessee, Knoxville, TN 37996-0840 and S.-S. Liu, Institute of Zoology, Chinese Academy of Sciences, Beijing, China.

Sonicated small unilamellar liposomes composed of phosphatidylethanolamine (PE) and a long chain fatty acid, such as oleic and palmitic acids, rapidly fuse with each other at room temperature when the medium pH is reduced to below 6.2. Negative-stain electron microscopy of liposomes showed 6-20 fold enlargement of liposome size with the acid treatment. Fusion was also monitored by the dilution of fluorescence phospholipids (NBD- and Rhodamine-PE) as described by Struck et al. (Biochem. 20(1981) 4093). Acid-induced fusion of liposomes requires the presence of a weakly acidic lipid such as fatty acids. Acidic phospholipids such as PS and cardiolipid (CL) do not fulfill this requirement. The presence of PE greatly enhanced fusion; while the presence of PC, PS, PI and CL inhibited fusion. Fusion competent liposomes, e.g. PE:oleic acid (8:2), also rapidly fuse with mitoplasts or isolated inner membranes of rat liver mitochondria. In contrast to the liposome-liposome fusion, however, liposome-mitoplast fusion showed a definitive pH optimum at 5.0-5.5, indicating additional requirement defined by the inner membranes of mitochondria. Liposome-mitoplast fusion also showed a less stringent requirement on the lipid composition. Partial fusion (30-40%) was observed with liposomes composed of PE/CL (8:2), PE/PS (8:2) or soybean phospholipids. This simple method may be useful in incorporating exogenous membrane lipids and proteins into the inner membranes of mitochondria. Supported by NIH grants CA 24553 and GM 31724 and a travel grant from National Research Council.

M-Pos62 PH SENSITIVE LIPOSOMES: ACID INDUCED FUSION AND IMPROVED CYTOPLASMIC DELIVERY. Jerome Connor, Milton B. Yatvin* and Leaf Huang, Dept. of Biochem., Univ. of Tenn., Knoxville, TN 37996-0840. *Dept. of Human Oncology, Univ. of Wisconsin, Madison, WI 53792.

Sonicated unilamellar vesicles (SUV) consisting of dioleoyl phosphatidylethanolamine (PE) and palmitoyl homocysteine (PHC) in an (8:2) molar ratio rapidly fuse, at a pH lower than 6.5, with vesicles of various lipid composition. Fusion was monitored by a) mixing of lipids as shown by resonance energy transfer, b) gel filtration and c) electron microscopy. The presence of phosphatidylethanolamine greatly enhanced fusion, while the presence of phosphatidylcholine, cholesterol and gangliosides inhibited fusion. The addition of 0.5 mM Ca^{++} synergistically increased the fusion, whereas the addition of 0.5 mM Mg^{++} had no effect. Fatty acid derivatized monoclonal anti-H2K^k was incorporated into reverse-phase evaporation vesicles (REV) consisting of the fusion competent PE-PHC (8:2) lipids by a modified method of Shen et al. (BBA 689(1982), 31-37). Mouse L929 cells (k haplotype) incubated with these immunoliposomes, containing calcein, revealed diffused fluorescence throughout the cell indicating a release of the dye into the cytoplasm. In contrast, cells incubated with pH insensitive immunoliposomes displayed only punctate fluorescence. In control experiments, mouse A31 cells (d haplotype) were incubated with immunoliposome and no fluorescence was observed. These results indicate that the immunoliposomes are specifically and effectively endocytosed by the target cells and the pH sensitive immunoliposomes are efficient in delivering their contents into the cytoplasm of target cells; possibly by fusing with the endosome membranes at low pH. (Supported by NIH Grant CA 24553 and GM 36227.)

M-Pos63 SENDAI VIRUS-LIPOSOME INTERACTIONS: FUSION, LEAKAGE AND OSMOTIC PRESSURE DEPENDENCE. Yung-Shyeng Tsao and Leaf Huang, Dept. of Biochem., University of Tennessee, Knoxville, TN 37996.

We have investigated the fusion between Sendai virus and large liposomes made by several cycles of freeze and thaw containing phosphatidylcholine, phosphatidylserine, phosphatidylethanolamine and gangliosides (1:2.60:1.48:0.08 molar ratio). To demonstrate fusion by the technique of resonance-energy-transfer 0.5% each of N-NBD-phosphatidylethanolamine and N-rhodamine-phosphatidylethanolamine were introduced into the liposomal membrane. To demonstrate Sendai virus-induced leakage which accompanied the fusion event a self quenching fluorescent dye, calcein, was entrapped in the liposomes. The enhancement of fluorescence at 520 nm was monitored as a function of time, temperature, etc. To demonstrate the effects of osmotic pressure on fusion or leakage different concentrations of salt were present either inside or outside of the vesicles. We have shown that the kinetics of both fusion and leakage are Sendai virus dosage dependent, fusion protein dependent, temperature dependent, and osmotically sensitive. Hypoosmotic condition is not absolutely required for fusion and leakage because these processes still occur in an isotonic environment; however, it can increase the rate of these processes. The $t_{1/2}$ of Sendai virus-induced leakage is less than 1 hr, while the $t_{1/2}$ of fusion is greater than 2 hrs in an isotonic environment, indicating that leakage occurs before fusion. The effect of liposomal composition upon fusion efficiency as well as the interactions of reconstituted vesicles containing F and/or HN proteins from Sendai virus and liposomes are also under investigation.

M-Pos64 CAPACITANCE INCREASE FOLLOWING INSEMINATION OF VOLTAGE-CLAMPED SEA URCHIN EGGS. D.H. McCulloh and E.L. Chambers. Physiology and Biophysics, Univ. Miami, School of Medicine, Miami FL 33101. (Intr. by Birgit Rose).

The exocytosis of cortical granules in sea urchin eggs has been observed as the elevation of a fertilization envelope starting 19s after initiation of the activation current in the voltage-clamped egg (Chambers and Lynn, Biophys. J. 41, 130a, 1983). The activation current consists of an inward shoulder which lasts 11.7s and culminates in a major inward current transient. The purpose of this study was to quantitatively determine the time course and extent of the exocytosis more directly, by monitoring the increase of membrane capacitance caused by fusion of cortical granule membranes with the plasma membrane. Capacitance was determined continuously before, and following insemination of *Lytechinus variegatus* eggs at 22°C by analyzing the amplitude of the capacitive current which flows during a 4-10 mV sine wave (50-200 Hz), superimposed upon the clamped membrane potential (-20 mV). A lock-in amplifier was used to discriminate currents through the capacitive admittance from those through the membrane conductance. The earliest detectable increase of capacitance began 14 ± 1.2 s (n=6) following the initiation of the activation current, and 1.8 ± 0.65 s after the onset of the major inward current. Capacitance continued to increase for 53 ± 5.7 s, resulting in a maximum capacitance 2.2 ± 0.12 times the initial value. The average rate of propagation for the cortical reaction was 4.2 ± 0.56 $\mu\text{m/s}$ (n=5) as determined from the rate of capacitance change. These data are comparable to those obtained at 15°C by Jaffe, Hagiwara and Kado (Dev. Biol. 67, 243, 1978). [Supported by NSF PCM 78-6178 and NIH HD-07129.]

M-Pos65 FLUORESCENCE RESONANCE ENERGY TRANSFER BETWEEN LABELLED LIPIDS EMBEDDED IN THE MEMBRANE BILAYER DETECTS CALCIUM-PROMOTED FUSION OF ISOLATED CHROMAFFIN GRANULES. Stephen J. Morris and Diane Bradley, Neurotoxicology Section, NINCDS, Bldg. 9 Room 1E127, NIH, Bethesda, MD 20205, USA.

Chromaffin granules isolated from bovine adrenal medulla were labelled by mixing with small unilamellar vesicles (SUV) composed of N-4-nitrobenzene-2-oxa-1,3-diazene dioleoyl phosphatidyl ethanolamine and/or N-lissamine rhodamine B sulfonyl dioleoyl phosphatidyl ethanolamine (NBD-PE and Rhodamine-PE) as donor and acceptor fluorophores. Incorporation of the labels could be followed by the relief of self quenching experienced when the labels were incorporated into the granule membrane. The mechanism of incorporation seemed to be fusion of the SUV with the granule membrane although transfer of label cannot be ruled out.

Granule-granule fusion can be detected either by fluorescence resonance energy transfer from donor to acceptor fluorophores or by donor quenching, in either of two different experimental designs: by reduction in donor fluorescence and increase in acceptor fluorescence when donor-labelled granules fused with acceptor-labelled granules or by corresponding reciprocal changes when granules containing both probes fused with unlabelled granules. It can be initiated by mM concentrations of Ca^{2+} ; Mg^{2+} is less effective. Mg-ATP has no effect. Fusion is inhibited by potassium glutamate and a variety of organic and inorganic cations and anions, which also inhibit granule-granule aggregation to a lesser extent. The conditions for promotion and inhibition of granule fusion are quite different from those reported by Knight and Baker [*J. Memb. Biol.* 68 (1982) 107-140] for exocytosis of granule contents from permeabilized chromaffin cells, who see a requirement for Mg-ATP and inhibition by Cl^- but not by glutamate. We conclude that the membrane fusion seen in this report is activated by a different mechanism.

M-Pos66 INHIBITION OF SENDAI VIRUS-INDUCED HEMOLYSIS BY FATTY ACIDS.

R. C. MacDonald, R. I. MacDonald and V. Dalle Ore. Department of Biochemistry, Molecular Biology and Cell Biology, Northwestern University, Evanston, IL 60201

Hemolysis by late-harvest virus is generally accepted to be a consequence of fusion of the viral membrane with the red cell membrane. To identify critical stages in the fusion of viral and target membranes, we have surveyed potential inhibitors of this process. Isostearic and cis-unsaturated fatty acids completely inhibited hemolysis at a few micrograms/ml. Saturated, normal fatty acids were partially inhibitory at concentrations several times greater. Trans-unsaturated fatty acids, as well as several other amphiphilic compounds were virtually non-inhibitory. In contrast to their different effects on viral activity, both cis- and trans-unsaturated fatty acids lyse red cells at concentrations of 25-50 micrograms/ml. Osmotic fragility of red cells was inversely related to inhibitory activity but not so as to explain the observed inhibition. Furthermore, it was unambiguously demonstrated that potent inhibitors, such as isostearic acid, affected the virus, not the target red cell, and inactivated the hemolytic, but not the hemagglutinating activity, of the virus. An inhibitory concentration of isostearate is well below that at which amphiphiles dissolve membranes and did not dissolve Sendai virus, as shown by sucrose gradient centrifugation and SDS-polyacrylamide gel electrophoresis. Inhibitory activity of fatty acids is inversely related to their critical micelle concentrations and directly related to their equilibrium surface pressures at air-water interfaces. In the case of isostearic acid, inhibition is proportional to concentrations below the C.M.C. but jumps abruptly at the C.M.C. Such behavior may indicate both lipid bilayer- and protein (presumably the fusion protein)-directed effects of the fatty acid inhibitors.

M-Pos67 DYNAMICS OF ADHESION, INSTABILITY AND FUSION OF MEMBRANES, CONSIDERED AS THIN VISCO-ELASTIC FILMS. D.S. Dimitrov, R.K. Jain, K. Miller, Department of Chemical Engineering, Carnegie-Mellon University, Pittsburgh, Pennsylvania 15213, D. Zhelev and T.T. Traykov, Central Laboratory of Biophysics, Bulgarian Academy of Sciences, Sofia 1113, Bulgaria

The process of mutual approach of membranes, resulting in adhesion or fusion, can be conveniently split into three main stages: 1) continuous approach of membranes; 2) destabilization of the membrane system, leading to the rupture of the intervening liquid film or of the film and the membranes and 3) expansion of the area of membrane contact during adhesion or of the hole during fusion. We have derived a general differential equation describing these stages. The membranes and the film between them have been modeled as thin viscoelastic films. The dispersion equation and the conditions for stability of a multilayered membrane system have been also derived. The results suggest that the destabilization of the film between membranes and/or the membranes themselves can increase the rate of membrane adhesion and fusion. Our experiments on the kinetics of haemolysis and fusion of red blood cells in dependence on the osmolarity and the concentration of surfactants (sodium dodecylsulfate and sodium tetradecylsulfate) seem to confirm the theoretical predictions. The membrane tension of rupture or/and fusion decreases with an increase of the surfactant concentration almost linearly at small concentration and depends on the time duration. Observations, carried out with a micropipette aspiration technique, have given similar results.

Supported by the NSF Grant No. INT 8209490.

M-Pos68 ANALYTICAL INTEGRATION OF THE STAVERMAN-KEDEM-KATCHALSKY TRANSPORT EQUATIONS. AND EXPERIMENTAL CONFIRMATION, A. Zelman, D. Gisser, M. Kupferschmid, Department of Biomedical Engineering, Rensselaer Polytechnic Institute, Troy, NY 12181

The Staverman-Kedem-Katchalsky "practical" flux equations have been solved analytically and simultaneously to obtain as a function of time the volumes and concentrations of the solutions bounding the membrane. Previous reports have estimated the transport parameters from linear regression methods which do not solve the differential equations simultaneously. In the analysis, the assumptions were made that c_{ss} is constant and defined as the arithmetic mean transmembrane solute concentration, the osmotic coefficients are unity, and transported volume is conserved. Direct experimental comparison of the transport coefficients by the zero volume flow method and the analytical solution indicates that the methods are consistent, but error analysis shows the analytical solution to be significantly more accurate. With the analytical solution, time dependent transmembrane volumes and concentrations can be predicted with less than 0.5% error, if L_p , σ and ω are known, or L_p , σ and ω can be determined from volume and concentration measurements as a function of time. In addition L_p , σ and ω can be roughly estimated from the analytical solution when only volume or only concentration is measured as a function of time. It should be recognized that transport coefficients measured with c_{ss} constant have general validity for any transport process since L_p , σ and ω are nearly independent of concentration. This research was supported in part by Public Health Service Contract AM7-2206 and NSF grant CPE81-15007.